ABSTRACT

Title of Dissertation: ROLES OF PLASMA MEMBRANE WOUNDING AND REPAIR IN B CELL ANTIGEN CAPTURE AND PRESENTATION

Jurriaan Jan Hein van Haaren
Doctor of Philosophy, 2022

Dissertation directed by: Dr. Wenxia Song, Professor, Cell Biology and Molecular Genetics

The B cell-mediated humoral immune responses play a crucial role in neutralizing pathogens and unwanted foreign substances. B cells become activated upon antigen binding of their B cell receptor (BCR), and then internalize and process antigen for presentation on their MHCII for T cell recognition. acquiring T cell signaling through antigen presentation is essential for B cell differentiation into high-affinity antibody-producing cells and memory B cells. *In vivo,* Antigen encountered by B cells is often tightly associated with the surface of pathogens and/or antigen-presenting cells. When B cells engage surface-associated antigen, BCR signaling induces reorganization of the cytoskeleton, causing spreading and contraction of the B cell on the antigen-presenting surface. This allows the B cell to engage more antigen and gather the antigen into a central cluster for internalization. Internalization of surface-associated antigen has been shown to require myosin-generated forces and the exocytosis of lysosomal enzymes. However, the mechanism that initiates lysosomal exocytosis remains unknown.

This research explored a possible mechanism for the triggering of lysosomal exocytosis of B cells during interaction with surface-associated antigen. We showed that BCR interaction with antigen tethered to beads, to planar lipid-bilayers (PLBs) or expressed on the surface of live cells causes permeabilization of the B cell plasma membrane (PM), an event that required strong BCR-antigen affinity, BCR signaling, and activation of non-muscle myosin IIA (NMIIA). Moreover, we showed that B cell PM permeabilization triggers a repair response that includes the exocytosis of lysosomes at the site of antigen interaction. Importantly, we showed that B cells undergoing PM permeabilization and subsequent repair internalize more antigen; and better activate T cells compared to unpermeabilized B cells. Thus, our research reveals a novel mechanism for B cells to capture surface-associated antigen: antigen affinity-dependent binding of the BCR indices localized B cell PM permeabilization and lysosome exocytosis as a repair response, which facilitates antigen internalization and presentation through the extracellular release of lysosomal hydrolases.

In addition, we explored the molecular mechanism required for B cell PM permeabilization in response to surface-associated antigen. We showed that B cells that undergo PM permeabilization in response to PLB-associated antigen spread over the PLB at a faster rate and to a larger area in comparison to cells that remain intact. Furthermore, we showed that B cells that undergo PM permeabilization recruit more NMIIA at a faster rate, and display a higher level of NMIIA organization at the immune synapse. We additionally discovered a 2^{o} B cell spreading and NMIIA recruitment event, approximately 25-30 minutes after antigen engagement, that facilitates B cell PM permeabilization. Thus, B cell PM permeabilization requires the engagement of a large amount of antigen through B cell spreading on the presenting surface, as well as strong NMIIA recruitment and organization at the immune synapse. This research suggests that B cell PM permeabilization in response to surface-associated antigen plays an important role in distinguishing B cells with various levels of

BCR activation, providing novel insights into the mechanisms responsible for affinity differentiation during B cell activation.

ROLES OF PLASMA MEMBRANE WOUNDING AND REPAIR IN B CELL ANTIGEN CAPTURE AND PRESENTATION

by

Jurriaan Jan Hein van Haaren

Dissertation submitted to the Faculty of the Graduate School of the
University of Maryland, College Park, in partial fulfillment
of the requirements for the degree of
Doctor of Philosophy
2022

Advisory Committee:
Wenxia Song, Ph.D., Chair
Norma Andrews, Ph.D.
Arpita Upadhyaya, Ph.D.
Sougata Roy, Ph.D.
Xiaoping Zhu, Ph.D.

Dedication

I dedicate this thesis to my family and friends for their encouragement and continued support. My Parents for being the best parents I could ask for and for always being there for me whenever I need them. My older sister for setting a great example for me to live up to. And my friends for always supporting me and helping me take some breaks from work whenever I need them.

Acknowledgments

First, and most importantly, I would like to thank Dr. Wenxia Song, for being a great advisor, not only for helping me develop my technical skills but also for allowing me to venture outside the lab and explore my interests. And for being supportive and patient with me and allowing me to learn from my mistakes. And finally, for respecting my needs and caring about my wellbeing in addition to my education.

I also want to thank Dr. Norma Andrews for always making me feel welcome in her lab and for encouraging me to work with Dr. Song on this project.

I further want to thank all my committee members, Dr. Wenxia Song, Dr. Norma Andrews, Dr. Arpita Upadhyaya, Dr. Sougata Roy, and Dr. Xiaoping Zu, for all their input and enlightening discussions.

I want to thank all the members of the Song lab, as well as the members of the Andrews lab and the Upadhyaya lab for engaging with me in discussions regarding this project and for their valuable input, and for creating a fun and engaging work environment. I specifically want to thank Anshuman Bhanja for being an awesome coworker, and more importantly, a great friend to go through this journey with. Having a friend alongside me in the lab has made work much more enjoyable and made it easier to get through the rough bits. Similarly, I want to thank Fernando Maeda, who like Anshuman was a great coworker and friend, and who was always fun to be around. Finally, I want to thank Katie Fallen for helping me get settled in the lab and teaching me most of what I needed to be successful in the Song lab.

I would also like to thank Amy Beaven for training me and helping me with any imaging needs.

Importantly, I would like to thank all my friends and family for supporting me and helping me to relax, stay sane, and to be able to enjoy my life outside the lab.

Finally, I want to thank the UMD Graduate Consulting Club, for helping me with my career development and ultimately helping me get a job in the field I want to work in.

Table of contents

List of Figures

List of Abbreviations

Ab	Antibody
Abp1	Actin binding protein 1
AID	Activation-induced cytidine deaminase
Ag	Antigen
APC	Antigen presenting cell
ASM	Acid sphingomyelinase
BAFF	B cell activating factor
BCR	B cell Receptor
BEL	Bromoenol Lactone
Bleb	Blebbistatin
BLNK	B-cell Linker protein
BTK	Burton's tyrosine kinase
CARC	Calcium release activated channels
CatS	Cysteine protease cathepsin
CFSE	Carboxyfluorescein succinimidyl ester
CIE	Clathrin independent endocytosis
CSR	Class switching recombination
CTL	Cytotoxic T-lymphocyte
CVID	Common variable immune deficiency
DAG	Diacylglycerol
DAMP	Damage-associated molecular patterns
DC	Dendritic cell
DEL	Duck egg lysozyme
D_H	Diversity region
DPA	Desipramine
ELISA	Enzyme-linked immunosorbent assay
ER	Endoplasmic reticulum
ERM	Ezrin/radixin/moesin
ESCRT	Endosomal Sorting Complex Required for Transport

Fc	Fragment crystallizable
FcyRIIB	Fc-gamma RII-B receptor
FDC	Follicular dendritic cell
FI	Fluorescence intensity
FIR	Fluorescence intensity Ratio
FO B cell	Follicular B cell
GC	Germinal center
GFP	Green fluorescence protein
Grb2	Growth factor receptor-bound protein 2
HEL	Hen Egg Lysozyme
HSC	hematopoietic stem cells
Ig	Immunoglobulin
IL	Interleukin
IP_3	Inositol triphosphate
IRM	Interference reflection microscopy
ITAM	Immunoreceptor Tyrosine-based Activation Motif
ITIM	Immunoreceptor Tyrosine-based Inhibitory Motif
J_H	Joining region
LAMP1	Lysosomal-associated membrane protein 1
LIMP2	Lysosomal integral membrane protein-2
MFI	Mean fluorescence intensity
MHCI	Major histocompatibility complex class-I
MHCII	Major histocompatibility complex class-II
mIg	Membrane bound immunoglobulin
MIIC	MHC Class-II containing multivesicular bodies
MTOC	Microtubule organization center
MZ B cell	Marginal zone B cell
N-WASP	Neuronal Wiskott-Aldrich syndrome protein
NFAT	Nuclear factor of activated T cells
NLR	Nod-like receptors

NMII	Non-muscle myosin-II
NMIIA	Non-muscle myosin IIA
PAMP	Pathogen-associated molecular patterns
PBS	Phosphate buffered saline
PI	Propidium Iodide
PI3K	Phosphoinositide 3 kinase
PIP2	Phosphatidylinositol 4,5-bisphosphate
PIP3	Phosphatidylinositol 3,4,5-trisphosphate
PLB	Planar lipid bilayer
PLCγ2	Phospholipase C-gamma 2
PM	Plasma membrane
pMLC	Phosphorylated myosin light chain
PRR	Pattern recognition receptors
pSyk	Phosphorylated Syk
Rag	Recombination-activating gene
SH2	Src homology 2
SHIP-1	SH2-domain-containing inositol 5-phosphatase
SHP1	SH2-domain containing protein tyrosine phosphatase
SLC	Surrogate Light chain
SLE	Systemic Lupus erythematosus
SLO	Streptolysin O
SMAC	Supramolecular activation complex
Syk	Spleen tyrosine Kinase
Syt	Synaptotamin
T1 B cell	Transitional 1 B cell
T2 B cell	Transitional 2 B Cell
TCR	T-cell receptor
TIRF	Total internal reflection fluorescence
Tf	Transferrin
T_{fh}	T follicular helper cell

TLR	Toll-like receptors
V_H	Variable region
WASP	Wiskott-Aldrich syndrome protein
XLA	X-linked agammaglobulinemia

Chapter 1: Introduction

1.1 B cell function in immune response

1.1.1 Innate Immunity

The immune system is essential in providing the human body with the necessary protection against foreign pathogens. It protects the body by attacking and neutralizing invading pathogens and toxins. The immune system consists of two major branches. First, there is the innate immune system, which protects against pathogens in a non-specific manner. The innate immune system works by recognizing common molecular patterns presented on pathogens and taking broad, non-specific action to neutralize the invading entities. For example, macrophages and other phagocytic cells recognize the surface molecules of pathogens, phagocytose these pathogens, and destroy them in phagolysosomes. The innate immune response is activated by receptors recognizing common pathogen-associated molecular patterns (PAMPs) on pathogen surfaces, or damage-associated molecular patterns (DAMPs) originating from damaged host cells[1,2]. PAMP receptors, known as pattern recognition receptors (PRRs), recognize lipoproteins, glycoproteins, lipopolysaccharide (LPS), and flagella present on the surface of bacterial cell walls and double-stranded RNAs of viruses. These receptors include toll-like receptors (TLRs), Nod-like receptors (NLRs), and retinoic acid-inducible gene (RIG-I) like receptors[1]. The innate immune system is generally thought of as a short-term response to invading pathogens and does not provide long-term protection against specific antigen (Ag). However, the innate immune system does function to initiate the second major branch of immunity, the adaptive immune response. Upon activation of PRRs, the innate immune system induces stimulatory cytokines that activate the rest of the innate immunity and also facilitate the activation of lymphocytes, which are essential components of the adaptive immune response[2–4]. The adaptive immune response provides long-lasting, specifically targeted protection against a wide variety of invading pathogens[2,5,6].

1.1.2 Adaptive immunity

The adaptive immune response can be divided into two major branches, the cell-mediated and the humoral (or antibody mediated) immune responses[7]. The cell mediated immune response largely depends on the function of T lymphocytes. T lymphocyte mediated immunity depends on the function of CD4+ T cells and CD8+ T cells. CD4+ T cells (or T helper cells, T_h) get activated by recognizing Ag presented with the major histocompatibility complex class II (MHCII) on the surface of professional Ag presenting cells (APCs). CD4+ T cells stimulate other leukocytes by releasing various stimulatory cytokines that induce various immune functions[8]. MHCII molecules are exclusively expressed by professional APCs, macrophages, dendritic cells, and B cells[7]. These cells internalize Ag, process it, and subsequently present the processed Ag on their MHCII[2,9,10]. Recognition of Ag presented on the MHCII through the T cell receptor (TCR) activates T_h cells and produces a stimulating signal in return to activate APCs[8,11,12]. CD8+ T cells (or Cytotoxic T cells, CTLs) recognize Ag presented on the major histocompatibility complex class I (MHCI)[7]. The MHCI is expressed by all cell types and is responsible for presenting antigen from intracellular pathogens, like viruses. Additionally, cancer cells can present miss-expressed protein on MHCI. CTLs recognize Ag presented on MHCI through TCR, which induces the release of cytotoxic proteins such as perforin, granzymes, and granulysin, consequently eliminating these cells[13,14].

The Humoral immune response relies on the production of Ag-specific antibodies (Abs) by B lymphocytes[9,15]. Antibodies are molecules that bind to Ag with specificity, neutralizing the Ag and tagging it to be degraded by other immune cells. To protect against a wide variety of possible pathogens and toxins, the human body produces a large variety of antibodies. Antibodies are produced by antibody producing cells, which differentiate from B lymphocytes that have been exposed to specific antigens. Antibodies function by binding to specific foreign substances in a process known as opsonization. Antibody binding can neutralize the foreign substance and help facilitate its clearance. Opsonization facilitates macrophages and other phagocytic cells to bind,

phagocytose and degrade the foreign substance. Additionally, opsonization induces the complement cascade, which kills the pathogenic cells by generating pores in their membrane. The research in this dissertation will focus mostly on the role of B cells in the humoral immune response. B cells circulate the body in search of foreign antigen through the blood and lymphatic system, although a large number of B cells can be found in secondary lymphoid tissues such as the spleen and lymph nodes. Here B cells interact with antigen presenting cells, such as macrophages and dendritic cells, that capture antigen and present it on their surface for B cell recognition. Although B cells do recognize soluble antigen, the presentation of antigen by APCs significantly increases the likelihood of B cells encountering antigen, and facilitates the interaction via costimulatory molecules present on the surface of the presenting cells[16]. B lymphocytes use their B cell receptor (BCR), a membrane associated immunoglobulin (Ig) receptor molecule, to recognize Ag. Once the BCR engages an Ag, the B cell will be primed to initiate signaling through the CD79a/CD79b heterodimer non-covalently associated with mIg. The intracellular domains of CD79a and CD79b contain intracellular signaling domains[17–19]. BCR signaling induces the activation of B cells and primes the internalization, processing, and presentation of the Ag on the MHCII [9]. The B cell will then receive an additional activation signal from Ag specific T_h cells[11,20]. Upon activation, B cells differentiate into Ab producing cells or memory B cells. Antibody producing cells generate Ag-specific Abs, with strong specificity to Ag. Alternatively, B cells can differentiate into memory B cells, which enter the circulation, and will be activated upon the next exposure to the same Ag. Activated B cells form germinal center reactions in the secondary lymphoid organs, where they undergo affinity maturation to improve Ab affinity to the specific antigen (further discussed below)[5,9]. Thus, providing rapid, high affinity, and long-lasting immunity against specific Ags[6,9].

1.2 B cell effector function

1.2.1 The antibody molecule

The main function of B Cells is to generate humoral immune responses by generating Ab. Antibodies function by binding with high specificity to Ag, which neutralizes the Ag by preventing pathogens with the Ag to colonize and invade host cells, by activating the compliment cascade, and by recruiting other immune cells through interaction with Fc receptors on their surfaces. An antibody is a glycoprotein complex consisting of two identical heavy chains and light chains, linked by disulfide bonds into a Y-shaped structure[21,22] (Figure 1.1). The antibody consists of two Ag binding regions (the Fab region) and a constant region (The FC region). Each of the two arms in an Ab (the Fab regions) contains a variable region used for binding Ag. The variable regions are generated through random VDJ rearrangement of Ig genes[21,22]. The tail (or the Fc region) is used to interact with complement proteins and the Fc receptors on various immune cells, and contains only a constant region which determines the isotype of the Ig antibody. The antibody molecule is made up of two heavy and two light chains. Each light chain consists of two Ig domains located in the Fab portion of the Ab molecule, and the heavy chain consists of four to five Ig domains (depending on the isotype class) spanning both the Fab and the Fc portion of the molecule. The N-terminus of the light and heavy chains form the variable region to bind Ag, while the C-terminal of the heavy chains forms the Fc region that binds to Fc receptors. Random rearrangement of the N terminus of the Ab molecule ensures that individual B cells have unique binding sites, and allows B cells to bind with high specificity to a wide range of Ag. The BCR is a surface-bound IgM or IgD Ab molecule, associated with a CD79a(Igα)/CD19b(Igβ) heterodimer that transduces Ag binding signal across the plasma membrane (PM). The BCR surveys Ag, and Ag binding initiates the process for B cells to differentiate into Ab producing cells, secreting Ab that specifically recognizes that Ag. In order to generate B cells with a wide variety of specificity, Ig genes undergo rearrangement in a process known as VDJ recombination during B cell maturation in the bone marrow[22–24]. VDJ

recombination is dependent on the recombination-activating gene (RAG1 and RAG2), which mediates the random recombination of the variable (V), diversity (D), and joining (J) gene segments of the Ig Heavy chain and the V and J segments of the Ig Light chain. This random gene recombination produces a large repertoire of B cell clones that will recognize a wide variety of Ag. Secreted Ab circulates the body to neutralize foreign Ag and will bind with high specificity to its target Ag. This opsonization neutralizes pathogens and allows them to be recognized by various immune cells expressing Fc receptors. Fc receptors will recognize the Fc portion of the Ab molecule. The binding of Fc receptors to Ag-Ab immune complexes and opsonized pathogens will activate the phagocytotic and intracellular kill functions of immune cells, such as macrophages and neutrophils, clearing the pathogens. Furthermore, Ab opsonizing pathogen can activate compliment cascades through their Fc region and induce compliment mediated cytolysis of pathogens.

Figure 1.1:

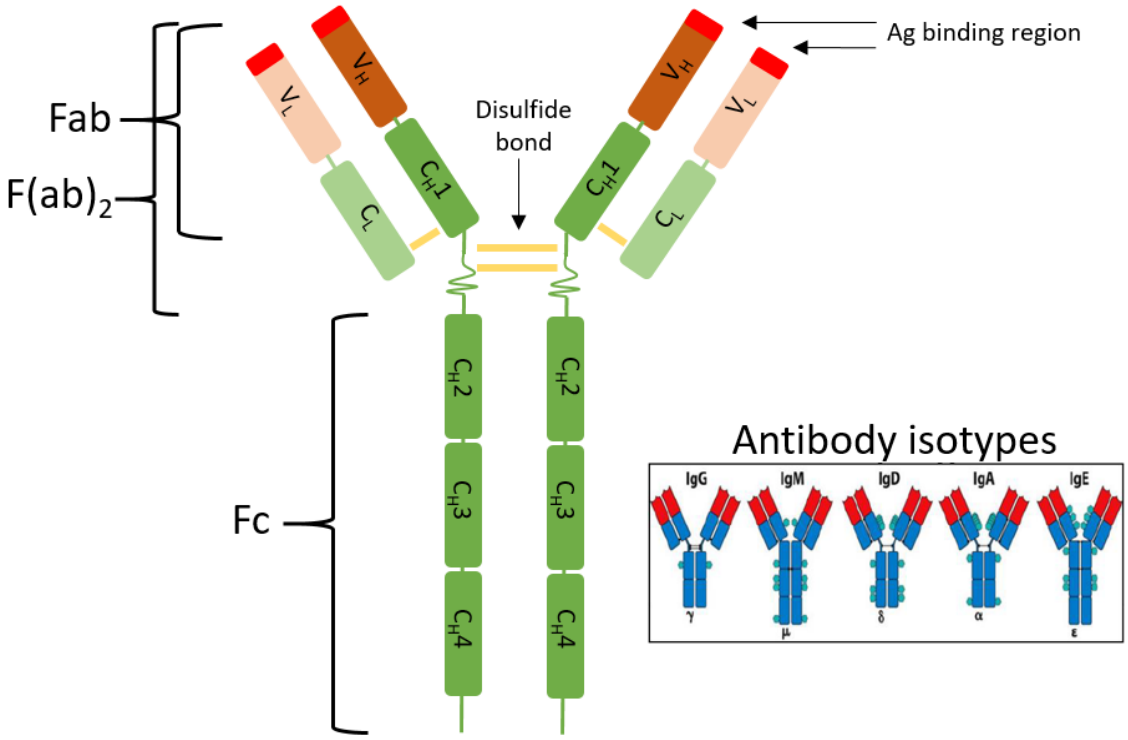

Figure 1.1: **Structure of the Ab molecule.** Abs are made up of 2 identical heavy and 2 identical light chains connected by disulfide bonds. Both the heavy and the light chain contain a variable (N-terminus) and constant (C-terminus) region. The variable region consists of one Ig domain and is located at the tip of both arms of the Ab molecule and is used to bind Ag. The constant region consists of 1 Ig domain in the light chain, and 3-4 Ig domains in the heavy chain, depending on the isotype of the Ab. The Fc (constant) region is made up of only the heavy chain constant regions and is used to bind Fc receptors. The Fab (antigen binding) region consist of one constant and one variable region of both the light and heavy chains and I used to bind to Antigen. The Fc and Fab regions are connected by a hinge region that gives the Ab flexibility to bind Ag.

1.2.2 Antibody function

There are five isotypes of the Ig molecule including IgM (μ), IgD (δ), IgE (ε), IgA (α) and IgG (γ)[25] (Figure 1.1). The isotype of the Ig is determined by the constant region (Fc region) of the molecule[25]. These isotypes determine their effector functions within the immune system. Naïve (Ag unexperienced) B cells express membrane IgD and IgM (B cell receptors), to survey for Ag. The C-terminus of the heavy chain of the mIgD and IgM molecules contain a hydrophobic transmembrane region, followed by three positively charged amino acids. B cell activation can induce Ig class switching recombination (CSR) changing from expression of mIgM and mIgD to expression of other Ig isotypes. Each Isotype has a unique, isotype specific, Fc-receptor it can bind to[25]. Binding to these Fc-receptors expressed on a variety of immune cells will induce various effector functions. Secreted Igs circulate the blood and lymph circulating systems, surveying foreign Ag. IgG is by far the most abundant circulating Ab and can be expressed as various subisoforms, such as IgG1, IgG2, IgG3, and IgG4 in the human. Besides activating complement IgG binds to isoform specific Fcγ receptors. Whereas the circulating IgG molecule exists as a monomer, the circulating IgM molecule exists as a pentamer. IgA is primarily secreted as dimers at the mucosal surfaces. IgE is the major player in allergic reactions and activates allergic reactions by binding FcεR on mast cells, basophils, and eosinophils, inducing degranulation. Thus, B cells play a wide variety of roles in the immune response to invading pathogens by secreting antibodies. Various Ig isotypes secreted by B cells can activate different immune cells through FcRs to fight infection. Under a sufficient activation condition, naïve B cells can differentiate into long-lived memory B cells and plasma cells, providing long-lasting immunity. Long-lived plasma cells maintain antibody levels in circulation. Memory B cells mount a rapid, robust, and highly specific immune response upon exposure to pathogens the host has previously been exposed to. Establishment of long-lived plasma and memory B cells is the fundamental basis of vaccines, the most effective preventatives for infectious diseases.

1.3 B cell development and activation

1.3.1 Early B cell development

Most B lymphocytes are originated from hematopoietic stem cells (HSC) in the bone marrow. B cells undergo a series of complex mutation steps and developmental stages before reaching the mature naive B cell stage. During B cell development, self-reactive B cells are eliminated (negative selection) to establish self-tolerance. B cells first emerge as pro-B cells, recognized by the surface expression of CD45R/B220. Pro-B cells express a pro-BCR, consisting of calnexin and Igα/Igβ before Ig genes undergo rearrangement[26]. B cells then undergo Rag1/2-mediated rearrangement of the Ig heavy chain genes and develop into Pre-B cells. Rearrangement of the Ig Heavy chain is initiated by IL-7, released by bone marrow stromal cells[23]. IL-7 induces the expression of the recombination-activating gene (rag). The diversity region (D_H) and the joining region (J_H) recombine first, followed by the variable region (V_H) to complete the VDJ recombination. During the Pre-B cell state, the rearranged Ig heavy chain is joined by a surrogate Light chain (SLC), consisting of λ5 and VpreB, to make up the mIg of the pre-BCR[26]. Ig gene rearrangement is critical for B cell development, as humans and mice with RAG1/2 deficiency do not develop mature lymphocytes[26,27]. Furthermore, immunodeficient SCID humans and mice fail to develop mature lymphocytes due to an inability to induce Ig gene rearrangement; however, introduction of genetically rearranged Ig molecules induces the generation of mature lymphocytes in SCID mice[28]. Successful assembly of the pre-BCR includes the association of the pre-BCR with the Igα/Igβ complex and will provide the B cell with an activation signal allowing the B cell to further develop. However, unsuccessful assembly of the pre-BCR will cause the B cell to undergo apoptosis, as these cells will lack a properly assembled BCR and will thus not be able to produce any intracellular signaling. At the immature B cell stage, B cells expressing self-reactive BCRs are negatively selected for elimination. The binding of the BCR to self Ag in the bone marrow with high affinities induces apoptosis, while low-affinity binding of the BCR to self Ag causes further VDJ rearrangement to change mIgM specificity[26,29]. Non-self-reactive B cells are selected to leave

the bone marrow and move to the secondary lymphoid tissues, where B cells further develop into transitional 1 (T1, IgD^{hi}/IgM^{low}), transitional 2 (T2 IgD^{hi}/IgM^{hi}), and mature follicular B cells.

Mature, Ag inexperienced naïve B cells, survive and survey Ag by circulating through the spleen and lymph nodes. Mature B cells can be divided into two major types, B1 and B2 B cells. B1 cells are responsible for generating Abs against common Ags (natural Abs). B1 cells exist in the pleural and peritoneal cavities and are responsible for generating Abs that respond to polymeric antigens such as polysaccharides and lipids. Unlike conventional B cells, these cells generate Ab responses independent of Ag stimulation through innate receptors, such as TLRs. Furthermore, these cells are self-renewing, requiring no BCR activation or T cell help to proliferate. B2 cells on the other hand, require Ag specific stimulation. In the secondary lymphoid tissues, there are two major populations of B-cells, marginal zone (MZ) B cells and follicular (FO) B cells. MZ B cells are non-circulating B cells located in the marginal zone of B cell follicles, while FO B cells are the dominant population of B cells in the secondary lymphoid tissue. Both MZ and FO B cells can be activated through the BCR[17,18,30]. BCR signaling is essential for B cell survival and activation. MZ B cells have a limited repertoire of BCRs that bind to common pathogen-associated Ag. They have a lower activation threshold than FO B cells and respond rapidly to Ag exposure, producing an antibody response within hours[31]. MZ B cells primarily respond to T cell independent Ag, such as polysaccharides or lipopolysaccharides that T cells do not recognize. T cell independent activation generally leads to short-lived Ab producing cells that primarily secrete IgM Abs. FO B cells circulate the body through the lymphatic system and pass through the follicles of the lymph nodes and spleen to survey Ag. FO B cells primarily respond to T cell dependent Ag, generally protein-based Ag, requiring a secondary signal from T helper (T_h) cells to differentiate into Ab producing cells or memory B cells. T cell help is essential for B cells to generate a high affinity, isotype switched Ab response, a process called affinity maturation[20,32].

1.3.2 B cell affinity maturation and the germinal center

The process of affinity maturation is essential for B cells to differentiate into high-affinity Ab producing cells or memory B cells. It is important that Ab producing cell and memory B cells are generated that can recognize an antigen with high specificity and strong binding affinity. Strong affinity and specificity will ensure the effective recognition and binding of the Ag and ensure an effective immune response. To accomplish the production of highly specific Ab producing and memory B cells, B cells undergo a number of processes to select for B cell clones with affinity and specificity of the BCR, and ultimately the Ab, against the antigen. This includes several rounds of somatic hypermutations as well as selective apoptosis and differentiation. The germinal center (GC) plays a crucial role in the affinity maturation of B cells. The germinal center is a specially organized cellular environment in secondary lymphoid tissues initiated by T cell stimulatory siganals[33,34]. GCs generally appear several days after initial exposure to an Ag, reach a peak after 1-2 weeks, and can last for several weeks[33]. The germinal center reaction is essential for the generation of high-affinity Ab producing cells and memory B cells, as its main function is to select for B cell clones with high affinity to the Ag (Figure 1.2). GC reactions are initiated after Ag recognition by the B cell. Upon Ag recognition, B cells internalize the foreign Ag, process it, and present it on the MHCII for T cell recognition. T_h cells activated by Ag-MHC-II complexes will prime B cells to migrate to the B cells follicle and undergo rapid proliferation, inducing germinal center reaction. B cells migrate from the B-T border of the B follicle by upregulating the CXCR5 receptor which recognize the chemokine CXCL13 produced by follicular dendritic cells (FDCs)[35]. FDCs are also responsible to presenting antigen to B cells in GC [5,32,34,36]. The Germinal center consists of two major regions, the dark zone, and the light zone[33,37]. The dark zone is a B cell dense area where Ag experienced B cells proliferate and undergo somatic hypermutation induced by activation-induced cytidine deaminase (AID). During somatic hypermutation, the variable (V), diversity (D), and Joining (J) regions of the Ig molecule undergo point mutations to alter the variable region of the Ig molecule and alter its affinity to the Ag. Somatic hypermutation further expands the B cell pool with a wide

range of affinity to the specific Ag[37]. After SHM, B cells will move from the dark zone to the light zone guided by the chemokine CXCL13 that is expressed by FDCs in the light zone and recruit $CXCR5^{hi}$ GC B cells[38,39]. The light zone contains FDCs that present surface bound Ag to the B cells, and Follicular T helper cells (T_{fh}) that provide B cells activation signals. In the light zone of the germinal center B cells survey and acquire Ag from APCs and consequently present processed Ag to T_{fh} cells to receive a T cell signal[40]. Cellular interactions between B cells and APCs, and B cells and T_{fh} Cells are critical in the light zone of the germinal center. Differentiation of high and low-affinity antigen during the acquisition of antigen from the surface of APCs is essential for proper affinity maturation of the B cells. Antigen affinity and density, as well as the nature of the presenting surface all affect the ability of the B cell to differentiate high- and low-affinity antigen (further discussed in chapter 1.6). Low-affinity B cells acquire less or no Ag and thus induce low levels of T cell signaling, priming low-affinity B cells to either undergo apoptosis or additional rounds of proliferation and somatic hypermutation. High-affinity B cells acquire more Ag and receive a strong T cell signal, priming them to class switching from IgM and IgD to IgG, IgA, and IgE and differentiate into Ab producing or memory B cells[37,41].

Figure 1.2:

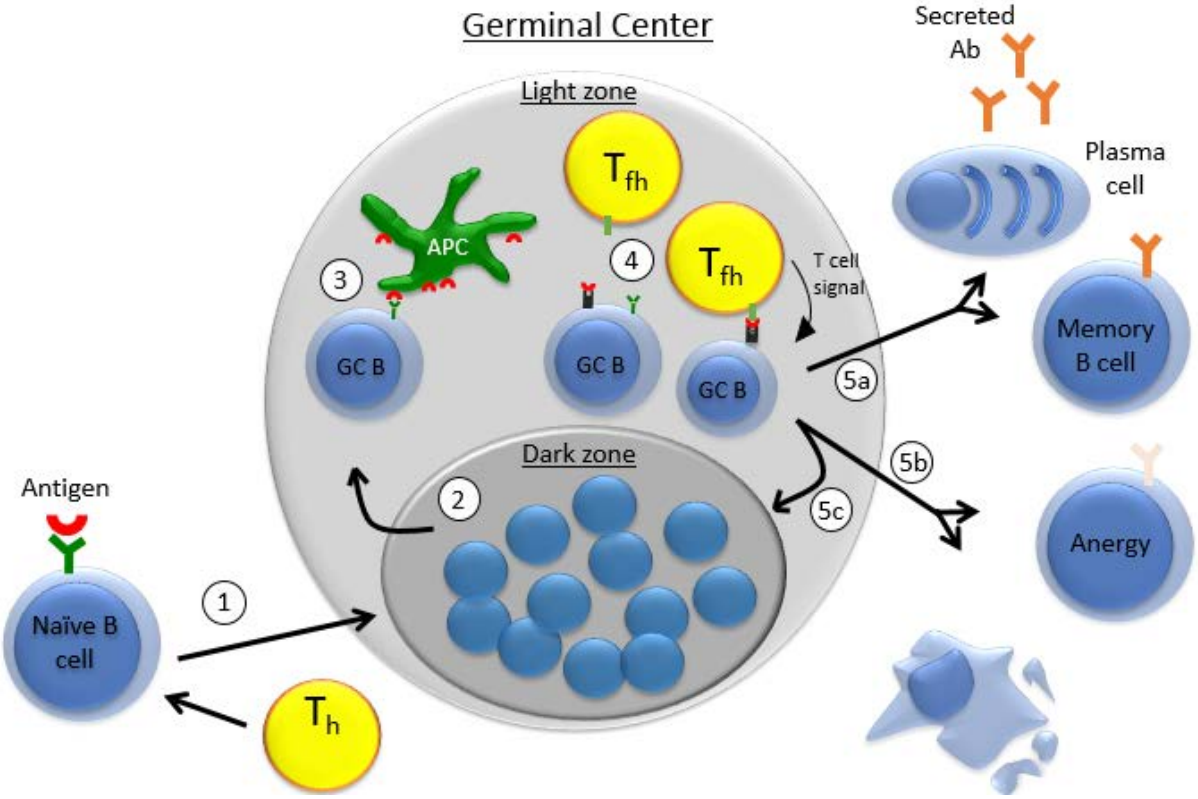
Germinal Center
Light zone
Dark zone
Secreted Ab
Plasma cell
Memory B cell
Anergy
Antigen
Naïve B cell
APC
GC B
GC B
GC B
T cell signal
1
2
3
4
5a
5b
5c

Figure 1.2: The Germinal center reaction. The germinal center reaction is essential for the process of affinity maturation in B cells. (1) Upon B cell activation by recognition of an Ag and an additional activation signal from a Th cell, a subset of B cells will be induced to enter a GC reaction. (2) In the dark zone of the germinal center B cells will proliferate and undergo somatic hypermutations of the BCR. This increases the B cell pool and increases the variability of the BCR's affinity to the Ag. (3) B cells move from the dark zone to the light zone, where they interact with APCs, mainly follicular dendritic cells (FDCs). B cells will engage Ag presented on the surface of the FDC and internalize, process, and present the AG on their MHC-II. (4) B cells then interact with Tfh Cells. The Tfh cell will recognize the Ag presented by the B cell on their MHC-II. The T cell will in return provide the B cell with an additional activation signal. The strength and nature of this signal depend on the BCR-Ag affinity. (5a) If the BCR-Ag interaction is strong, the B cell will receive a strong T cell signal and will be induced to undergo Class switching recombination (CSR) and differentiation into memory B cells or Ab producing cells. (5b) If the BCR-Ag interaction is weak, the B cell will receive a weak, or no, T cell signal and will be induced to either enter a stage of anergy (non-reactiveness) or the B cell will undergo apoptosis. (5c) if the BCR-Ag affinity is moderate, the B cell will receive some T cell signal and will be induced to migrate back to the dark zone and undergo additional rounds of proliferation and somatic hypermutations, to increase its BCR-Ag affinity.

1.4 BCR signaling pathway

B cells recognize Ag through the BCR. The BCR is a membrane associated protein complex consisting of a trans-membrane immunoglobulin (mIg), responsible for Ag recognition, non-covalently associated with a heterodimer of Igα and Igβ (CD79a/b), responsible for intracellular signaling. Upon engaging Ag, the BCR generates an intracellular signaling response through the Igα/Igβ. B cell activation requires a certain threshold level of BCR signaling, which prevents spontaneous B cell activation, or activation in response to low-affinity Ag. The extent of BCR signaling is dependent on the avidity of the BCR-Ag interaction[42]. Avidity is determined by the affinity of the BCR-Ag interaction as well as the valency (the abundance of epitopes) of the Ag. Research from the Batista and Pierce labs showed that Ag with high affinity will induce a stronger BCR signal when compared to low-affinity antigen mutants[42–45], and similarly, Ag with a higher number of repeated epitopes will also induce a stronger BCR signal [46,47]. Both affinity and valency of the antigen to the BCR are important for B cell affinity discrimination. This allows the B cells to differentiate between high and low affinity BCR-Ag interactions and prevents activation of the B cell in response to weak Ag interactions. Furthermore, it allows the B cells to effectively undergo the affinity maturation processes.

1.4.1 BCR signaling cascade

To initiate BCR signaling, the BCR must recognize an Ag that can crosslink surface BCRs. This requirement was demonstrated by the fact that exposure of B cells to a $F(ab)_2$ fragment of anti-BCR antibody (containing 2 Ag binding sites) induces BCR activation, but exposure to a Fab fragment of anti-BCR antibody (containing one Ag binding site) does not[48]. Crosslinking of the BCR will lead the BCR to self-aggregate into lipid raft associated BCR microclusters[17,18] (Figure 1.3). Lipid rafts are dynamic plasma membrane (PM) structures rich in cholesterol and glycosphingolipids that can physically and biochemically include or exclude

surface molecules. Aggregated BCR clusters and BCR co-stimulatory receptors such as CD19, a costimulatory molecule that lowers the activation threshold of the BCR, prefer to locate in lipid rafts. It has been shown that translocation into lipid raft domains will induce a conformational change of the BCR that alters the conformation of the Igα/Igβ heterodimer to expose its cytoplasmic signaling domain[30,49,50]. Both Igα and Igβ are transmembrane proteins with a cytoplasmic domain containing an immunoreceptor tyrosine-based activation motif (ITAM), responsible for intracellular signaling (figure 1.4). The ITAM is a signal transduction motif consisting of a conserved sequence of a tyrosine, followed by two amino acids and a leucine or isoleucine; with a 6-8 spacer ($YxxL/I\ x_{(6-8)}\ YxxL/I$)[19]. The ITAM is recognized by various signaling molecules important for the immune responses. Importantly, phosphorylated ITAM is a docking site for the spleen tyrosine Kinase (Syk), which plays an important role in early BCR signaling initiation[51,52]. Upon the formation of BCR microclusters and localization of these microclusters into lipid rafts, the BCR ITAM is phosphorylated by lipid raft resident Src tyrosine kinase Lyn; further underlining the importance of localization of the BCR into lipid raft domains[18,53] (Figure 1.4). The phosphorylated ITAM provides the docking site for Src homology 2 (SH2) domain containing Syk and enables Lyn to phosphorylate Syk. Activation of Syk is critically important, as inhibition of Syk majorly reduces B cell signaling and activation[54]. phosphorylated Syk activates various downstream signaling molecules, including the adaptor protein B-cell Linker protein (BLNK), which serves as a scaffold for the recruitment of various signaling molecules, including Burton's tyrosine kinase (BTK), phospholipase C-γ 2 (PLCγ2), and Vav[9] (Figure 1.4). The recruitment of B cell adaptor molecules, such as BLNK and Grb-2, facilitates the formation of a BCR signalosome (a collection of B cell signaling molecules) at the Ag binding site[55]. This organized signalosome can activate and regulate BCR signaling by recruiting additional stimulatory and inhibitory signaling molecules[9,56]. BCR signalosomes induce signaling cascades, leading to the activation of transcription factors that induce cell survival and proliferation. For example, BTK activated by Syk-mediated phosphorylation and self-

phosphorylation can activate PLCγ2[57]. PLCγ2 in turn cleaves Phosphatidylinositol 4,5-bisphosphate (PIP_2) to generate inositol triphosphate (IP_3) and Diacylglycerol (DAG). IP_3 bind to ER associated receptors, inducing the release of Ca^{2+} from ER, the intracellular Ca^{2+} storage. ER Ca^{2+} release activates calcium release activated channels (CARC) on the plasma membrane, causing an influx of extracellular Ca^{2+}. Ca^{2+} and DAG subsequently activation of PKC-β, which induces the activation of both the MAPK/ERK and Nuclear factor of activated T cells (NFAT) signaling cascades, leading to further activation of transcription factors responsible for B cell activation, proliferation, and differentiation[58]. Activation of the BTK and Ca^{2+} influx also induces the reorganization of the cytoskeleton important for sustained BCR signaling (Further discussed in chapter 1.5). BTK activates the actin nucleation promoting factors WASP and WAVE2 through Rho family GTPase Rac1 and Cdc422 initiating Actin polymerization[59,60]. Cdc42 further induces the polymerization of microtubulin and the polarization of the microtubule organization center (MTOC)[61]. Ultimately, BCR signaling increases the expression of co-stimulatory molecules for T cell activation, such as MHC-II, CD40, CD80/86, ICOS-L, and ICAM-1. BCR signaling also activates the endocytic machinery involved in internalizing the BCR-Ag complex, enabling B cells to capture, process, and present Ag to T cells to acquire additional activation signals[9,56].

Figure 1.3:

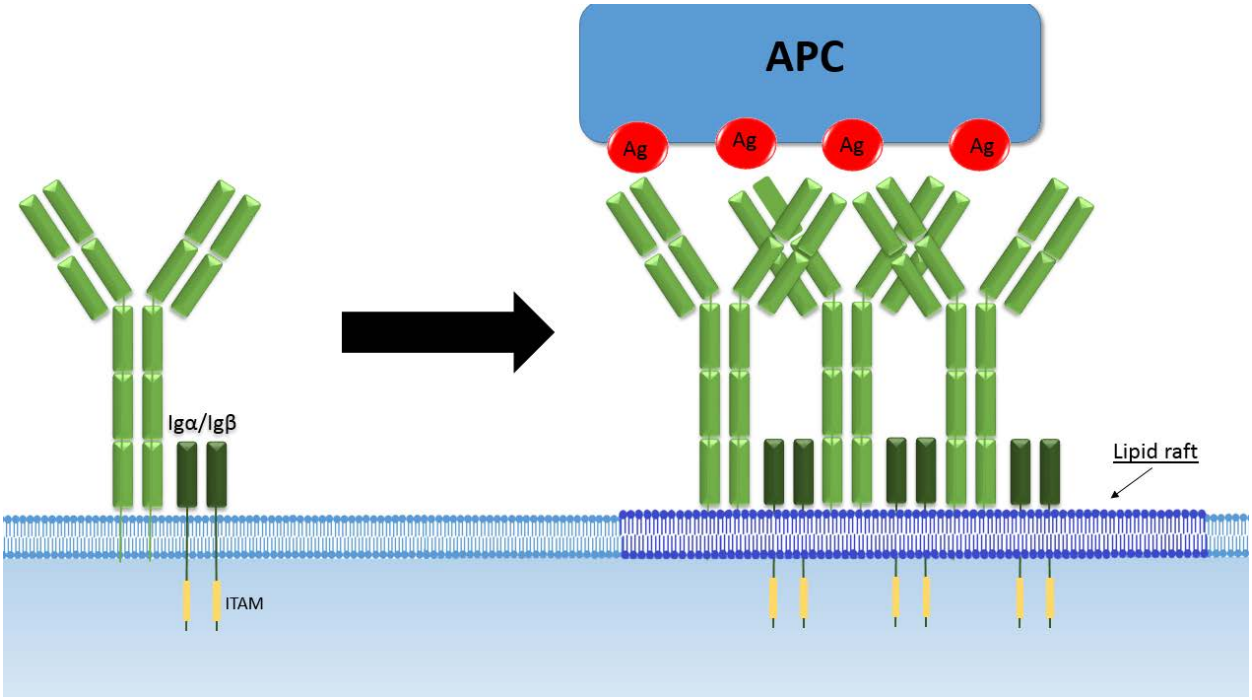

Figure 1.3: The BCR and BCR activation. The B Cell receptor is made up of a membrane-associated Ig (mIg), either IgM or IgD. The mIg is non-covalently associated with an Iga/Igb (Cd79a/b) heterodimer containing a cytoplasmic tail with an ITAM domain. The ITAm domain of the Iga/Igb is responsible for inducing intracellular signaling. Upon binding multivalent Ag, the BCR is induced to form BCR microclusters and localizes to a lipid raft membrane domain. Upon entering lipid rafts the BCR undergoes a conformational change that alters the structure of the Iga/Igb to an open position, exposing the ITAM domain. The lipid rafts domain is home to the signaling kinase Lyn. Which will induce phosphorylation of the ITAm domain and induce BCR signaling.

Figure 1.4:

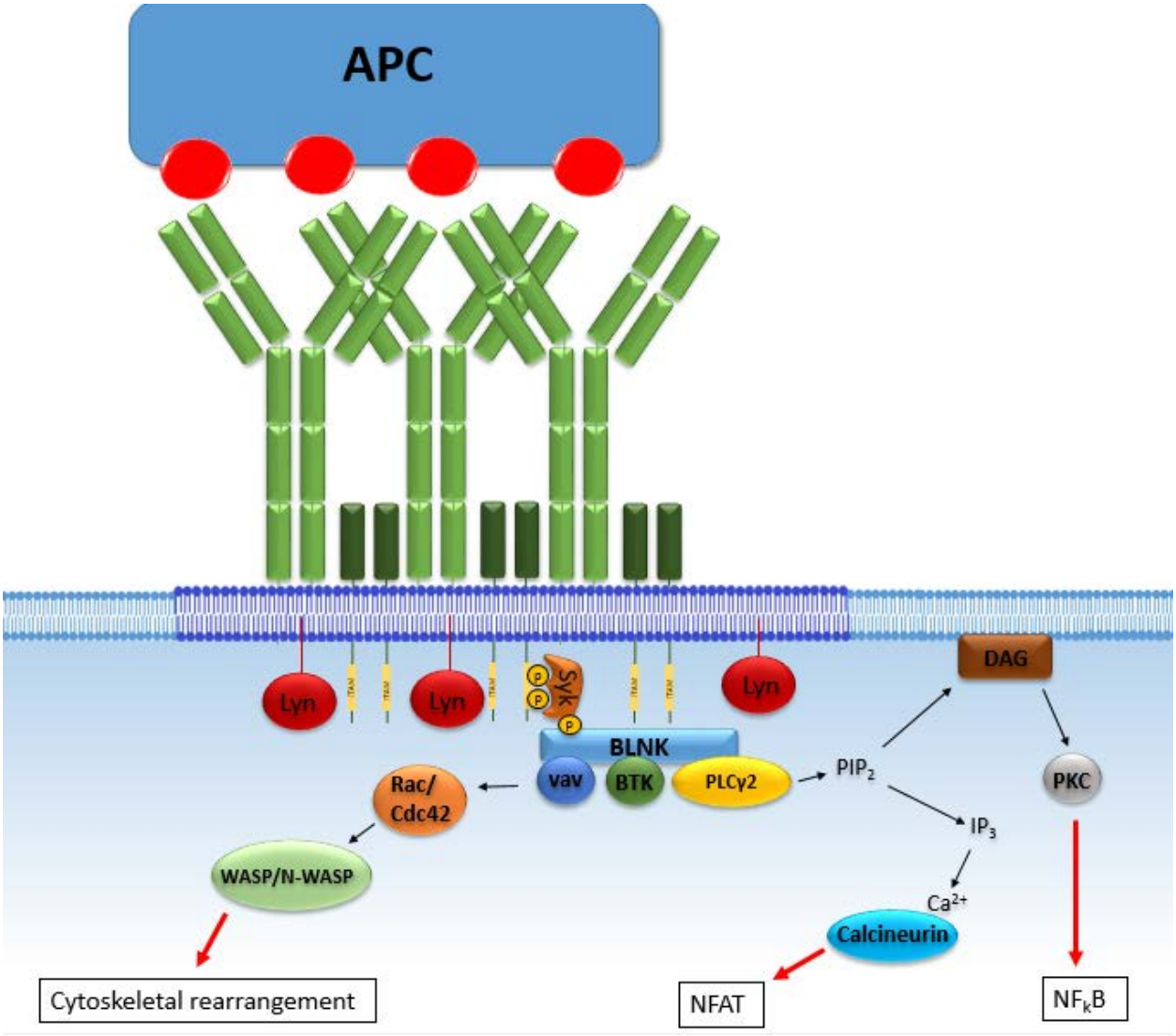
APC
Lyn
Lyn
Syk
Lyn
BLNK
vav
BTK
PLCγ2
Rac/
Cdc42
WASP/N-WASP
Cytoskeletal rearrangement
PIP2
DAG
PKC
IP3
Ca2+
Calcineurin
NFAT
NFkB

Figure 1.4: BCR signaling. BCR signaling is a complex process involving multiple signaling molecules that induce various cellular fates. This figure represents a largely simplified model of the early BCR signaling cascade. Upon localization of the BCR into lipid raft domains, the ITAM domain of the Iga/Igb is exposed and phosphorylated by lipid raft resident Lyn. Syk recognizes and binds to the phosphorylated ITAM and gets phosphorylated by Lyn. Phosphorylated syk then serves as a docking site for various B cell adaptor proteins, such as BLNK. BLNK recruits and provides a docking site for various other B cell signaling kinases, including BTK, PLCy2, and Vav. Vav activated the small GTPase Rac and Cdc42, which induce the rearrangement of the cytoskeleton by activating actin regulators WASP and N-WASP. BTK activates PLCγ2 which cleaves PIP_2 to generate IP_3 and DAG. DAG activates PKC and induces the downstream NF_kB signaling pathway. IP_3 induces the release of Ca^{2+} from calcium stores. Ca^{2+} will bind calcineurin and induce the NFAT signaling cascade. This BCR signaling will activate transcription factors that ultimately lead to B cell activation, proliferation, survival, and differentiation.

Proper regulation of B cell signaling in response to Ag is essential as dysregulation of BCR signaling can lead to various immune disorders. In addition to BCR signaling molecules, B cells express various co-stimulatory and co-inhibitory receptors. The co-stimulatory receptor CD19 works to lower the activation threshold of the BCR [62]. CD19 is associated with the complement receptor CD21, and the tetraspanin family protein CD81 on the B cell surface. Complement opsonized Ag brings the BCR and CD19 together, which prolongs BCR signaling by providing additional docking sites for BTK and PI3K[9,63]. CD19 deficiency leads to reductions in B cell activation and humoral immune responses in mice[64]. On the other hand, BCR activation is negatively regulated by inhibitory co-receptors and various phosphatases. The inhibitory co-receptor FcyRIIB inhibits B cell activation by decreasing BCR signaling[56,65]. Ab opsonized Ag co-ligates FcyRIIB with the BCR, which inhibits BCR clustering and BCR signalosome formation. The cytoplasmic domain of FcyRIIB contains an immunoreceptor tyrosine-based inhibitory motif (ITIM). Upon BCR-FcγRIIB coligation, the ITIM is phosphorylated by lipid raft resident kinase Lyn. Phosphorylated ITIM then provides a docking site for inhibitory phosphatases such as SH2-domain-containing inositol 5-phosphatase (SHIP-1) and SH2-domain containing protein tyrosine phosphatase (SHP1). SHP1 works to inhibit BCR signaling by dephosphorylating signaling molecules. SHIP1 inhibits PIP_3 and the activation of BTK, AKT, and PLCγ2 by removing their plasma membrane docking sites [56,65]. The negatively regulatory role of SHIP1 in BCR signaling is critical for maintaining autoreactive B cells in an anergic (non-responsive) state.

1.4.2 The impact of miss-regulation of BCR signaling

Understanding early B cell activation is critical, as dysregulation of B cell signaling can lead to a myriad of complications. Impaired BCR signaling activation leads to humoral immune deficiencies. For example, patients suffering X-linked agammaglobulinemia (XLA), have a point mutation in the Plenkstrin domain (PH) domain of BTKl, which prevents it from binding to

$PI(3,4,5)P_3$ on the plasma membrane and being activated, causing B cell development blockage and B cells and antibody deficiencies[15,66]. Another example is the common variable immune deficiency (CVID) due to mutations in the BCR co-stimulatory receptor CD19 or T-cell stimulatory molecules such as CD40L[15]. On the other hand, if B cell maturation or activation is not properly controlled, it could lead to autoimmune complications[15,67]. Overactive signaling, or a lack of negative signaling regulation can lead to the generation of auto-reactive B cells, as it promotes the survival of self-reactive clones that would otherwise be negatively selected for during the B cell maturation process. This in turn leads to the generation of antibody producing cells that produce self-reactive antibodies. Self-reactive antibodies have been observed in patients with numerous autoimmune disorders such as systemic lupus erythematosus (SLE), Type I diabetes, and rheumatoid arthritis[15,67]. Rheumatoid arthritis, for example, is caused by the production of antibodies against the joints. This can take place when B cell activation is not properly regulated, and B cells become activated in response to a weak BCR signal. Another example is Systemic Lupus Erythematosus (SLE)[67]. Among other causes, a patient can have a large amount of B cell activating factor (BAFF) expression, important for providing activation and proliferation signals to B cells[15]. This can increase the numbers of self-reactive B cells, increasing the production of self-antibodies. Another example of how miss regulation of B cell activation can lead to immune dysfunction is in the case of Wiskott-Aldrich syndrome[68]. This disease is caused by a mutation in the gene expressing the Wiskott Aldrich syndrome protein (WASP) and can lead to various immune deficiencies and autoimmune complications. WASP plays an important role in the regulation and organization of actin. Since Actin regulation is essential for proper B cell activation, patients suffering from Wiskott-Aldrich syndrome often display dysfunction of proper B cell responses. Additionally, if BCR signaling goes unchecked and is activated in the absence of antigenic challenge, it can induce the formation of B cell lymphomas by continuously producing a proliferation signal[15]. Miss regulation of B cell signaling can cause defects in various developmental stages of the B cell, leading to the generation of

various types of lymphomas. Fortunately, our understanding of the B cell signaling process has identified various successful treatment methods for B cell lymphomas[69]. For example, BTK inhibitors, such as ibrutinib are used as an effective source of treatment for B cell lymphomas, by inhibiting B cell signaling cascades and preventing continuous B cell proliferation[69]. However, not all B cell lymphomas are responsive to this kind of treatment. Thus, it is essential that B cell activation is regulated properly. And understanding the process of B cell activation is essentially important for the treatment of B cell related immune diseases as well as B cell lymphomas.

1.5 B cell antigen interaction and the cytoskeleton

Interactions between immune cells are an important part of the adaptive immune response[3]. In addition to soluble Ag, B cells encounter Ag presented by antigen presenting cells (APCs) in the secondary lymphoid tissues, such as follicular dendritic cells and macrophages. APCs present Ag on their surface through complement or Fc receptors[70,71]. Intravital imaging has shown that APCs can hold the Ag on their surface for several days for B cells to recognize[72]. Although B cells are capable of detecting soluble Ag, the majority of Ag encountered by B cells in vivo is Ag bound to the surface of APCs and pathogenic cells; therefore, the interaction between B cells and APCs and surface associated Ag plays an essential role in B cell activation[70,71,73,74]. The interaction of B cells with APCs induces the formation of a super signaling molecular complex at the interaction site often referred to as the immune synapse[75,76]. Although the immune synapse was first described in T cell interaction with antigen presenting cells, a similar interaction occurs during B cell interaction with antigen presenting surfaces. The immune synapse consists of a dynamic organized structure of signaling receptors, co-stimulatory molecules, and adherence molecules, and is responsible for regulating the interaction between two immune cells (described below). Although not required for B cell activation during interaction with APCS, surface adhesion molecules can help facilitate the formation of the

immune synapse and BCR clustering[77]. The B cell-APC interaction site serves as a site for B cell signaling organization, as well as a site for antigen extraction from the presenting surface.

1.5.1 BCR-Ag interaction

Upon encountering Ag presented on the surface of an APC, B cells first establish contact with the presenting surface. Ag engagement induces BCR aggregation into microclusters in lipid rafts. The BCR interaction with surface Ag induces conformational changes, exposing the ITAMs in the cytoplasmic domain of the BCR[51,52]. Early BCR signaling induces the growth of these BCR microclusters, amplifying BCR signaling and causing them to move centripetally into the center of the contact zone where they form a large central BCR cluster[56]. The formation of a large central cluster is a critical event for B cell activation as it downregulates BCR signaling and serves to facilitate antigen internalization into the B cell[56,78]. Inhibitory co-receptors, such as FcγRIIB, downregulate BCR signaling and inhibit the BCR clustering[65]. Furthermore, BCR clustering is enhanced in cells exposed to surface bound Ag compared to cells exposed to soluble Ag, giving a possible explanation for the enhanced activation of B cells in response to surface bound Ag[56,79].

1.5.2 B cell-APC interaction

The formation of a stable B cell-APC interaction site is essential for proper BCR signaling and antigen internalization. The interaction site not only stabilizes the interaction between the B cell and the APC, but also helps to regulate BCR signaling. The formation of an organized interaction site observed during B cell interaction with an antigen presenting surface appears reminiscent of the immune synapse described in T cells[80,81]. The immune synapse is described to include various organized regions with individual functions, together referred to as a supramolecular activation complex (SMAC). This organized structure consists of 3 main regions, the central SMAC (cSMAC), peripheral SMAC (pSMAC) and distal SMAC (dSMAC)[77,82,83]. The cSMAC refers to the center of the organized immune synapse, this region is densely populated by

signaling receptors and co-signaling molecules and is generally devoid of actin cytoskeleton. The pSMAC surrounds the cSMAC and is occupied by adhesion molecules that stabilize the cellular interaction such as LFA-1. Unlike T cells, B cells do not require the presence of adhesion molecules to generate a stable immune complex; however, the presence of adhesion molecules does stabilize the interaction site and improves B cell signaling at lower antigen density[77]. Finally, the dSMAC, surrounding the pSMAC is an area of filamentous actin at the edge of the contact zone, this actin uses retrograde flow to shuttle receptor clusters to the center of the contact zone, into the cSMAC[77,82,83]. The formation of such an organized structure thus helps facilitate the central movement of BCR-Ag clusters to generate a large central BCR cluster that allows for effective Ag extraction into the B cell[44,84]. B cell interaction with antigen presenting surfaces further facilitates the re-organization of the functional components of the entire B cell. It was shown that B cells polarize to the Ag contact zone, recruiting functional cellular components, including signaling molecules, endocytic machinery, and lysosome vesicles, to the site of Ag interaction[61,77,85,86]. The centrosome plays an important role in determining cell polarity, as it controls spindle pole formation and the organization of membrane organelles[87]. In response to Ag engagement, the centrosome, or microtubule organization center (MTOC), is recruited to the Ag interaction site[88–90]. Repositioning of the centrosome to the Ag interaction site is mediated by the microtubule-associated motor protein dynein and by the small GTPase Cdc42, which activates polarity proteins such as Par3 and PKC[61,90]. Polarization towards the Ag interaction site is crucial for Ag extraction and presentation, as polarization recruits essential machinery responsible for antigen extraction and processing[77,85,86]. Importantly, cell polarization localizes lysosomal vesicles to the antigen interaction site, which facilitates processing of the antigen before loading on the MHCII. Furthermore, lysosomal exocytosis has been proposed to play a role in antigen extraction from the presenting surface[89]. The importance of cell polarity is supported by the finding that a lack of proteins important for cellular polarization in B cells significantly inhibits

the cells' ability to internalize and process Ag for presentation on the MHCII, a process essential for further B cell activation[89,91].

1.5.3 Cytoskeleton organization at the immune synapse

The B cell cytoskeleton plays an essential role in BCR clustering and the formation of a stable immune synapse (Figure 1.5). BCR signaling induces the reorganization of the cytoskeleton through various signaling cascades. Early BCR signaling will cause the rapid breakdown of cortical actin. Cortical actin is the actin network associated with the inner leaflet of the plasma membrane, where actin is linked to the plasma membrane by ERM proteins, including Ezrin, Radixin, and meosin. Cortical actin creates barriers along the plane of the plasma membrane to limit free lateral diffusion of plasma membrane associated protein, including BCR and BCR-associated co-receptors[92,93]. Early BCR signaling induces activation of Rab-GTPase, which causes dephosphorization of ERM protein, releasing the connection between the actin and the plasma membrane. Rab-GTPase additionally activates cofilin, further inducing actin de-polimerization[94,95].The degradation of the cortical actin at the interaction site allows for free diffusion and increased mobility of BCRs inducing the generation of larger microclusters, increasing the size of BCR signalosomes, and increasing overall BCR signaling. The breakdown of the cortical actin structure is essential for B cell activation, as studies show that treatment with the actin stabilizing drug, Jasplakinolide, inhibits the formation of a stable BCR cluster[79]. Furthermore, treatment of B cells with Latrunculin A, a drug that induces actin de-polymerization, shows that B cells will induce a BCR signal in the absence of Ag challenge by inducing spontaneous BCR cluster formation[79]. The increased BCR signaling caused by microcluster formation induces rapid re-organization of the actin cytoskeleton. It has been shown that the activity of actin regulatory molecules and actin nucleating molecules can affect the mobility of the BCR and thus impact B cell activation[96,97]. The BCR signaling molecule BTK is known to activate WASP and Neuronal-WASP (N-WASP) which induce the nucleation of new

actin filaments through the activation of the ARP2/3 complex[60]. WASP is expressed exclusively in immune cells, while N-WASP is expressed in all cell types[98,99]. The WASP/N-WASP mediated re-organization of the actin structure is of critical importance, as cells exhibiting BTK dysfunction are unable to form stable contact with presenting surfaces[100]. During cell spreading, BTK recruits WASP family actin regulators through phosphorylation of signaling molecules such as Vav and PIP5K, which generate PIP_2 and recruit WASP and N-WASP. WASP family proteins then activate the actin nucleating factor APR2/3 to induce B cell spreading on the presenting surface by generating branched actin structures[101]. Actin is recruited to the leading edge of the B cell, inducing the formation of filopodia and lamellopodia that causes the B cell to spread on the presenting surface and increase the contact area between the B cell and the Ag presenting surface[44,56,102]. As The B cell spreads on the presenting surface more Ag is engaged and new BCR microclusters form at the edge of the contact area. The increase in total BCR signaling causes the BCR clusters to be recruited into one large BCR cluster, located at the center of the contact zone, called a central cluster[56,79]. During this process, the cell continues to spread, as actin filaments accumulate at the outer edge of the cell, while BCR-Ag complexes are shuttled into a central cluster devoid of actin. As B cell spreading on the antigen presenting surface facilitates the recruitment of BCR clusters into a central cluster, it is clear that B cell spreading is critical for proper B cell activation. This is further supported by research showing that cells which are unable to spread show a reduced B cell activation response and can cause immune deficiencies[103]. Generation of a central BCR cluster will reduce BCR signaling, as BCR present in the central cluster is shown to have reduced signaling[56]. This reduced BCR signaling ultimately causes the B cell to contract and reduce its contact area with the presenting surface[56]. B cell contraction is mediated by inhibitory signaling molecules such as SHIP, which downregulate BCR signaling. Additionally, B cell contraction is facilitated by the N-WASP mediated reorganization of the actin cytoskeleton around the central cluster, by non-muscle myosin IIA (NMIIA) generated forces[104], and by microtubule-associated motor protein dynein[78,105]. Although both WASP and N-

WASP play a critical role during B cell spreading and early signaling, only N-WASP seems to play an essential role in B cell contraction and signaling attenuation[56]. Post-contraction, the BCR molecules recruited into the central cluster show a reduction in BCR signaling. It has been shown that B cell contraction and BCR accumulation into a central cluster are important to attenuate BCR signaling and to prevent B cells from being over-stimulated, as inhibition of contraction causes excessive BCR signaling, which can induce autoimmune conditions[78]. This is further confirmed by an increase in autoantibody production in the absence of SHIP or N-WASP[78,106]. Additionally, upon formation of an organized interaction site, and a central BCR cluster, B cells can further reduce BCR signaling through BCR endocytosis

Figure 1.5:

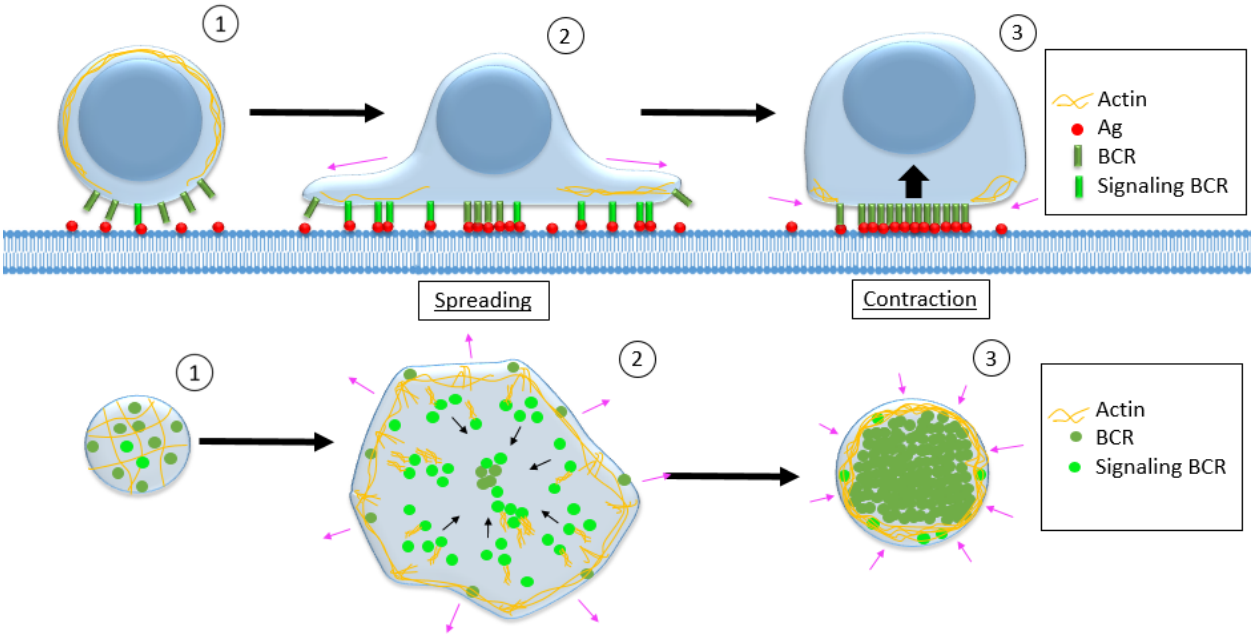

Figure 1.5: Formation of the immune synapse. Upon engaging surface-bound Ag, the B cell will spread and contract on the presenting surface to create a stable immune synapse. (1) Upon recognition of Ag by the BCR, the formation of BCR microclusters will induce BCR signaling and will cause the breakdown of cortical actin. The breakdown of cortical actin, together with the regionalization of actin induced by BCR signaling, allows the B cell to spread on the presenting surface and engage more Ag. (2) Increased engagement of Ag and increased BCR signaling will induce the BCR microclusters to be moved to the center of the cell where they form a larger central BCR cluster. BCR in the central cluster loses BCR signaling ability, reducing BCR signaling. (3) Reduced BCR signaling will again induce the rearrangement of the actin cytoskeleton and induce contraction of the cell, collecting the Ag-engaged BCR into a large central cluster.

It is clear that both actin remodeling and myosin play a critical role in the generation of a central BCR cluster at the immune synapse[79,95,101]. This was supported by a study showing inhibition of actin polarization using low concentrations of Latrunculin A inhibits the formation of BCR clusters[97]. It was furthermore shown that inhibition of actin nucleators, such as Arp2/3 and WASP family proteins reduces BCR diffusivity[107]. Currently, the exact mechanisms by which actin dynamics regulate BCR movement at the immune synapse are not fully understood. However, recent research found evidence of the formation of actin arcs associated with myosin IIA[101], bearing a resemblance to actomyosin arcs observed to facilitate the centralizing movement of signaling molecules in T cells[108]. Actin is observed to form a ring-like structure around the central BCR cluster and myosin seems to be recruited to the interaction site and associated with actin filaments[56,100,109]. It has been proposed that B cells use a similar mechanism as T cells use to form a central TCR cluster, where they use myosin-associated actin arcs to move BCR-Ag clusters towards the center of the contact area[56,109]. Additionally, myosin was shown to play a central role in BCR signaling downregulation and B cell contraction, as NMIIA deficient B cells show an increase in autoantibody generation[104,110]. These findings suggest that actin, as well as myosin, plays a role in the formation of a central BCR cluster prior to antigen endocytosis. It is clear that spreading and contraction increases the ability of B cells to internalize antigen. However, the direct impact of spreading and contraction on antigen internalization remains unknown.

1.6 Ag uptake, processing, and presentation

In order for B cells to become activated and differentiate into high-affinity Ab producing cells or memory B cells, they require two activation signals: an initial BCR signal upon engaging Ag and an additional signal from T helper cells. To acquire a T cell signal, B cells capture, internalize, process, and present Ag as complexes with MHCII for T cell recognition. Therefore,

Ag endocytosis is a critical step to generate the second signal, as it determines the level of Ag presentation and T cell activation. The more Ag B cells internalize the stronger the T cell activation signal will be generated. Ag endocytosis is regulated by both external and internal conditions of the B cell as well as the properties of the Ag such as antigen affinity, antigen density, and the stiffness of the presenting surface; these properties determine the efficiency of Ag endocytosis.

1.6.1 BCR-Antigen endocytosis

A major mechanism by which the BCR internalizes Ag is through clathrin-mediated endocytosis[85,111] (Figure 1.6). Engagement of Ag by BCR induces the recruitment of endocytic machinery, including clathrin, adaptor protein 2 (AP2), and dynamin. The lipid raft localization of BCR-Ag complexes facilitates the recruitment of endocytic machinery[17]. Clathrin-mediated endocytosis is dependent on conserved tyrosine based endocytosis motifs present on the cytoplasmic tails of receptors. Endocytic adaptor proteins are recruited to the membrane by interacting with phosphatidyl inositol polyphosphate lipids and recruit adaptor proteins such as AP2 which in turn recruits clathrin to the plasma membrane[112]. Clathrin and its associated proteins will generate inwards curvature of the membrane, forming clathrin-coated pits. To complete the endocytic process, these clathrin-coated pits require membrane scission [112]. This process is mediated by the GTP binding protein dynamin as well as the actin cytoskeleton[112]. Actin binding protein 1 (Abp1) interacts with both dynamin and actin filaments, recruiting F-actin to the site of vesicle scission[113]. Actin accumulation around the neck of clathrin-coated pits will then further pull the invagination into the cytoplasm. Dynamin associates with the neck of the clathrin-coated pit and constricts the neck to pinch off the vesicle from the plasma membrane. In the case of surface associated antigen, NMII is required for endocytosis[85]. Actomyosin generates the pulling force allowing dynamin to pinch off the vesicle (figure 1.6). Although clathrin-mediated endocytosis seems to be the main mode of Ag endocytosis, it was shown that inhibition

of clathrin expression only partially reduced antigen endocytosis[114]. Furthermore, various research has shown the ability of B cells to internalize antigen through clathrin-independent modes of Ag endocytosis[114–116]. Once the B cell successfully internalized Ag, the Ag is processed and presented to T cells for further activation.

Figure 1.6:

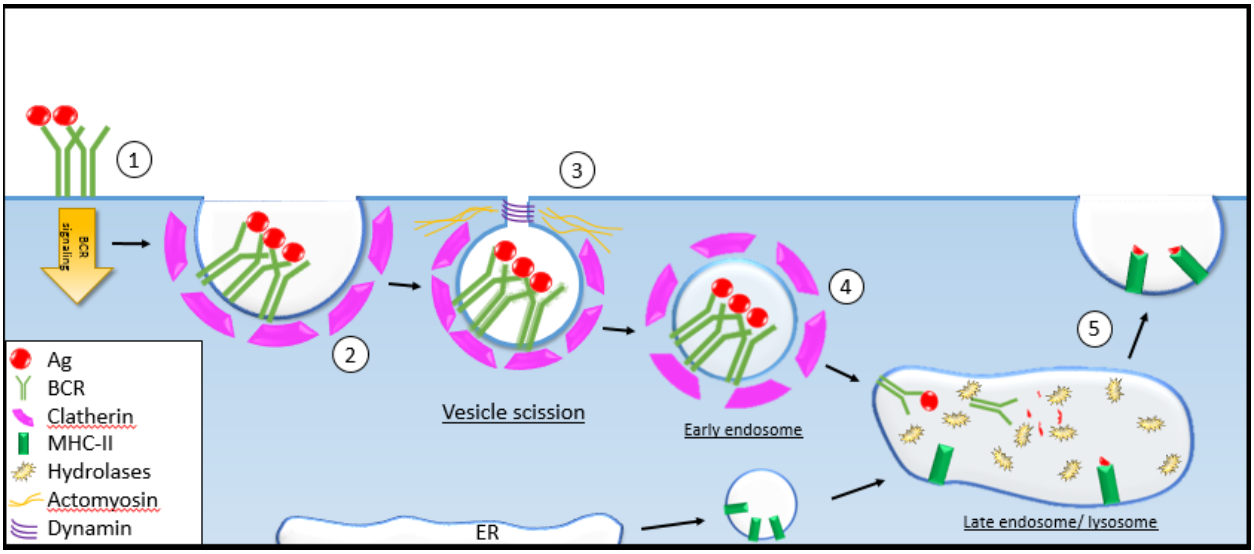

Figure 1.6: Ag endocytosis, processing, and presentation on the MHC-II. Upon Ag engagement, the BCR-Ag complex will be internalized, processed, and presented on the MHC-II for T cell recognition. (1) Ag engagement by the BCR induces BCR signaling, which provides the B cell with a survival signal and also induces the recruitment of endocytic machinery to the Ag interaction site. (2) The BCR-Ag complex is pulled into the cell by cytoskeletal forces, generating a clathrin-coated pit containing the BRC-Ag complex. (3) The vesicle is pulled further into the B cell, assisted by actomyosin structures generated around the neck of the vesicle. The scission protein dynamin locates around the neck of the vesicle and facilitates the scission of the vesicle from the membrane. (4) The early endosome, containing the BCR-Ag complex will then merge with a late endosome/lysosome compartment rich in MHC-II. Here the Ag is degraded, and Ag fragments are loaded onto the MHC-II. (5) Ag-loaded MHC-II is then shuttled to the cell surface where it is exposed for T cell recognition.

The binding avidity of Ag to the BCR directly impacts Ag endocytosis of surface associated antigen, as B cells internalize high affinity or highly dense Ag with higher efficiency than low affinity or low-density Ag, priming a stronger T cell signal[32,43,117]. This provides the B cell with a mode of Ag affinity discrimination. When Ag is limited, high avidity Ag is more competitive to bind to the BCR than low avidity Ag. It was shown that Hen Egg Lysozyme (HEL) as high-affinity Ag induces higher levels of BCR signaling and Ag endocytosis in MD4 B cells from mice with Ig transgenes, compared to MD4 B cells exposed to a low affinity mutated HEL Ag[44,45,118,119]. Similarly, B cells exposed to highly dense surface associated Ag show increases in both BCR signaling and Ag endocytosis, compared to the same Ag with low density[46,47]. This effect is due to the stronger ability of high valent Ag to induce BCR crosslinking than low valent Ag, consequently enhancing the formation of BCR clusters[17,18]. Because Ag valency affects Ag endocytosis, the mode of Ag presentation is said to play an essential role in the efficiency of Ag endocytosis[120]. Soluble Ag is rapidly internalized through caveolin-dependent endocytosis. However, *in Vivo* the majority of Ag encountered by B cells is bound to the surface of antigen presenting cells, bound to their Fc receptors or MHCII. The physical properties of the Ag presenting surface play an essential role in facilitating Ag endocytosis. To capture Ag from presenting surfaces, the B cell will form an organized interaction site with the presenting cell. B cells in various developmental and activation states utilize different methods to extract Ag from presenting surfaces. For example, naïve B cells are shown to internalize Ag after gathering the Ag into a central cluster of the contact zone; however, GC B cells are shown to create small clusters scattered throughout the contact zone to internalize ag[76,121]. This difference in the mode of Ag endocytosis may play an important role in affinity discrimination, allowing GC B cells to select high-affinity BCR-Ag interactions, and allowing naïve B cells to use load sharing of large clusters to capture low-affinity B cells to become activated in response to lower affinity Ag[121]. Moreover, the stiffness of an antigen presenting surface can also determine the ease by which Ag is extracted from the presenting surface. Strong attachment of Ag to a stable surface

makes it more difficult for B cells to extract Ag from the APC, whereas weak attachment to a malleable surface makes it easier for the B cell to extract the Ag. For example, FDCs, found in germinal center reactions, were found to have higher membrane stiffness compared to dendritic cells (DCs). This higher stiffness allows B cells to be able to better discriminate for the affinity of Ag, as a stiffer membrane is more resistant to B cell pulling forces[120]. Providing an additional method by which GC B cells can more efficiently discriminate between low and high-affinity Ag.

1.6.2 BCR-Ag endocytosis from presenting surface

The majority of Ag encountered by B cells *in vivo* is Ag bound to the surface of APCs. It is thus critical to understand how B cells interact with antigen presented on a surface and to understand how this antigen is extracted from the surface for B cell endocytosis. Previous research had identified two mechanisms by which B cells extract Ag from presenting surfaces. First, B cells utilize NMII-generated contractile forces to pull Ag from presenting surfaces [85,121]. Non-muscle myosin II exerts forces at BCR Ag engaging sites, pulling Ag in membrane invaginations into the B cell [85]. This pulling action also assists in affinity discrimination, as low-affinity BCR-Ag interactions will be disrupted by this pulling force, aborting antigen endocytosis. However, Ag internalization is only possible when BCR-Ag affinity is strong enough to withstand the pulling action[122]. Furthermore, when Ag is associated with a soft surface, B cells can internalize Ag with fragments of the presenting surface[120]. However, if the Ag is strongly associated with a stiff presenting surface, B cells may not be able to apply enough force to extract the Ag from the presenting surface[120,123–125]. In this case, B cells utilize proteases released from lysosomes to cleave the Ag from its presenting surface facilitating antigen internalization[89,120]. However, it is unknown what induces the lysosome release of hydrolases into the extracellular space. Accumulated studies have shown that the strength by which the Ag is tethered to presenting surfaces and the stiffness of Ag presenting surfaces can influence the effectiveness of B cell Ag extraction, and consequently B cell Ag presentation, activation, and differentiation. The

two proposed methods of Ag extraction provide methods for B cells to differentiate various types of Ag and discriminate between high and low-affinity Ag. As low-affinity BCR-Ag interactions will be disrupted by the pulling force, and high-affinity Ag interactions will induce the release of hydrolases to facilitate efficient Ag endocytosis. However, it remains unclear what induces the switch between the two mechanisms during antigen extraction.

1.6.3 Antigen processing and presentation

Upon Antigen endocytosis, B cells process the internalized antigen and present it on the MHCII molecule where the antigen fragment can be recognized by $CD4^+$ T cells. The internalization of the BCR-Antigen complex both initiates antigen processing and presentation on the MHCII and serves as a mechanism for down regulating BCR signaling. Upon internalization, vesicles containing the BCR-Antigen complexes are trafficked into endocytic compartments facilitated by continued BCR signaling and cytoskeletal dynamics[111,126]. Vesicle trafficking is mediated by the ubiquitination of Syk protein associated with the BCR. It has been shown that mice lacking the E3 ubiquitin ligase Cb1 accumulate BCR-antigen vesicles at the Ag interaction site, highlighting the importance of BCR signaling and ubiquitination for effective trafficking of the BCR-Ag complex[127]. Following ubiquitination, the BCR-antigen vesicles are trafficked to the endosome compartments where the antigen will be degraded by various proteases. Simultaneously, MHCII molecules are shuttled from the ER and Golgi, to form a large late endosome compartment, called Class-II containing multivesicular bodies (MIIC). BCR-Ag complex trafficking to the late endosome MIIC is mediated by the ubiquitination of the BCR Ig Heavy chain[126]. In these vesicles, MHCII combine with the processed antigen and is loaded with antigen fragments. To prevent MHCII loading with endogenous protein, the MHCII associates with a type II transmembrane protein called Ii. Upon entering the late endosome, Ii is removed with the help of the chaperone protein H2-DM and the cysteine protease cathepsin (CatS), allowing the processed antigen fragments to be loaded onto the MHCII molecule. Antigen loaded

MHCII molecules are then shuttled to the plasma membrane, where the MHCII-Antigen complex is exposed and can be recognized by the T-cell receptor (TCR) of T cells[128]. Proper antigen processing and presentation of antigen fragments on the MHCII is essential as cells lacking this ability are unable to receive T cell help and produce a proper humoral immune response.

A complete understanding of the process of Ag endocytosis and processing, and how it is affected by the mode of Ag presentation, provides opportunities for the intelligent design of vaccines. As B cells response varies based on the affinity, valency, and the mode of Ag presentation, these properties could be manipulated by utilizing complex biomaterials to produce stronger Ab responses. Furthermore, the ability of B cells to discriminate high and low-affinity Ag depends strongly on the Ag presenting surface, this provides us with potential mechanisms to enhance the generation of a high-affinity Ab response to vaccines.

1.7 B-T cell interaction

B cells require a second activation signal from CD4+ T helper cells to differentiate into high-affinity Ab producing or memory B cells. Once B cells engage protein Ag in B cell follicles in the secondary lymphoid tissue, BCR signaling will prime the B cell to internalize the Ag and present Ag fragments on their MHCII for T cell recognition. Antigen driven activation of the B cell will induce the upregulation of chemoattractant receptors CCR7 and EB2I and costimulatory molecules for B-T cell interaction, which will facilitate the recruitment of activated B cells to the T cell zone of B follicles[25,35,129]. Like B cells, naïve T cells can also be activated by Ag presented by FDC and other APCs and move to the T cell zone of B cell follicles[25]. BCR and TCR signaling induce the expression of surface molecules important for effective B-T cell interaction[8]. At the interface of the B cell and the T cell zone, activated B cells will engage CD4+ Tfh cells[35]. The interaction between B and T cells can last for 45 minutes or longer and induces the activation and

proliferation of both T and B cells[31]. B-T cell interactions play an important role in affinity maturation during the germinal center reaction. After exposure to antigen on the surface of APCs, B cells process and present the antigen on their MHCII for recognition by T_{fh} cells. The nature of this interaction determines the fate of the B cells. B cells which are able to internalize high amounts of antigen will be more likely to form stable immune synapses with T cells and induce proper T cell activation. This in turn will allow the B cell to receive a strong T cell signal and differentiate into high-affinity antibody producing cells or memory B cells.

Similar to B cell-APC interaction, B and T cells form an organized interaction site during recognition of the MHCII-Ag complex by the TCR [130–132] (Figure 1.7). The T Cell-APC synapse is highly organized containing a cSMAC, pSMAC, and dSMAC region of organized signaling molecules, adhesion molecules, and organized cytoskeletal structure, respectively. Rearrangement of the cytoskeleton is also essential in the formation of a stable T cell synapse as it facilitates recruitment of the TCR into a central cluster (not unlike the formation of a central BCR cluster)[132]. Regulation of T cell synapse formation is essential for proper activation of the T cell, and unlike B cell-APC interactions it does require co-stimulatory and adhesion molecules. The B-T interaction is regulated by various surface molecules on both the B and T cell[8,25,133]. At the center of this interaction lies the interaction of the TCR with the MHC-Ag complex. Similar to the BCR, the TCR has a variable region that is generated through V(D)J gene rearrangement, producing a large population of TCRs with unique specificities [134]. The TCR is associated with the CD3 signaling complex that transduces an intracellular signal through their ITAM domain[135]. The TCR is expressed on mature T cell surface with either a CD4 or CD8 co-receptor. CD8-associated TCR interacts exclusively with MHCI while CD4-associated TCR interacts exclusively with MHCII[134]. The CD4-TCR will specifically recognize Ag on the MHCII of APCs and will induce T cell activation through intracellular signaling cascades. Like the BCR, the TCR only responds to high-affinity interactions, and it is known that the TCR exerts force on the Ag to

gauge the binding affinity of the ag and release low-affinity Ag[136]. Similar to the BCR, the TCR localizes to lipid rafts where its intracellular ζ-domain and CD3 co-stimulatory ITAM sites are phosphorylated, and TCR signaling is transduced through ZAP-70 signaling molecules to induce various downstream effects[137]. The amount of MHC expressed on the presenting surface plays an important role in determining the efficiency of the T cell activation[138]. Besides the TCR-MHC binding, the B-T cell interaction is regulated by a variety of other costimulatory and adhesion molecules. The integrin LFA-1 on T cells will bind ICAM1 and ICAM 2 on B cells and facilitate T cell activation by stabilizing the interaction between the 2 cells[25,138]. Additionally, various co-stimulatory molecules are involved in B-T cell interaction. Thus, like B cell activation, the activation of T cells is also tightly regulated by various stimulatory and inhibitory mechanisms.

Figure 1.7:

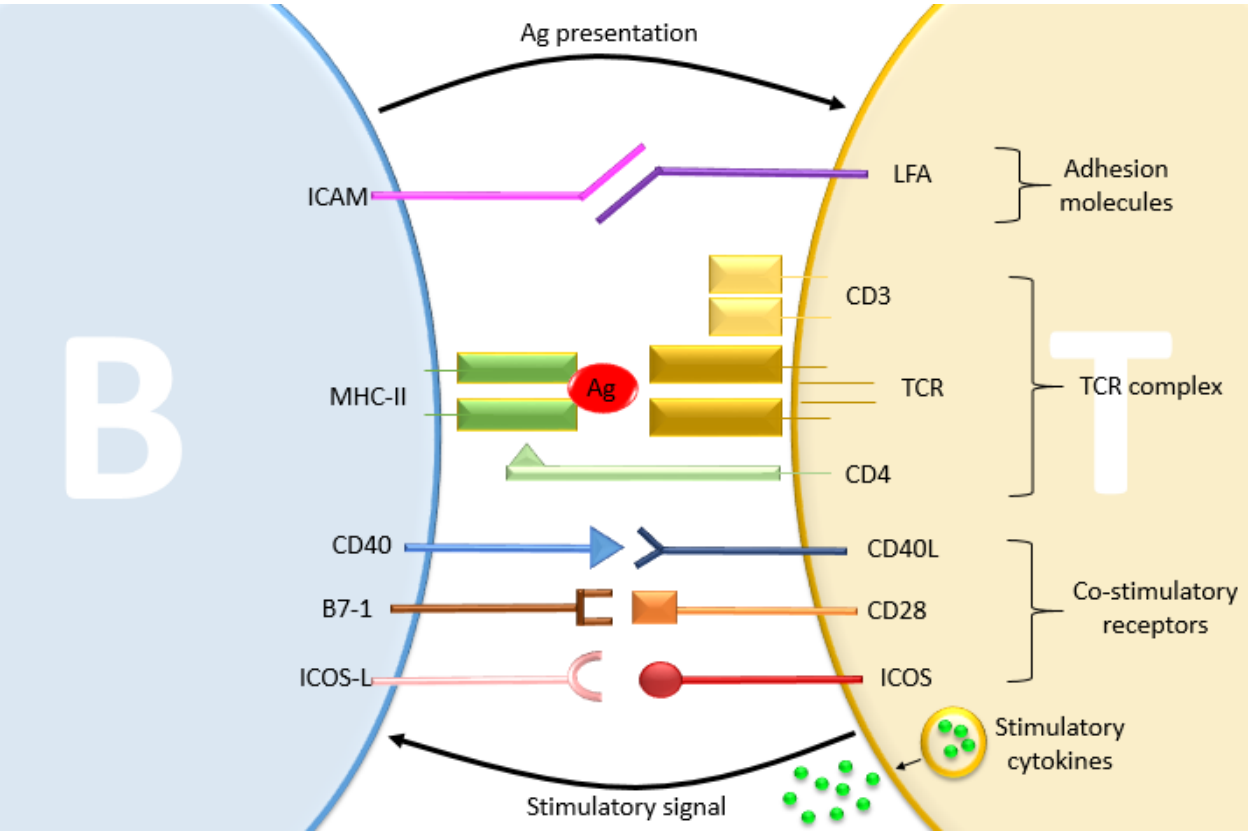

Figure 1.7: B-T cell interaction. B cell- T cell interaction relies on a variety of signaling, co-stimulatory, and adhesion molecules. B cells present Ag to T cells in order to receive a stimulatory signal, allowing them to further develop. B cells present Ag on their MHC-II, which is recognized by the TCR-CD3 complex, together with the CD4. This induces TCR signaling and induces the T cell to produce stimulatory cytokines to induce further B cell activation. This interaction is dependent on sufficient TCR-Ag affinity and various co-stimulatory and adhesion molecules. CD40, B7-1, and ICOS-L on the B cell surface bind to CD40L, CD28, and ICOS on the T cell surface, respectively. These receptors provide co-stimulatory signals. ICAM, on the B cell surface, and LFA, on the T cell surface, are adhesion molecules that play an important role in stabilizing the B-T cell interaction. Upon activation induced by TCR signaling, the T cell will release stimulatory cytokines that bind to receptors on the B cell and further induce B cell activation.

T cells activated by B cells provide B cells with activation signals through costimulatory molecule interaction and secreting cytokines, which drive B cell proliferation and differentiation to Ab producing plasma cells or memory B cells. Proliferating B cells form germinal centers (GC). In GC, B cell undergoes somatic hypermutation and affinity maturation, which rely on further T cell help. Follicular helper T cells (T_{fh}) are a specialized subset of T_h cells that are located in the light zoon of GCs[25]. T_{fh} cells express a high level of CXCR5, which guide T_{fh} towards GCs where the CXCR5 ligand CXCL13 is expressed by follicular dendritic cells[35]. Here the Tfh cells will provide additional activation signals to GC B cells, inducing only high-affinity B cells to differentiate further. Upon activation, T cells will release cytokines, such as IL-2, IL-4, IL-5, and IL-21, which support B cell activation[8,35] through cytokine receptors on B cells. T_{fh} secreted IL-4 and IL-21 induce B cell class switching and differentiate into long-lived plasma cells or memory B cells[41].

1.8 Membrane wounding/repair

Plasma membrane wounding

Membrane disruptions occur regularly in most cell types and can occur by a number of mechanisms (McNeil 1997). Disruption of the Plasma membrane can be caused by mechanical stress, pore forming toxins, or cellular interactions, and the nature of these disruptions varies depending on the cause and mechanism of the disruption. Mechanical disruptions have been observed to occur *in Vivo* in a wide variety of cell types[139,140]. Many cells experience mechanical forces such as tensile, compressive, and shear stresses. These mechanical stresses can lead to physical disruptions of the plasma membrane by creating tears in the membrane[139,140]. For example, muscle and epithelial cells often get wounded through mechanical stress caused by muscle contraction, or through cuts or punctures of the epithelial surface[140,141]. Another way the plasma membrane can get disrupted is through the action of pore forming proteins. Pore forming

proteins can originate from a variety of sources, such as toxins released by pathogens, pore forming proteins produced by host cells, and complement proteins[142–145]. Pore forming proteins differ in the mechanism by which they attack the membrane, and generate membrane pores of various sizes[144,145]. Pathogens can release pore forming toxins in order to perforate host cell plasma membranes[142]. For example, Streptolysin O (SLO), a toxin released by Group A streptococcus, forms a transmembrane pore that can induce cytolysis[142]. In addition to pore forming toxins released by pathogens, pore forming proteins produced by host cells can also cause disruptions of plasma membranes[144]. For example, complement protein and cytolytic T cells of the host immune system developed to kill pathogens and pathogenic cells by creating pores in their membranes. However, off-target effects of these mechanisms can cause disruptions of healthy host cells[144]. Finally, the plasma membrane can be wounded by cell-cell interactions, as cellular interactions often generate mechanical forces at interaction sites. Plasma membrane wounding has been observed to occur during interactions between immune cells[123–125]. For example, B and T cells have been observed ripping the membrane of APCs during extraction of Ag, and both B and T cells have been observed internalizing small membrane fragments of the APC surface[120,124]. As membrane wounding is a regularly occurring event, cells have developed various mechanisms to repair disrupted plasma membranes and prevent cell death. To study cell wounding, plasma membrane disruptions can be detected using membrane impermeable dyes that can only enter and incorporate into the cell upon plasma membrane disruption, such as dextran and propidium iodide (PI)[146,147].

1.8.1 Plasma membrane repair

Plasma membrane disruption is detrimental to cells, causing cytolysis. Disruption of the plasma membrane causes a rapid influx of extracellular Ca^{2+}, as Ca^{2+} in the cytoplasm is at nanomolar levels and extracellular Ca^{2+} is present at the micromolar range[148]. In order to prevent cell death caused by membrane disruptions, cells have developed mechanisms to rapidly repair their plasma membrane, generally repairing their membrane within several seconds to a minute of

membrane disruprions[149]. It has been shown that membrane disruptions and subsequent calcium influx induce rapid movement of intracellular vesicles to the site of membrane disruption to patch the membrane wound[150–153]. The role of calcium in membrane wound repair was further solidified by research showing that cells are unable to repair their disrupted plasma membrane in the absence of calcium[154]. The intracellular vesicle patch was one of the earliest proposed models for membrane repair. This model hypothesizes that cells prevent membrane leakage by crowding the wounded area with intracellular vesicles, followed by vesicle fusion to the plasma membrane. Alternative models of membrane repair involve membrane repair through loosening the membrane tension. The influx of extracellular Ca^{2+} triggers the rearrangement of cortical actin, inducing the formation of membrane blebs and loosening membrane tension, allowing the membrane room to repair its disruptions[155,156]. Alternative models of membrane repair involve fusion of intracellular vesicles, namely lysosomes, with the plasma membrane to loosen membrane tension and provide additional membrane surface to facilitate membrane repair[157,148,149]. This is supported by the finding that lysosomal exocytosis can be induced by an increase in Ca^{2+} in the cytosol[158]. The importance of lysosomal exocytosis during membrane repair was further supported by an increase in the presence of lysosomal-associated membrane protein 1 (LAMP1) on the surface of cells post membrane disruption[159–161]. Additionally, an increase of extracellular b-Hexosaminidase, a lysosomal enzyme, was detected upon disruption of the cell membrane[154]. Finally, inhibition of lysosomal exocytosis with the inhibitor Bromoenol Lactone (BEL) was shown to disrupt membrane repair[154]. Together this research suggests a critical role for lysosome exocytosis in membrane repair. Although loosening membrane tension will provide flexibility to the membrane, the exact mechanism by which cells reseal their disrupted membrane is not fully understood.

1.8.2 Endocytosis dependent repair

More recently, an alternative model of membrane repair has been proposed where cells actively remove disrupted portions of the plasma membrane through shedding or endocytosing patches of disrupted membrane rather than repairing the disrupted membrane directly[148,149] (Figure 1.8). These methods of membrane repair provide a more plausible mode for the repair of membranes disrupted by pore forming protein complexes. After disruption of the plasma membrane, rapid exocytosis was observed at the wounding site. in addition, accumulation of endocytic vesicles was observed at the site of wounding[146,156]. It has been proposed that cells utilize vesicle shedding or endocytosis methods to either shed vesicles containing the membrane pore, or endocytose the pore containing vesicle to destroy the pore forming protein in degradation compartments[155,162,163]. Cells have been observed to form blebs of disrupted portions of the membrane and proceed to shed these blebs to retain membrane integrity[163]. Fusion of intracellular vesicles with the plasma membrane is dependent on actin cytoskeleton dynamics and a variety of fusion proteins. Vesicles are targeted to the membrane SNARE complex, a protein complex that facilitates vesicle docking to the plasma membrane. The v-SNARE protein Vamp-7 was observed in B cells to be recruited to facilitate lysosomal exocytosis[164]. Synaptotagmin (Syt) is a transmembrane protein that binds to both phospholipids and the SNARE complex and provides a mode of fusion of two membranes. Exocytosis of lysosomal vesicles is induced by an influx of calcium through the Ca^{2+} sensitive synaptotagmin VII (Syt-VII)[159]. Membrane vesicle shedding is further mediated by the Endosomal Sorting Complex Required for Transport (ESCRT), a protein that has been shown to facilitate membrane remodeling and scission in various cellular processes such as cytokinesis and viral budding[165,166]. It has been observed that ESCRT-III is recruited to disrupted membrane sites to facilitate repair in response to laser induces membrane wounding[155]. Additionally, recent research showed that ESCRT proteins are recruited to Cytotoxic T-lymphocyte (CTL) attack sites to facilitate repair in response to membrane damage[167,168].

Suggesting the ESCRT protein complex plays an essential role in vesicle fusion dependent PM repair.

Figure 1.8:

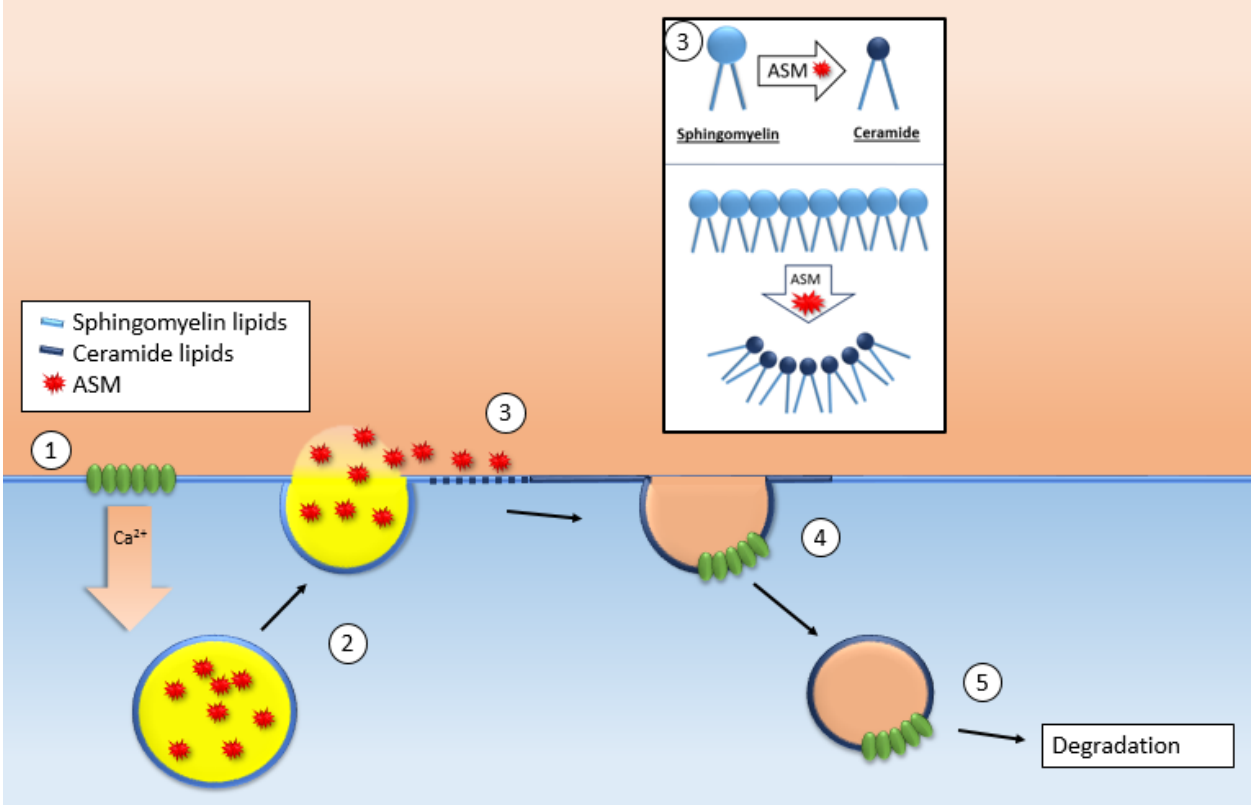

Figure 1.8: Endocytosis mediated membrane repair. Membrane repair is essential to prevent cell death upon small disruptions of the plasma membrane. (1) Disruption of the plasma membrane, either by mechanical rupture or by pore-forming protein, induces an influx of extracellular calcium into the cytoplasm. (2) The influx of extracellular calcium induces the exocytosis of lysosomes at the site of membrane disruption. (3) Lysosomal exocytosis causes the release of various lysosomal enzymes, including ASM, into the extracellular space. ASM then modifies sphingomyelin to generate ceramide lipids. (4) Generation of ceramide-rich membrane domains will induce the inward curvature of the plasma membrane. This inward curvature induces endocytosis of the disrupted membrane. (5) Endocytosis of the disrupted membrane removes the lesion from the plasma membrane, effectively repairing the membrane. Pore-forming proteins are ultimately shuttled to degradative compartments.

In addition to removing disrupted portions of the PM through vesicle shedding, cells have been observed to internalize disrupted portions of the PM and proceed to degrade associated pore forming protein[162]. Research from Dr. Andrews' lab shows that various cell types can rapidly repair membrane damage through an endocytosis-dependent mechanism[154,159,169] (Figure 1.8). This mode of membrane repair relies on the Ca^{2+} mediated exocytosis of lysosomes. The release of lysosomal enzymes, specifically acid sphingomyelinase (ASM), into the extracellular space induces the generation of ceramide from sphingomyelin lipids. ASM, a phosphodiesterase, removes the sphingomyelin head group, leading to the formation of ceramide and phosphocholine rich lipid raft domains at the wounding site[154,170]. Since ceramide lipids contain a smaller head group, they produce an inwards curvature in the membrane, promoting the formation of membrane pits called caveolae. Caveolae are 60-80 nm membrane invaginations stabilized by intracellular caveolin proteins and are known to play a role in endocytic pathways[149,171]. The presence of lipid raft domains as well as caveolin pits facilitates membrane endocytosis[169,172]. This leads to caveolin-mediated clathrin-independent endocytosis (CIE) of membrane lesions, effectively repairing the plasma membrane. This mode of membrane repair is supported by studies showing that inhibition of ASM activity through treatment with Desipramine (DPA), prevented cells from repairing plasma membrane disruptions[115,154]. Furthermore, the release of extracellular acid sphingomyelinase was shown to be sufficient to recover membrane repair[161]. Disruptions in cavin protein, important in the formation of caveolae, also reduce the ability of cells to repair their plasma membrane[173]. Interestingly, patients with Duchenne muscular dystrophy, caused by defects in caveolin protein expression, show a decreased ability to recover from muscle contraction induced cell wounding[169]. B cells are known to lack expression of caveolin protein[174]. However, research from our lab showed that B cells are, nonetheless, able to repair SLO induces membrane disruption using a lysosome exocytosis and lipid raft dependent repair mechanism[115]. Upon wounding with SLO, there was an increase in exposure of extracellular lysosomal integral membrane protein-2 (LIMP2) as well as an increase in lipid raft

mediated endocytosis. Interestingly, in contrast to cells that do produce caveolin protein, B cells utilize a lipid raft dependent tubular endocytosis pathway during repair in response to the pore forming toxin SLO[146]. Surprisingly, SLO-induced wounding significantly reduced BCR endocytosis in response to antigenic challenge. This is likely caused by a spatial competition for the recruitment of lipid raft domains, as both mechanisms are dependent on lipid raft mediated endocytosis.

1.9 Rationale and Aims

B cell activation requires BCR signaling, antigen uptake, and antigen processing. B cells are known to utilize lipid raft domains to organize BCR signalosomes and endocytosis machinery[17], and utilize lysosomal enzymes to release antigen from presenting surfaces for endocytosis and process antigen for later presentation. Our lab has previously shown that B cells can repair membrane disruptions by triggering lysosome exocytosis and clathrin and caveolin independent and lipid raft dependent endocytosis[115]. Importantly, B cell membrane repair interferes with B cell activation, likely due to a spatial competition in the recruitment of lipid raft membrane domains, since both BCR activation and membrane repair rely on lipid raft domains[18,146,154]. Furthermore, it is well established that B cell interaction with surface associated antigen through the BCR generates cellular forces, including traction forces during spreading and contraction and the pulling forces excreted by B cells at BCR-antigen interacting sites for internalization[175,176].

I hypothesized that BCR interactions with surface associated antigen can disrupt the B cell PM at interaction sites, likely due to cellular forces, and because this occurs at BCR-antigen interacting sites, this membrane permeabilization and subsequent repair will facilitate B cell activation. Based on what we have learned about membrane wound repair, I predict that

membrane disruptions at the BCR-Ag interaction site induce the repair response that induces lysosome exocytosis and recruits lipid rafts, facilitating BCR signaling, Ag uptake, and antigen processing. This dissertation addresses the question of whether BCR-antigen interactions can cause membrane disruption at interacting sites, what the impact of membrane disruption is on B cell antigen capture and presentation, and what is required to induce B cell PM disruption. Specifically, this research shows, for the first time, that BCR interaction with various models of surface associated antigen, but not soluble Ag, can cause B cell PM permeabilization. B cell PM disruptions induce lysosome exocytosis as a repair response, which facilitates both Ag uptake and Ag presentation to T cells. High-affinity surface associated antigen, BCR signaling, and the motor activity of NMII are required for this antigen induced B cell PM permeabilization. Furthermore, fast, strong, and persistent B cell spreading and NMIIA recruitment, and the formation of an actomyosin ring at the interacting surface may also be required for antigen induced B cell PM permeabilization.

1.9.1 Aim 1: To determine if antigen can cause B cell plasma membrane permeabilization and how permeabilization impact B cell antigen internalization and presentation

This aim was designed to determine whether antigen-induced B cell PM permeabilization occurs or not and explore its role in B cell activation. To determine whether B cell membrane permeabilization and subsequent repair occur during interactions with surface bound Ag, we developed various models of surface bound Ag, including Ag tethered to latex beads, Ag tethered to planar lipid bilayers, and a membrane anchored Ag expressed on the surface of live COS-7 cells. To determine whether the B cells became permeabilized, we proposed to use various membrane impermeable dyes, including propidium iodide (PI), FM, SYTOX, and Ponceau-4R, and measure the entry of these dyes into the cytoplasm, as indicators of PM permeabilization by live cell spinning disc and total internal fluorescence microscopy, and flow cytometry. To determine whether B cells can reseal PM permeabilization, we track the cytoplasmic entry of

various membrane impermeable dyes administered at early and late time points. We also determined the frequency and location of lysosome exocytosis events by detecting the extracellular exposure of the luminal domain of the lysosomal protein LIMP2 and the fusion of dye-loaded lysosomes with the B cell PM at BCR-antigen interacting sites. We further examined whether BCR signaling and myosin activity were required for antigen-induced B cell PM permeabilization using inhibitors. To determine the role for BCR-Ag binding affinity in inducing B cell membrane permeabilization, we utilized B cells from mice expressing Ig transgene MD4 that specifically binds hen egg lysozyme (HEL) with high affinity, and used duck egg lysozyme as a low-affinity antigen to pair with HEL. Finally, we determined if antigen induced B cell PM permeabilization could facilitate Ag uptake and presentation to T cells, using a fluorescent Ag and T cells hybridoma that specifically recognizes Ag presented on the B cell surface, and by examining the effect of NMII inhibitor, which inhibited antigen induced B cell PM permeabilization, on antigen internalization and B cell activation of T cells by antigen presentation.

1.9.2 Aim2: To examine the cellular mechanisms required to induce B cell plasma membrane permeabilization during interaction with surface-associated antigen

This aim was designed to explore the cellular mechanisms required for B cell permeabilization during engagement with surface associate antigen. We proposed to use antigen coated planar lipid bilayers, which allows us to directly image B cell-antigen interaction sites live using total internal reflection fluorescence (TIRF) microscopy and interference reflection microscopy (IRM). We proposed to compare the kinetics, the extent, and the persistency of B cell spreading on the antigen presenting surface between B cells that eventually did and did not permeabilization become permeabilized. We proposed to examine the recruitment kinetics and levels of NMIIA to and its persistence and organization at the B cell contact zone using transgenic mice expressing GFP-NMIIA and TIRF microscopy and compare these parameters

between B cells that did and did not eventually become permeabilized. Lastly, we propose to use live imaging probes for lysosomes (SiR-Lysosome) and TIRF and spinning disc fluorescence microscopy to compare the level of lysosome polarization toward antigen binding sites in B cells that did and did not become permeabilization.

Chapter2: Surface-associated antigen induces permeabilization of primary mouse B-cells and lysosome exocytosis facilitating antigen uptake and presentation to T-cells.

2.1 Abstract

B-cell receptor (BCR)-mediated antigen internalization and presentation are essential for humoral memory immune responses. Antigen encountered by B-cells is often tightly associated with the surface of pathogens and/or antigen-presenting cells. Internalization of such antigens requires myosin-mediated traction forces and extracellular release of lysosomal enzymes, but the mechanism triggering lysosomal exocytosis is unknown. Here we show that BCR-mediated recognition of antigen tethered to beads, to planar lipid-bilayers or expressed on cell surfaces causes localized plasma membrane (PM) permeabilization, a process that requires BCR signaling and non-muscle myosin II activity. B-cell permeabilization triggers PM repair responses involving lysosomal exocytosis, and B-cells permeabilized by surface-associated antigen internalize more antigen than cells that remain intact. Higher affinity antigens cause more B-cell permeabilization and lysosomal exocytosis and are more efficiently presented to T-cells. Thus, PM permeabilization by surface-associated antigen triggers a lysosome-mediated B-cell resealing response, providing the extracellular hydrolases that facilitate antigen internalization and presentation.

2.2 Introduction

B-cells are responsible for generating antibody responses that neutralize pathogens and attract other immune cells. B-cell activation is initiated by the B-cell receptor (BCR), which surveys antigen through its membrane-anchored immunoglobulin[177]. Antigen-BCR interaction induces signaling cascades and antigen internalization, followed by intracellular processing and surface presentation to T-cells. Antigen presentation is essential for the activation of B-cells and their differentiation into high-affinity memory or antibody-secreting cells[178]. A property that is critical for maximizing humoral protection is the ability of clonal-specific BCRs to recognize antigens in their different physical, chemical, and biological forms.

Antigen encountered by B-cells *in vivo* is often tightly associated with the surface of pathogens, such as parasites, bacteria and viruses, and/or antigen-presenting cells, such as follicular dendritic cells[179]. Internalization, processing, and presentation of such surface-bound antigens are essential for specific B-cells to obtain T-cell help, which is critical for B-cell activation and differentiation. Follicular dendritic cells, which are uniquely present in germinal centers of secondary lymphoid organs, internalize antigens that drain into these organs and present them to B-cells[72,180]. Competition between high and low-affinity B-cells to acquire antigen from follicular dendritic cells is a critical step in the selection of high-affinity cells that differentiate into memory B-cells and long-lived plasma cells.

B-cells, follicular B-cells in particular, are thought to have a limited ability to phagocytose large insoluble antigen particles[181]. However, B-cells are able to extract and endocytose antigen that is tightly associated with non-internalizable surfaces[45]. Importantly, the efficiency of antigen presentation by B-cells appears to depend more strongly on the BCR-antigen binding affinity when the antigen is associated with non-internalizable surfaces, compared to antigen bound to internalizable particles[45]. Recent studies using antigen-coated

beads, planar lipid bilayers, or plasma membrane (PM) sheets revealed two major mechanisms by which B-cells extract antigen from non-internalizable surfaces for endocytosis. Mechanical forces, generated by non-muscle myosin II (NMII) activation at sites of antigen-BCR interaction, can directly pull antigen from presenting surfaces for endocytosis. When mechanical forces alone are not sufficient, hydrolases released from lysosomes cleave surface-associated antigen to facilitate internalization[85,89,120,175]. Surface-associated antigen was previously shown to induce polarization of B-cell lysosomes towards antigen-binding sites[89], but the mechanism responsible for triggering lysosome exocytosis and release of hydrolytic enzymes was unknown.

When cells are permeabilized by physical tearing or pore-forming proteins, Ca^{2+} influx triggers rapid exocytosis of lysosomes as part of the process that repairs the PM and prevents cell death[149,159]. Since its discovery several decades ago[182], Ca^{2+}-dependent exocytosis of lysosomes has been observed in many cell types[183–186]. We previously reported that permeabilization of the PM of mouse splenic B-cells with the pore-forming toxin streptolysin O (SLO) triggers lysosomal exocytosis, releasing hydrolases extracellularly and exposing the luminal epitope of the lysosome-associated protein LIMP-2 on the cell surface. B-cells rapidly reseal these PM lesions in a process that requires lysosomal exocytosis[146]. Surprisingly, in this study we found that interaction of the BCR with surface-associated antigen can permeabilize the B-cell PM, triggering a resealing mechanism that involves exocytosis of lysosomes. We investigated this process by determining if antigen-induced PM permeabilization depends on the BCR-antigen binding affinity, BCR signaling and NMII motor activity, and if it influences the ability of mouse primary B-cells to internalize and present surface-associated antigens to T-cells.

2.3 Results

2.3.1 BCR interaction with surface-associated antigen induces B-cell PM permeabilization at antigen-binding sites

We initially utilized two experimental models previously used to study BCR-mediated internalization of surface-associated antigen: F(ab')$_2$-anti-mouse IgM+G (αM, which binds and activates mouse BCRs) immobilized on beads or tethered to planar lipid bilayers (PLB) by biotin-streptavidin interaction. Beads or PLB coated with transferrin (Tf) at similar surface density as αM were used as controls, as Tf does not activate the BCR and interacts with the Tf receptor with similar affinity as the *bona fide* antigen hen egg lysozyme (HEL) binds to the BCR of transgenic MD4 mouse B-cells[118,187]. Strikingly, live imaging revealed influx of the membrane-impermeable dye propidium iodide (PI) at sites of primary mouse B-cell contact with αM-beads, indicating that PM permeabilization occurred at bead-binding locations (*Figure 2.1A, Figure 2.1-figure supplement 1 and Videos 1-3*). While similar percentages of B-cells bound αM- or Tf-beads (*Figure 2.1B)*, a significantly higher fraction of B-cells binding αM-beads became PI-positive (*Figure 2.1C*). Flow cytometry analysis confirmed the increased PI entry in B-cells binding αM-beads when compared to Tf-beads (*Figure 2.1D-G and Figure 2.1-figure supplement 2*). Addition of soluble F(ab')$_2$-anti-mouse IgM+G (sαM, also capable of binding and activating the BCR) did not increase the frequency of PI entry in B-cells binding to Tf-beads (*Figure 2.1F*). The percentage of cells positive for cleaved caspase-3, an early apoptotic marker, was similar in B-cells interacting or not with αM- or Tf-beads and only increased significantly after treatment with staurosporine (*Figure 2.1-figure supplement 3*), suggesting that PM permeabilization is not associated with apoptosis. Similar observations were made using the PLB system that allows lateral movement of the tethered antigen[188]. Significantly more B-cells became PI-positive when contacting αM-PLB when compared to Tf-PLB (*Figure 2.1H-J*).

Figure 2.1:

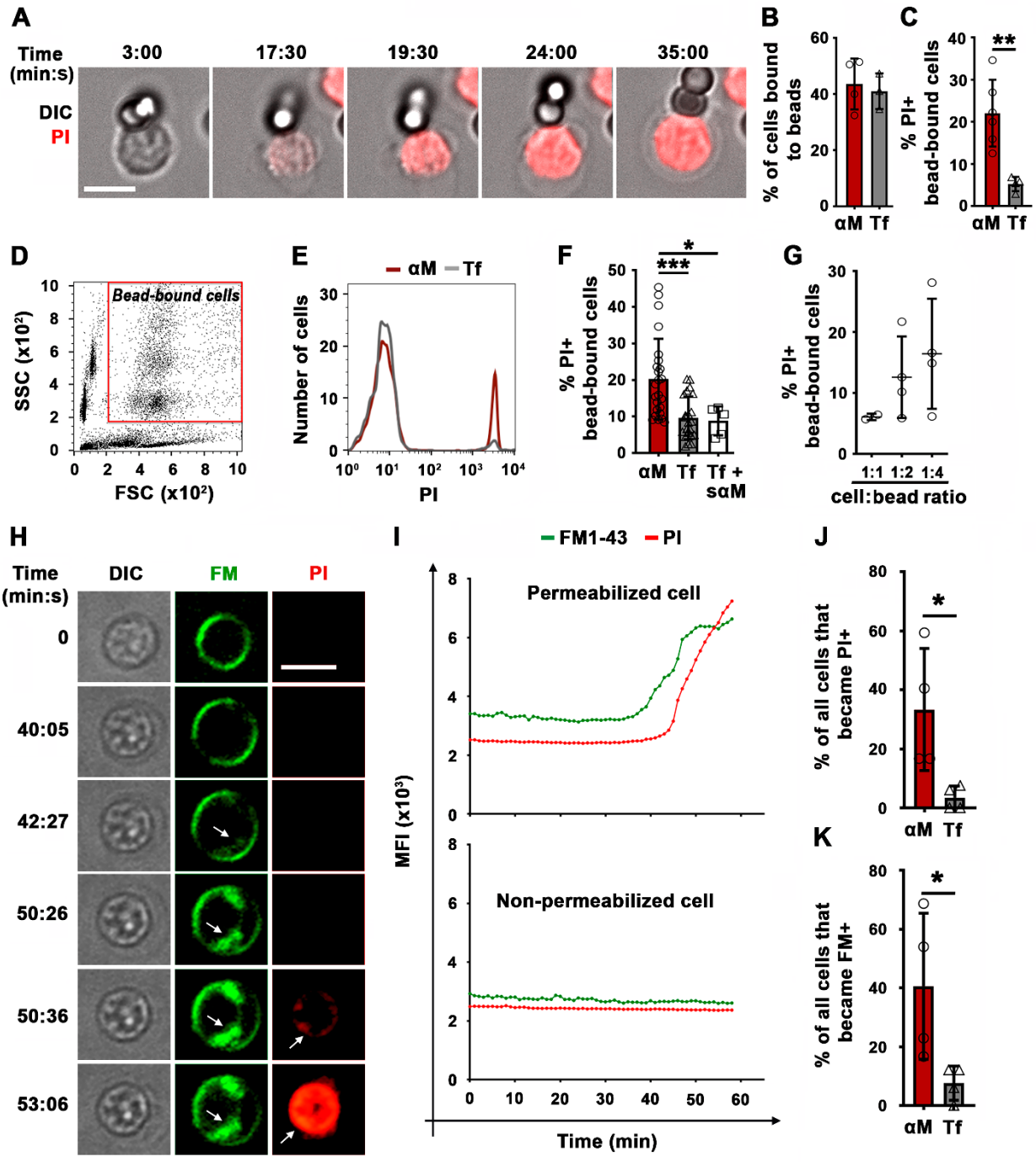
A
Time (min:s)
3:00
17:30
19:30
24:00
35:00
DIC
PI
B
% of cells bound to beads
αM
Tf
C
% PI+ bead-bound cells
**
αM
Tf
D
Bead-bound cells
SSC (x10²)
FSC (x10²)
E
αM
Tf
Number of cells
PI
F
% PI+ bead-bound cells
*
***
αM
Tf
Tf + sαM
G
% PI+ bead-bound cells
1:1
1:2
1:4
cell:bead ratio
H
Time (min:s)
DIC
FM
PI
0
40:05
42:27
50:26
50:36
53:06
I
FM1-43
PI
Permeabilized cell
Non-permeabilized cell
MFI (x10³)
Time (min)
J
% of all cells that became PI+
*
αM
Tf
K
% of all cells that became FM+
*
αM
Tf

Figure 2.1. BCR binding to surface-associated ligands causes B-cell PM permeabilization. (**A**) Time-lapse images of a splenic B-cell incubated with αM-beads (1:2 cell:bead ratio) in the presence of PI *(Video 1)*. (**B**) Percentages of B-cells bound to beads. (**C**) Percentages of PI-positive (PI+) cells in bead-bound B-cells at 30 min. (**D**) Gate for bead-bound B-cells in forward and side scatter flow cytometry dot plot. (**E**) Histograms of PI fluorescence intensity (FI) of αM- and Tf-bead-bound B-cells after 30 min incubation, showing 1,000 cells per condition. (**F**) Percentages of PI+ bead-bound B-cells after 30 min incubation with αM- or Tf-beads with or without soluble αM (sαM). (**G**) Percentages of PI+ bead-bound B-cells after 30 min at indicated cell:αM bead ratios. (**H**) Time-lapse images of a B-cell interacting with αM-PLB in the presence of FM1-43 and PI (arrows, FM1-43 or PI entry, *Video 4*). (**I**) Mean fluorescence intensity of FM1-43 (green lines) and PI (red lines) in a defined intracellular region of a permeabilized (top) and non-permeabilized (bottom) cell over time. (**J**) Percentages of PI+ B-cells interacting with αM- or Tf-PLB for 60 min. (**K**) Percentages of B-cells interacting with αM- or Tf-PLB for 30 min showing intracellular FM staining (FM+). Data points represent independent experiments (mean ± SD) (B, C, F, G, J, K). Bars, 5 μm. *$p \leq 0.05$, **$p \leq 0.01$, ***$p \leq 0.005$, unpaired Student's *t*-test (B, C, J, K) or one-way ANOVA (F). Work for figures 2.1-B, D, E, F, G, H, and I was executed by Fernando Maeda.

PM permeabilization in B-cells binding to αM-PLB was also observed using membrane-impermeable lipophilic FM probes. These fluorescent dyes have been used extensively to assess PM integrity, because they only label the outer PM leaflet of intact cells but rapidly stain intracellular membranes when entering the cytosol[189–191]. After >30 min of interaction with αM-PLB, we observed sudden, massive increases in FM1-43 staining of intracellular membranes, including the nuclear envelope (*Figure 2.1H and I, Figure 2.1-figure supplements 4, 5 and Video 4*). Consistent with the PI entry results (*Figure 2.1J)*, significantly more B-cells showed a sudden increase in intracellular FM staining when contacting αM-PLB compared to Tf-PLB (*Figure 2.1K*). This characteristic pattern of sudden FM influx with staining of the nuclear envelope was only observed in B-cells that eventually became PI-positive, not in cells that remained PI-negative during interaction with αM-PLB (*Figure 2.1- figure supplement 4*). Since FM lipophilic dyes can also be internalized through surface receptor endocytosis, we activated BCR endocytosis by cross-linking surface BCRs using soluble $F(ab')_2$ goat-anti-mouse IgM+G antibodies followed by fluorescent $F(ab')_2$ anti-goat-IgG[192,193]. Under these conditions, which did not cause PM permeabilization, we observed FM1-43 uptake appearing as small peripheral puncta that colocalized with BCR cross-linking antibodies. Such endosome-associated FM1-43 staining pattern was markedly different from the sudden, massive FM influx observed shortly before PI entry in permeabilized cells (*Figure 2.1-figure supplement 6* and *Video 4*). Collectively, these data show that the sudden, massive influx of FM dyes during αM-PLB binding is caused by B-cell permeabilization, and not by a gradual endocytosis of the PM-associated tracer triggered by BCR engagement.

As an independent method to demonstrate antigen-induced permeabilization of B-cells, we took advantage of the ability of membrane-impermeable Ponceau 4R to quench cytosolic fluorophores upon entering cells[194]. Instead of monitoring nuclear or intracellular membrane staining by membrane-impermeable fluorescent dyes, we determined the percentage of B-cells

pre-loaded with carboxyfluorescein succinimidyl ester (CFSE) that lost their cytosolic fluorescence as a consequence of Ponceau 4R entry during PM permeabilization. To validate this method, we first permeabilized B-cells with the pore-forming toxin streptolysin O (SLO). In the presence of Ponceau 4R, the percentage of B-cells with reduced CFSE fluorescence increased significantly after exposure to SLO (*Figure 2.2A and B*), mimicking what we previously observed for PI entry in SLO-treated B-cells[146]. Thus, quenching of cytoplasmic CFSE by the membrane-impermeable Ponceau 4R is a potent indicator of PM permeabilization. Using this method, we compared B-cells incubated with αM- or Tf-PLB by live imaging. A significantly higher fraction of CFSE-labeled B-cells showed fluorescence quenching when interacting with αM-PLB, quantified as the percentage of cells that lost >70% of their initial CFSE fluorescence (*Figure 2.2C and D and Video 5*). The average time for detection of αM-PLB-induced B-cell permeabilization measured by this quenching method was similar to what was observed for FM entry, while the average time for intracellular detection of PI showed a ~8 min delay (*Figure 2.2E, Figure 1-figure supplements 4 and Video 4*). An analysis of the cumulative rate of influx of the three distinct tracers confirmed the small delay in PI detection (*Figure 2.2F*). Thus, FM influx and Ponceau 4R-mediated quenching are more sensitive methods for detecting the onset of B-cell PM permeabilization when compared to PI influx, which is only clearly visualized after intercalation into double-stranded DNA inside the nucleus. Based on consistent results obtained with three different methods, we conclude that BCR binding to αM-coated surfaces (but not to soluble αM) causes localized permeabilization of the B-cell PM.

Figure 2.2:

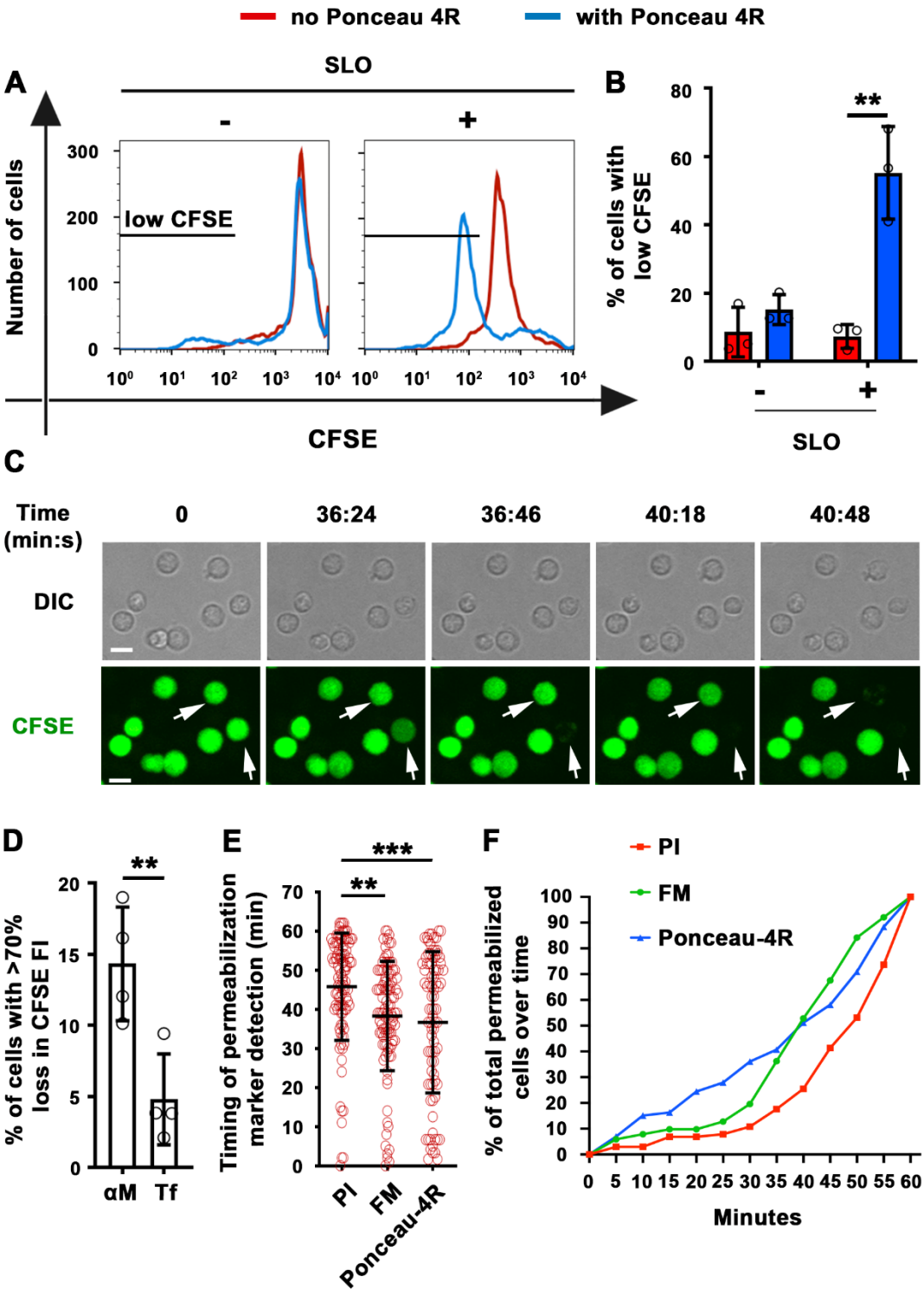
no Ponceau 4R
with Ponceau 4R
A
SLO
-
+
Number of cells
low CFSE
CFSE
B
% of cells with low CFSE
**
SLO
C
Time (min:s)
0
36:24
36:46
40:18
40:48
DIC
CFSE
D
% of cells with >70% loss in CFSE FI
**
αM
Tf
E
Timing of permeabilization marker detection (min)
***
**
PI
FM
Ponceau-4R
F
% of total permeabilized cells over time
PI
FM
Ponceau-4R
Minutes

Figure 2.2. Extracellular Ponceau 4R quenches cytoplasmic CFSE in αM-PLB-permeabilized B-cells. (A) Flow cytometry histograms of CFSE FI in B-cells incubated with or without SLO for 10 min in the presence or absence of Ponceau 4R, showing 8,500 cells per condition**. (B)** Percentages of cells with reduced CFSE in the presence or absence of Ponceau 4R after treatment with or without SLO. Data points represent independent experiments (mean ± SD). **(C)** Time-lapse images of B-cells pre-stained with CFSE interacting with αM-PLB in the presence of Ponceau 4R (arrows, cells with Ponceau 4R quenching of cytoplasmic CFSE) *(Video 5)*. **(D)** Percentages of B-cells with more than 70% loss of CFSE FI after 60 min interaction with αM- or Tf -PLB. Data points represent independent experiments (mean ± SD). **(E)** Timing of PI, FM1-43 entry or Ponceau 4R-mediated CFSE quenching in B-cells interacting with αM-PLB. Data points represent individual cells in at least four independent experiments (mean ± SD). **(F)** Cumulative percentages of total permeabilized B-cells detected over time in four independent experiments. Bars, 5 μm. $^{**}p \leq 0.01$, $^{***}p \leq 0.005$, unpaired Student's *t*-test (B, D) or one-way ANOVA (E). Work for figures 2.2-A, B, C, and D was executed by Fernando Maeda.

We next determined whether HEL, a *bona fide* antigen recognized by the BCR from MD4 mice, also caused B-cell permeabilization when tethered to artificial surfaces or presented as an integral membrane protein (mHEL) on the surface of live cells[75]. Flow cytometry analysis revealed that similar fractions of MD4 B-cells become PI-positive after binding beads coupled to αM or to HEL (*Figure 2.3A-C*). In contrast, WT B-cells binding to HEL- beads showed a low percentage of PI-positive cells, similar to what is observed with Tf-beads (*Figure 2.1F and Figure 2.3A-C*). Importantly, transmembrane mHEL-GFP expressed on the surface of live COS-7 cells co-clustered with the BCR at sites of interaction with MD4 B-cells, followed by PI influx. This dramatic clustering pattern followed by permeabilization was not observed in WT B-cells, whose BCR is incapable of specifically recognizing HEL (*Figure 2.3D* and *Videos 6 and 7*). A significantly higher percentage of MD4 B-cells showed PI influx after interaction with COS-7 cells expressing mHEL-GFP, when compared to WT B-cells (*Figure 2.3E*). The percentage of PI-positive MD4 B-cells was also significantly higher after incubation with mHEL-expressing COS-7 cells than with mock-transfected cells (*Figure 2.3F*). Collectively these results show that BCR binding to surface-associated antigen can cause permeabilization of the B-cell PM.

Figure 2.3:

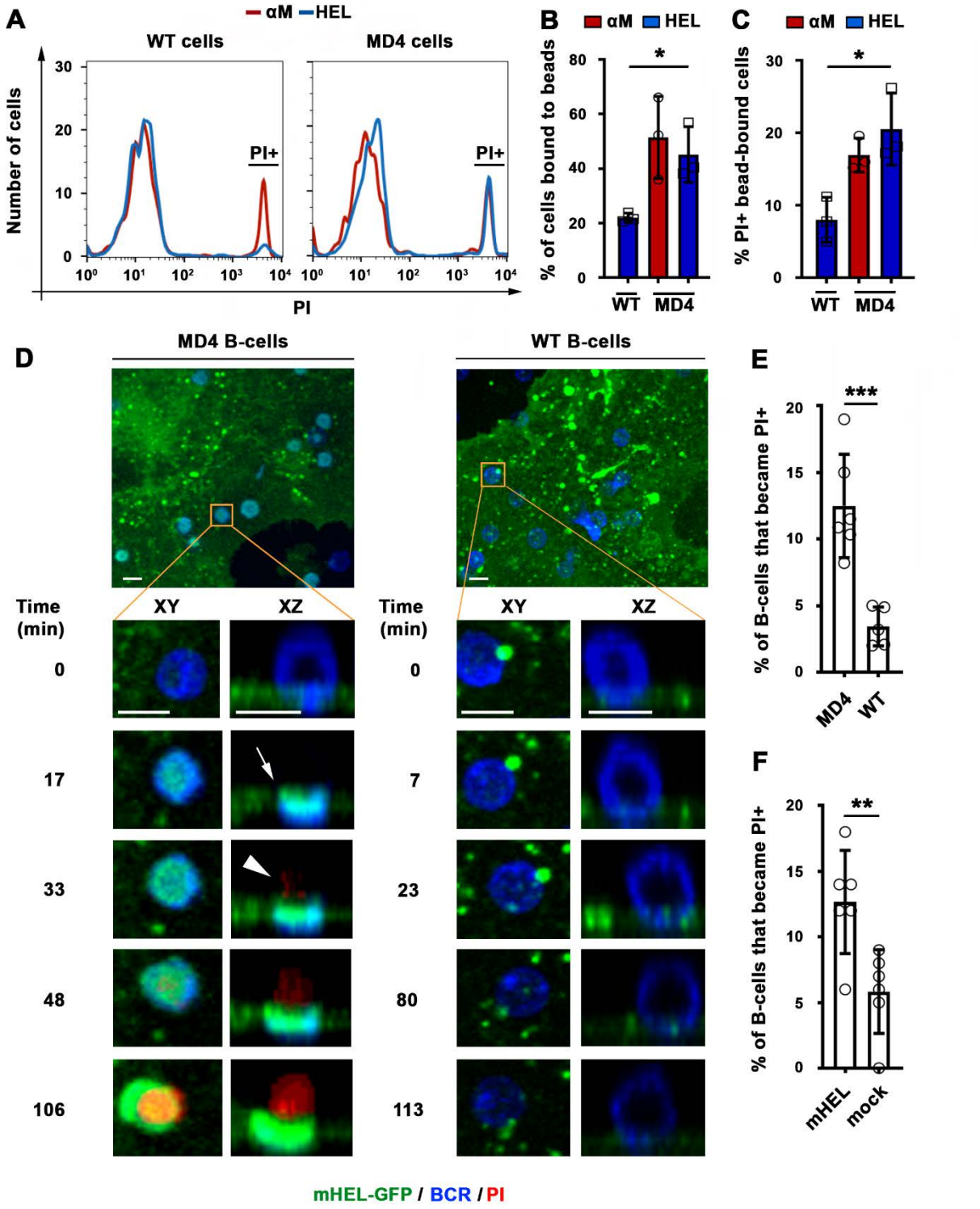
A
αM HEL
WT cells
MD4 cells
Number of cells
PI+
PI
B
αM HEL
% of cells bound to beads
WT MD4
C
αM HEL
% PI+ bead-bound cells
WT MD4
D
MD4 B-cells
WT B-cells
Time (min)
XY
XZ
0
17
33
48
106
0
7
23
80
113
mHEL-GFP / BCR / PI
E
% of B-cells that became PI+
MD4 WT
F
% of B-cells that became PI+
mHEL mock

Figure 2.3. BCR-mediated binding of HEL coupled to beads or expressed as a transmembrane protein on COS-7 cells causes B-cell PM permeabilization. (A) Flow cytometry histograms of PI FI in WT or MD4 B-cells incubated with αM- or HEL-beads for 30 min by flow cytometry, showing 1,000 cells per condition. (**B**) Percentages of WT and MD4 B-cells binding αM- or HEL-beads. Data points represent independent experiments (mean ± SD). (**C**) Percentages of PI+ bead-bound WT or MD4 B-cells after 30 min incubation. Data points represent independent experiments (mean ± SD). **(D)** Spinning disk time-lapse images of a MD4 B-cell (left panels) and a WT B-cell (right panels) interacting with a mHEL-GFP-expressing COS-7 cell in the presence of PI *(Videos 6 and 7).* Arrows, clustering of mHEL-GFP during B-cell binding; arrowheads, PI entry in the B-cell. **(E)** Percentages of PI+ MD4 and WT B-cells interacting with COS-7 cells transfected with mHEL-GFP. **(F)** Percentages of PI+ MD4 B-cells interacting with COS-7 cells transfected with mHEL-GFP or mock-transfected. Data points (E and F) represent individual videos from 3~4 independent experiments (mean ± SD). Bars, 5 μm *$p \leq 0.05$, **$p \leq 0.01$, ***$p \leq 0.005$, unpaired Student's *t*-test (E, F) or one-way ANOVA (B, C). Work for Figures 2.3-A, B, and C was executed by Fernando Maeda.

2.3.2 Antigen-induced B-cell permeabilization requires high-affinity BCR-antigen binding, BCR signaling, and NMII motor activity

High-affinity binding of the BCR to antigen associated with non-internalizable surfaces induces high levels of BCR signaling, cytoskeleton reorganization, and antigen endocytosis[44,45,118]. To examine the impact of the BCR binding affinity on antigen-induced PM permeabilization, we incubated MD4 B-cells with beads coated with equal densities of HEL or the duck egg lysozyme isoform DEL-I. The MD4 BCR binds DEL-I with >100 fold lower affinity than it binds HEL[119]. As expected, the percentage of B-cells binding multiple beads was reduced when the BCR-antigen affinity decreased (*Figure 2.4-figure supplement 1A*), but B-cells binding one single bead were detected for both HEL and DEL-I and also Tf (*Figure 2.4-figure supplement 1*). In these single bead-bound populations, DEL-I-beads caused significantly less PI entry than HEL-beads (*Figure 2.4A*). Inhibition of signaling with the Src kinase inhibitor PP2[30] (iSrc) or the Bruton's Tyrosine Kinase inhibitor AVL-292 (Aalipour and Advani 2013) (iBTK) (*Figure 2.4B and C*) also reduced PI entry in cells binding HEL-beads (*Figure 2.4D*). After contact with αM-PLB or αM-beads but not Tf-PLB or Tf-beads, surface BCRs became polarized towards PLB- or bead-binding sites within ~10 min, a period markedly shorter than what is required for detection of PM permeabilization through FM influx (*Figure 2.4E-H, Figure 2.4-figure supplement 2, and Video 8*). Importantly, the activated form of the actin motor protein NMII, detected through its phosphorylated light chain (pMLC), accumulated along with the BCR at αM-bead-binding sites (*Figure 2.4G, Figure 2.4-figure supplement 3 and Video 9*). The fluorescence intensity ratios (FIR) of surface BCRs and pMLC were significantly higher in B-cells binding αM-beads than in cells binding Tf-beads (*Figure 2.4H and I*). Notably, inhibition of NMII motor activity with blebbistatin (Bleb) markedly reduced the number of B-cells that became PI-positive during interaction with αM-beads, without affecting the cells' ability to bind the beads (*Figure 2.4J and K*). Live imaging detected PI entry following a "tug-of-war' between two B-cells simultaneously engaging an αM-bead (*Video 3 and Figure 2.1-figure supplement*

1C), further supporting a role for NMII-mediated traction forces in antigen-induced PM permeabilization. Thus, our results indicate that PM permeabilization caused by surface-associated antigen requires strong BCR-antigen interaction and the subsequent activation of signaling and NMII motor activity.

Figure 2.4:

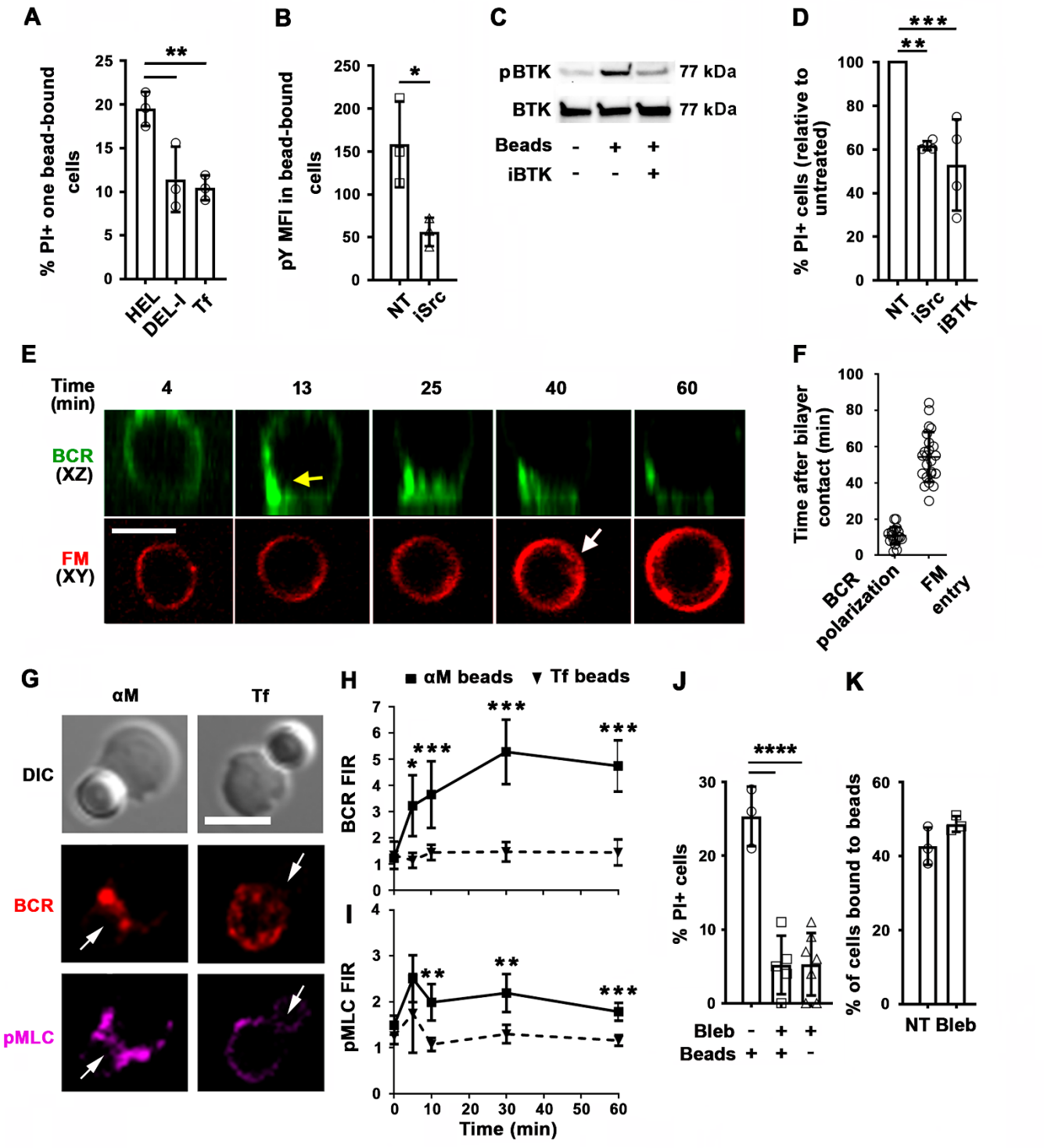
A
% PI+ one bead-bound cells
HEL
DEL-I
Tf
B
pY MFI in bead-bound cells
NT
iSrc
C
pBTK
BTK
77 kDa
Beads
iBTK
D
% PI+ cells (relative to untreated)
NT
iSrc
iBTK
E
Time (min)
4
13
25
40
60
BCR (XZ)
FM (XY)
F
Time after bilayer contact (min)
BCR polarization
FM entry
G
αM
Tf
DIC
BCR
pMLC
H
αM beads
Tf beads
BCR FIR
I
pMLC FIR
Time (min)
J
% PI+ cells
Bleb
Beads
K
% of cells bound to beads
NT
Bleb

Figure 2.4. PM permeabilization induced by surface-associated antigen depends on high-affinity BCR-antigen binding, BCR signaling, and non-muscle myosin II (NMII) motor activity. (**A**) Percentages of PI+ single bead-binding B-cells after incubation with HEL-, DEL-I- or Tf-beads (1:4 cell:bead ratio) for 30 min. Data points represent independent experiments (mean ± SD). (**B**) Mean fluorescence intensity (MFI) of phosphotyrosine (pY) in HEL-bead-bound B-cells treated or untreated (NT) with a Src kinase inhibitor (iSrc) by flow cytometry. Data points represent independent experiments (mean ± SD). (**C**) Western blot analysis of phosphorylated BTK (pBTK) and BTK in B-cells incubated with HEL-beads in the presence or absence of a BTK inhibitor (iBTK) for 30 min. (**D**) Percentages of PI+ HEL-bead-bound cells treated with iSrc or iBTK relative to not-treated (NT) at 30 min. Data points represent independent experiments (mean ± SD). (**E**) Spinning disk time-lapse images of BCR polarization (yellow arrow) in a B-cell incubated with αM-PLB in the presence of FM4-64 (white arrow, intracellular FM). (**F**) Timing of BCR polarization and FM entry of individual cells interacting with αM-PLB *(Video 8)*. Data points represent individual cells in three independent experiments (mean ± SD). (**G**) Confocal images of BCR and phosphorylated NMII light chain (pMLC) staining in B-cells interacting with αM- or Tf-beads (arrows, bead binding sites). (**H** and **I**) FI ratio (FIR) of BCR (**H**) and pMLC (**I**) staining at the bead-binding site relative to the opposite PM in αM- and Tf-bead-bound cells over time. Data represent the averages of three independent experiments (mean ± SD). (**J**) Percentages of PI+ bead-binding B-cells incubated with αM-beads for 30 min with or without blebbistatin (Bleb). Data points represent individual videos from three independent experiments (mean ± SD). (**K**) Percentages of bead-bound B-cells incubated with αM-beads for 30 min in the presence or absence of Bleb. Data points represent independent experiments (mean ± SD). Bars, 5 μm. *$p \leq 0.05$, **$p \leq 0.01$, ***$p \leq 0.005$, ****$p \leq 0.001$, unpaired Student's *t*-test (B, H, I, K) or one-way ANOVA (A, D, J). Work for figures 2.4-A, B, C, and D was executed by Fernando Maeda.

2.3.3 Antigen-induced B-cell permeabilization triggers lysosomal exocytosis as a PM repair response

Permeabilization with the pore-forming toxin SLO triggers exocytosis of lysosomes in mouse primary B-cells[146], a response to Ca^{2+} influx that is observed in several cell types and is required for the resealing PM wounds[159]. To determine if permeabilization by surface-associated αM or HEL triggered exocytosis of lysosomes in B-cells, we first examined whether luminal epitopes of the lysosomal membrane protein LIMP-2 were exposed on the cell surface. Flow cytometry detected surface LIMP-2 in a higher percentage of B-cells binding αM-beads than in B-cells binding Tf-beads (*Figure 2.5A and B*). Notably, surface exposure of LIMP-2 was lower in MD4 B-cells binding DEL-I-beads compared to HEL-beads (*Figure 2.5C*). These results reveal a close correlation between the extent of PM permeabilization (*Figure 2.4A*) and lysosomal exocytosis induced by surface-associated αM, HEL or DEL-I (*Figure 2.5B-C*). Surface LIMP-2 was predominantly detected at sites of αM-bead binding (*Figure 2.5D and Figure 2.5-figure supplement 1*) and this polarized pattern, measured by FIR, increased after ~30 min of interaction with αM- but not Tf-beads (*Figure 2.5E*). Notably, this timeframe was similar to the average period required for PM permeabilization (*Figure 2.2E*). Next, we performed live total internal reflection fluorescence (TIRF) microscopy of B-cells preloaded with the luminal lysosomal probe SiR-Lyso (a membrane-permeable fluorescent peptide that binds to the lysosomal enzyme cathepsin D) while contacting αM-PLB. Exocytosis events were identified by rises in the fluorescence intensity of SiR-Lyso puncta (reflecting lysosome entry into the TIRF evanescent field adjacent to the PM) followed by sharp decreases within ~2 s (reflecting dye dispersion upon fusion of lysosomes with the PM) (*Figure 2.5F and G, Figure 2.5-figure supplement 2 and Video 10*). Exocytosis events were observed in the majority of individual PI-positive cells interacting with αM-PLB (*Figure 2.5H*) and occurred predominantly ~30-45 min after αM-PLB contact (*Figure 2.5H and I*), a timing similar to PM permeabilization and LIMP-2 exposure. Lysosomal exocytosis events were significantly more frequent in permeabilized B-cells when compared to B-

cells that remained intact (*Figure 2.5J*). These results show that permeabilization of B-cells by surface-associated antigen triggers exocytosis of lysosomes.

Figure 2.5:

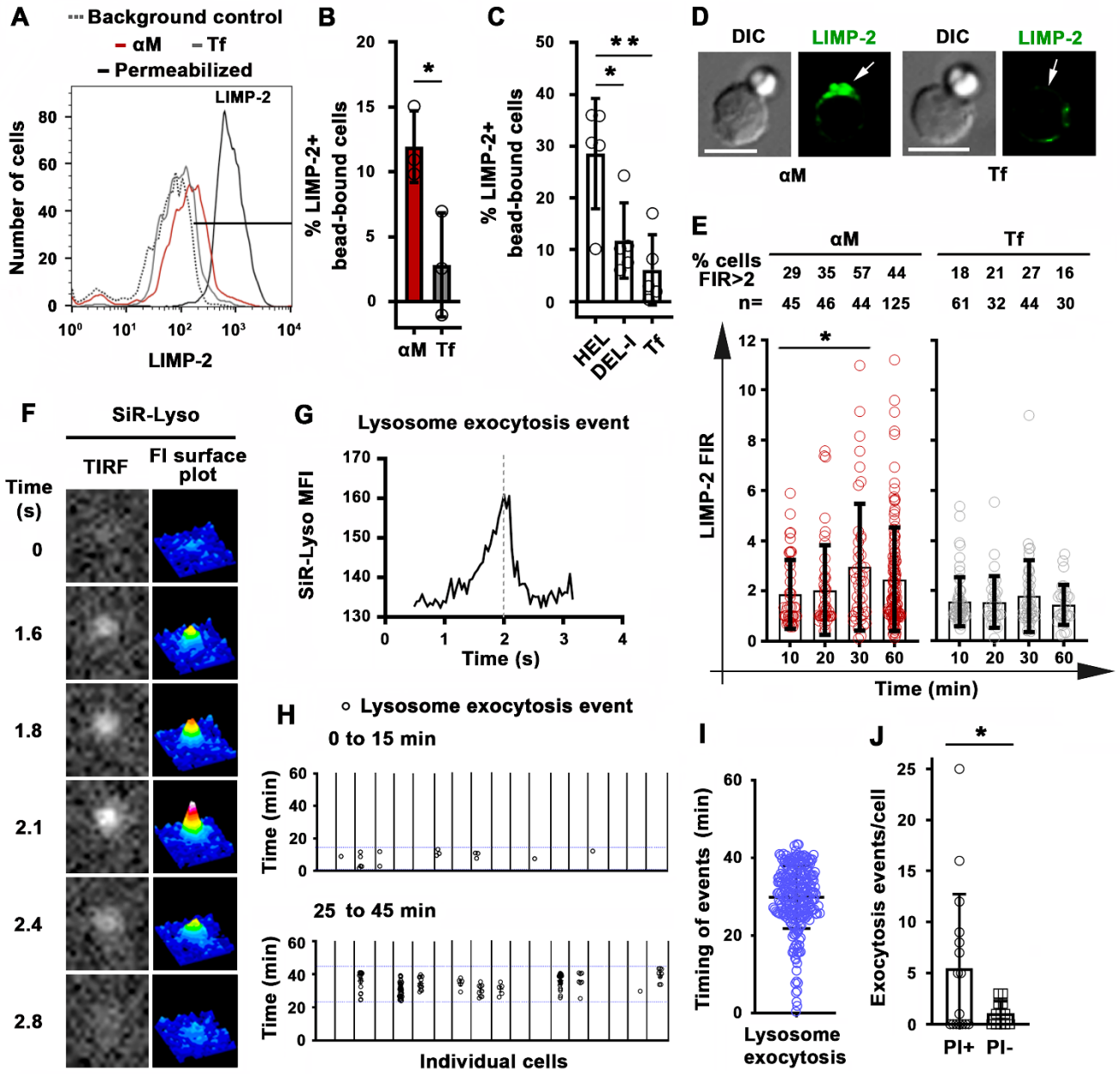
A
Background control
αM
Tf
Permeabilized
LIMP-2
Number of cells
LIMP-2
B
% LIMP-2+ bead-bound cells
αM
Tf
C
% LIMP-2+ bead-bound cells
HEL
DEL-I
Tf
D
DIC
LIMP-2
DIC
LIMP-2
αM
Tf
E
αM
Tf
% cells FIR>2
29 35 57 44
18 21 27 16
n=
45 46 44 125
61 32 44 30
LIMP-2 FIR
Time (min)
F
SiR-Lyso
TIRF
FI surface plot
Time (s)
0
1.6
1.8
2.1
2.4
2.8
G
Lysosome exocytosis event
SiR-Lyso MFI
Time (s)
H
Lysosome exocytosis event
0 to 15 min
25 to 45 min
Time (min)
Individual cells
I
Timing of events (min)
Lysosome exocytosis
J
Exocytosis events/cell
PI+
PI-

Figure 2.5. Antigen-induced permeabilization triggers lysosomal exocytosis. (**A**) Flow cytometry analysis of surface-exposed (no detergent permeabilization) and/or intracellular LIMP-2 (with detergent permeabilization) of bead-bound B-cells after incubation with αM- or Tf-beads for 30 min, showing 3,000 cells per condition. (**B** and **C**) Percentages of cells with surface-exposed LIMP-2 (relative to values with secondary antibody alone) in bead-bound B-cells incubated with αM- or Tf-beads (**B**) or with HEL-, DEL-I- or Tf-beads (**C**) for 30 min. Data points represent independent experiments (mean ± SD). (**D**) Confocal images of surface-exposed LIMP-2 in B-cells incubated with αM- or Tf-beads (arrows, bead-binding sites). (**E**) FIR (bead-binding site:opposite PM) of surface-exposed LIMP-2 in individual cells over time. Data points represent individual cells (mean ± SD). (**F**) Total internal reflection microscopy (TIRF) images (left) and FI surface plots (right) of SiR-Lyso at the B-cell surface contacting αM-PLB (*Video 10*). (**G**) Representative MFI versus time plot of a SiR-Lyso-loaded lysosome undergoing exocytosis. (**H**) SiR-Lyso exocytosis events (circles) in individual B-cells during the first 0-15 min or 25–45 min of incubation with αM-PLB. (**I**) Timing of individual SiR-Lyso exocytosis events in B-cells incubated with αM-PLB for 45 min. Data points represent individual SiR-Lyso exocytosis events from three independent experiments (mean ± SD). (**J**) Numbers of SiR-Lyso exocytosis events per B-cell permeabilized (PI+) or not permeabilized (PI-) by αM-PLB during 45 min. Data points represent individual cells from three independent experiments (mean ± SD). *$p \leq 0.05$, **$p \leq 0.01$, unpaired Student's *t*-test (B and J) or one-way ANOVA (C and E). Bars, 5 μm. Work for figures 2.5-A, B, C, D, and E was executed by Fernando Maeda.

We next determined if B-cells were capable of resealing their PM, by using an assay involving sequential exposure to two different membrane-impermeable fluorescent dyes[159]. Resealed cells were quantified by flow cytometry as the percentage of permeabilized cells binding αM-beads (stained intracellularly with FM4-64 kept throughout the assay) that excluded the membrane-impermeable dye SYTOX Blue (added only during the last 10 min of the assay) (*Figure 2.6A*). Under these conditions, ~50% of B-cells permeabilized by surface-associated antigen resealed their PM within the assay period (*Figure 2.6B*). Inhibition of lysosomal exocytosis with bromoenol lactone (BEL)[154,195] significantly reduced the percentage of resealed cells (*Figure 2.6A and B*). We found no evidence that the reduction in resealed cells after BEL treatment was due to toxicity of this inhibitor. B-cell populations with low forward-scatter versus side-scatter values typical of dead cells did not increase after BEL treatment (*Figure 2.6-figure supplement 1*). Exposure to BEL also did not increase the small fraction (<7%) of Tf-bead-binding B-cells that was permeable to SYTOX Blue (*Figure 2.6-figure supplement 1*). These data suggest that lysosomal exocytosis is required for the resealing of B-cells permeabilized by binding to surface-associated antigen. To confirm that individual antigen-permeabilized B-cells resealed, we used live imaging to visualize cells incubated with αM-PLB in the presence of SYTOX Green. PI was then added for the last 10 min of the 4 h incubation. Time-lapse images showed that B-cells that became permeable to SYTOX Green during interaction with αM-PLB subsequently excluded PI – a direct indication that their PM resealed during the 4 h assay period (*Figure 2.6C and Video 11*). As expected, cells that were already permeable to SYTOX Green at the beginning of the incubation (likely non-viable cells that were damaged prior to the incubation) were also permeable to PI (which causes strong quenching of the SYTOX green fluorescence upon entering cells - *Figure 2.6C and Video 11*). Interestingly, primary B-cells permeabilized during interaction with αM-beads (*Figure 2.1A and Video 1*) or αM-PLB (*Figure 2.1H, Figure 2.6C and Video 11*) often displayed a shape change visualized as an increase in cell diameter, but after resealing this morphological change was gradually reversed (*Figure 2.6C, Figure 2.6-figure*

supplement 2, Videos 11 and 12). Collectively, our results indicate that B-cell PM permeabilization by binding to surface-associated antigen is a reversible event, and that lysosomal exocytosis is required for PM resealing as previously shown for other cell types[149].

Figure 2.6:

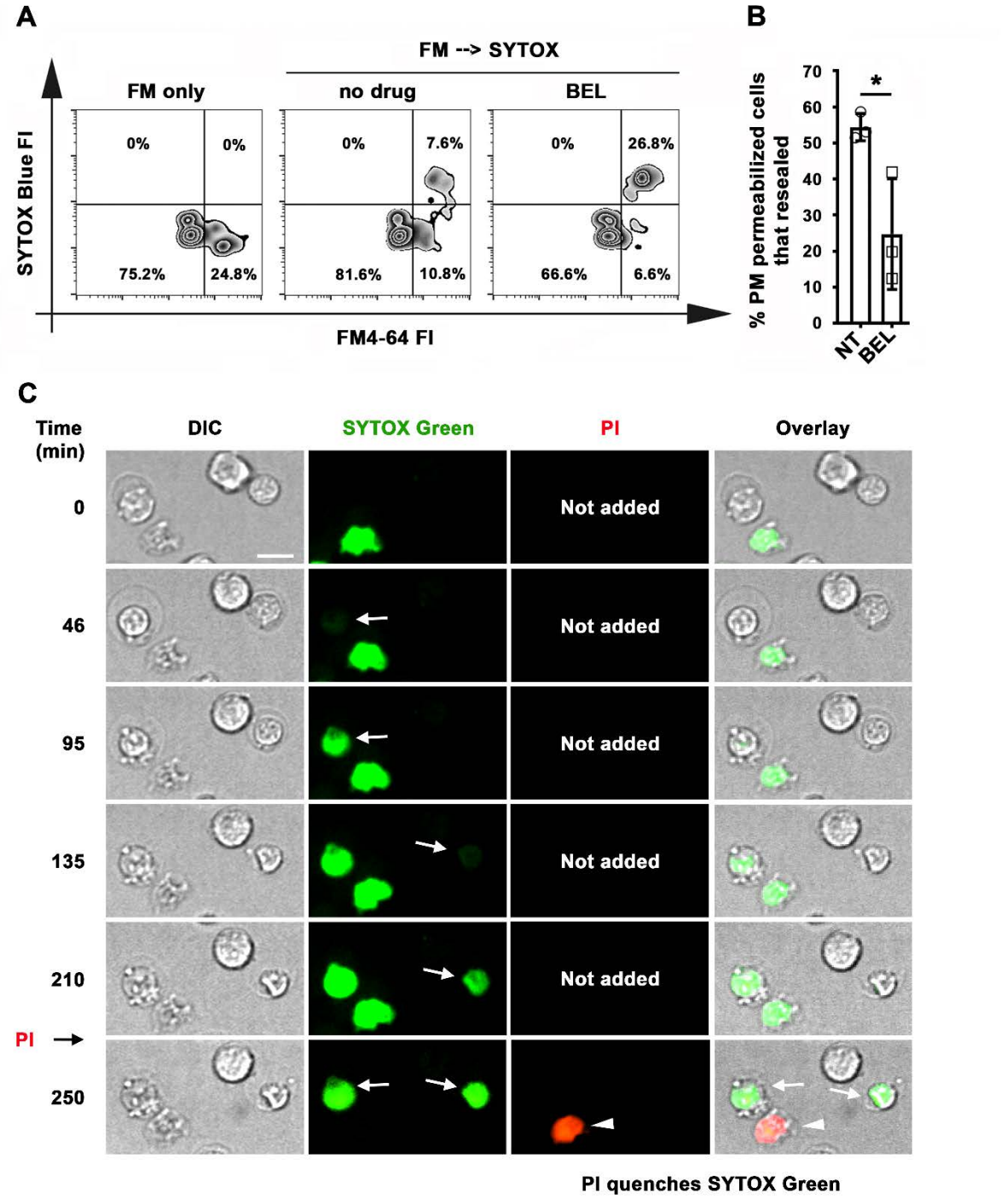
A
FM --> SYTOX
FM only
no drug
BEL
SYTOX Blue FI
FM4-64 FI
0%
0%
75.2%
24.8%
0%
7.6%
81.6%
10.8%
0%
26.8%
66.6%
6.6%
B
% PM permeabilized cells that resealed
70
60
50
40
30
20
10
0
*
NT
BEL
C
Time (min)
DIC
SYTOX Green
PI
Overlay
0
46
95
135
210
PI
250
Not added
Not added
Not added
Not added
Not added
PI quenches SYTOX Green

Figure 2.6. Antigen-permeabilized B-cells reseal their PM in a lysosomal exocytosis-dependent manner. (**A**) B-cells were incubated with αM-beads and permeabilized/resealed cells were assessed by flow cytometry of FM4-64 (added from the start) and SYTOX Blue (added in the last 10 min) FI, in the presence or absence of BEL. (**B**) Percentages of permeabilized αM-bead-bound cells that resealed in the presence or absence of BEL. Data points represent independent experiments (mean ± SD). **(C)** Time-lapse images of splenic B-cells incubated with αM-PLB in the presence of SYTOX Green. PI was added for 10 min at the end *(Video 11)*. Arrows, cells that became permeabilized after contacting the αM-PLB and later excluded PI; arrowhead, cell that was SYTOX+ since the start of the video and did not exclude PI. *$p \leq 0.05$, unpaired Student's *t*-test (B). Bar, 5 μm. Work for figure 2.6 was executed by Fernando Maeda.

2.3.4 B-cell permeabilization and lysosomal exocytosis facilitate internalization and presentation of surface-associated antigen

We investigated the relationship between PM permeabilization by surface-associated antigen and antigen internalization using fluorescent αM covalently bound to beads or tethered to PLB. Live imaging detected αM puncta moving away from bead-binding sites into B-cells, increasing progressively between 30 and 60 min of interaction (*Figure 2.7A and B and Video 13*). In contrast, intracellular fluorescent puncta were markedly less abundant during the same time period in cells not binding αM-beads, or binding Tf-beads (*Figure 2.7B*). Inhibition of antigen-mediated PM permeabilization with blebbistatin significantly reduced extraction and internalization of αM coupled to beads (*Figure 2.7C*). When similar experiments were performed with PLB, the fraction of cells containing internalized αM and the total amount of αM uptake were significantly higher in permeabilized cells with high levels of intracellular FM staining (FM-high), compared to non-permeabilized cells with low FM staining (FM-low) (*Figure 2.7D-F*). These data suggest that αM-induced PM permeabilization, rapidly followed by lysosomal exocytosis, promotes extraction and internalization of αM from non-internalizable surfaces.

Figure 2.7:

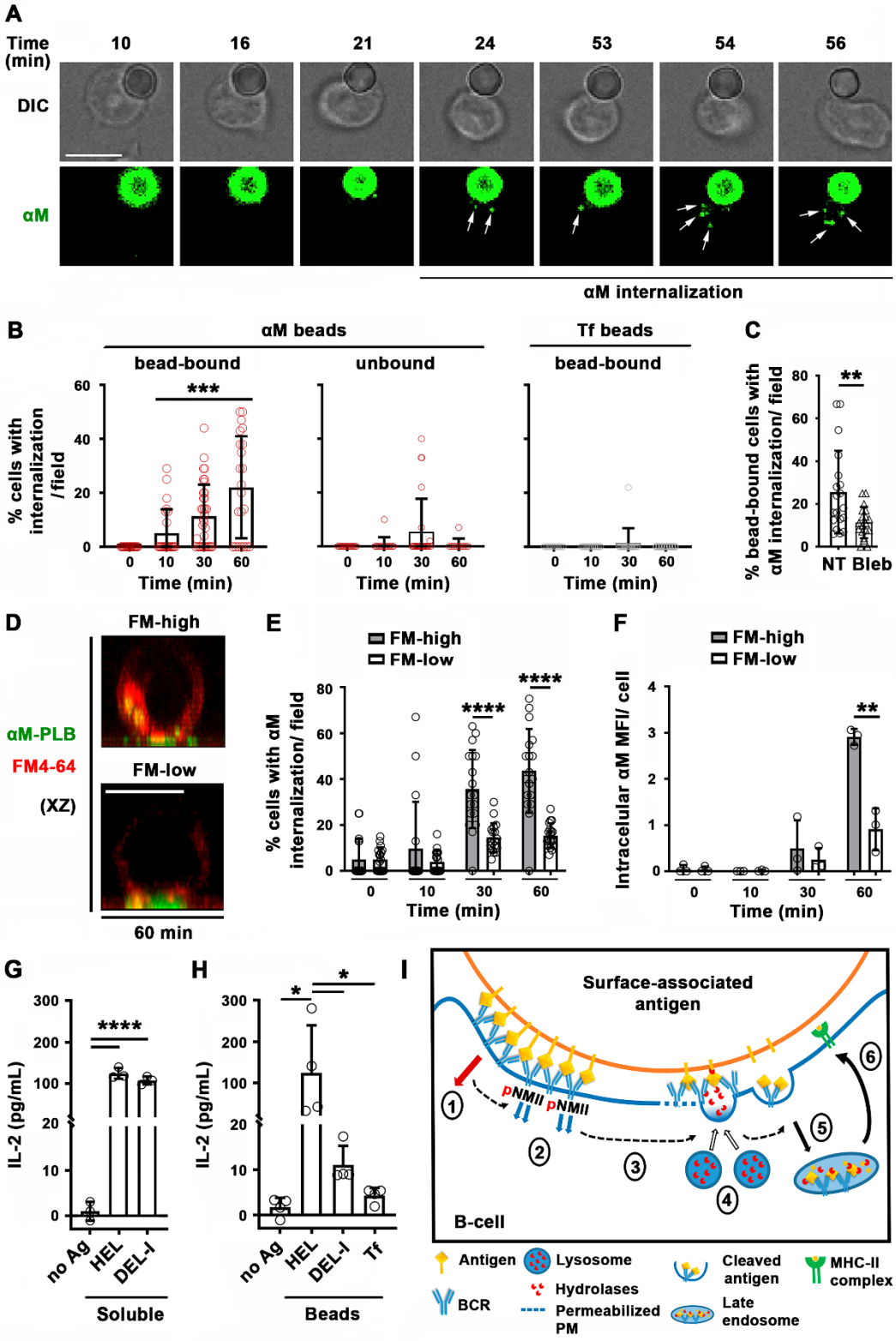
A
Time (min)
10
16
21
24
53
54
56
DIC
αM
αM internalization
B
αM beads
Tf beads
bead-bound
unbound
bead-bound
% cells with internalization / field
***
Time (min)
C
% bead-bound cells with αM internalization/ field
**
NT
Bleb
D
FM-high
FM-low
αM-PLB
FM4-64
(XZ)
60 min
E
FM-high
FM-low
% cells with αM internalization/ field
****
****
Time (min)
F
FM-high
FM-low
Intracelular αM MFI/ cell
**
Time (min)
G
IL-2 (pg/mL)
****
no Ag
HEL
DEL-I
Soluble
H
IL-2 (pg/mL)
*
*
no Ag
HEL
DEL-I
Tf
Beads
I
Surface-associated antigen
pNMII
pNMII
B-cell
Antigen
BCR
Lysosome
Hydrolases
Permeabilized PM
Cleaved antigen
Late endosome
MHC-II complex

Figure 2.7. Antigen-induced PM permeabilization promotes antigen internalization and presentation. (**A**) Confocal live imaging of a B-cell interacting with fluorescent αM-beads (arrows, internalized αM). (**B**) Percentages of cells containing internalized αM or Tf, bound or not to αM- or Tf-beads, over time. Data points represent individual fields in three independent experiments (mean ± SD). (**C**) Percentages of bead-bound B-cells with internalized αM in the presence or absence of Bleb after 60 min. Data points represent individual fields in four independent experiments (mean ±SD). (**D**) Confocal images (xz) of αM internalization in B-cells permeabilized (FM-high) or not permeabilized (FM-low) by αM-PLB after 60 min. € Percentages of B-cells, permeabilized (FM-high) or not permeabilized (FM-low) by αM-PLB, containing internalized αM over time. Data points represent individual fields in three independent experiments (mean ± SD). (**F**) MFI values of internalized αM in individual B-cells permeabilized (FM-high) or not (FM-low) by αM-PLB over time. Data points represent independent experiments (mean ± SD). (**G**) IL-2 secretion by 3A9 T-cells activated by B-cells incubated with or without (no Ag) soluble HEL or DEL-I (10 μg/ml) for 72 h. Data points represent independent experiments (mean ± SD). (**H**) IL-2 secretion by 3A9 T-cells activated by B-cells incubated with or without HEL-, DEL-I- or Tf-beads (1:4 cell:bead ratio) for 72 h. Bars, 5 μm. Data points represent independent experiments (mean ± SD). *$p \leq 0.05$, **$p \leq 0.01$, **$p \leq 0.005$, ****$p \leq 0.0001$, unpaired Student's *t*-test (C,E,F), one-way ANOVA (G,H) or Kruskal-Wallis non-parametric test (B). (**I**) Cartoon depicting a working model for the spatiotemporal relationship of events initiated by the interaction of the BCR with surface-associated antigen. High-affinity binding stabilizes BCR-antigen interaction and induces strong BCR signaling (1) and NMII activation (2). Activated NMII generates local traction forces that permeabilize the PM (3), triggering a localized PM repair response mediated by lysosomal exocytosis. Lysosome exocytosis releases hydrolases that cleave antigen off surfaces (4), facilitating endocytosis (5) and presentation to T-cells (6). Figure 2.7 I was generated by Fernando Maeda.

Next, we investigated whether antigen internalization enhanced by PM permeabilization and lysosomal exocytosis impacts antigen presentation by B-cells. We compared levels of IL-2 secretion by the 3A9 T-cell hybridoma line[196] after activation by B-cells exposed to HEL- or DEL-I-beads. B-cells exposed to high concentrations of soluble HEL or DEL-I induced similar levels of IL-2 secretion (*Figure 2.7G*), demonstrating that the primary B-cells used in these assays could process and present the conserved peptide present in both HEL and DEL-I for T-cell activation. In contrast, when the B-cells were exposed to lower amounts of surface-associated antigens, B-cells exposed to HEL-beads activated T-cells to produce IL-2 at markedly higher levels than cells exposed to DEL-I-beads *(Figure 2.7H*). These results indicate that B-cell permeabilization resulting from high-affinity antigen-BCR interaction, with its corresponding lysosomal exocytosis response, facilitates the presentation of antigen associated with non-internalizable surfaces.

2.4 Discussion

Extracellular release of lysosomal enzymes by B-cells was previously proposed to cleave antigens tightly associated with non-internalizable surfaces, facilitating internalization and presentation to T-cells[89,120]. However, it was unclear which mechanism was responsible for inducing lysosomal enzyme release when B-cells engaged insoluble antigen. In this study, we show that interaction of the BCR with surface-associated antigen can permeabilize the B-cell PM, triggering lysosomal exocytosis as part of the PM repair response[159,182]. Antigen-dependent PM permeabilization occurs at antigen-binding sites and is reversible under conditions that allow lysosomal exocytosis. We further demonstrate that PM permeabilization and lysosomal exocytosis require high-affinity binding of the BCR to antigen, BCR signaling and activation of NMII motor activity, and that this process facilitates antigen internalization, processing, and presentation. Thus, our study identifies a critical novel step in the affinity-dependent process by

which B-cells capture antigen tightly associated with surfaces, for effective internalization and subsequent presentation to T-cells.

Capture and internalization of antigen tightly associated with surfaces is an important immunological process, as B-cells encounter this type of antigen *in vivo* on parasites, bacteria and viruses, as well as immune cells such as follicular dendritic cells. Follicular dendritic cells capture antigen drained into lymph nodes and present it on their surface to germinal center B-cells. In this manner, follicular dendritic cells enhance BCR antigenic stimulation by increasing antigen avidity, in addition to providing costimulatory molecules[16]. While the exact percentage is unknown, studies have suggested that the majority of antigens that B-cells encounter *in vivo* are in a membrane-associated form[197]. Importantly, the capture, internalization, and presentation of such surface-associated antigens to T-cells play a critical role in selecting specific B-cells for survival, clonal expansion and differentiation into long-lived high-affinity memory B-cells and antibody-secreting cells[198].

We found that B-cell PM permeabilization induced by surface-associated antigen depends on the motor activity of NMII. Following BCR polarization, activated NMII accumulates at sites of B-cell binding to αM- or HEL-beads or PLB before permeabilization occurs. These findings are consistent with previous studies showing that internalization of surface-associated but not soluble antigen requires NMII-mediated traction forces at antigen-binding sites[85,121]. Collectively, our results support the notion that NMII-mediated traction forces generated during BCR-antigen interaction are responsible for permeabilization of the B-cell PM. Whether this permeabilization is due to tearing of the lipid bilayer[149] or the opening of mechanosensitive membrane channels [199,200] is currently unknown. However, our finding that three distinct membrane-impermeable probes, PI, FM lipophilic dyes, and Ponceau 4R readily gain access to the cytosol after B-cell interaction with surface-associated antigen suggest that NMII-mediated

membrane tearing is the mechanism underlying antigen-dependent B-cell PM permeabilization. In this context, it is noteworthy that Endophilin A2, a protein that facilitates the resealing of PM wounds[201], also contributes to BCR-mediated internalization of membrane-associated antigen[116].

We were initially surprised to observe B-cell PM permeabilization during BCR-mediated binding of surface-associated antigen, a process that is known to generate myosin-mediated forces as a mechanism to capture antigen. To confirm that permeabilization occurs, we utilized three different membrane-impermeable probes, two types of BCR ligands, and three types of presenting surfaces. All generated similar results. We first detected B-cell permeabilization during interaction with surface-associated antigen by following the entry of membrane-impermeable DNA-binding or lipophilic dyes. While these compounds bind to different intracellular structures, both showed sudden rather than gradual increases in intracellular staining, consistent with PM permeabilization. To strengthen these results, we designed an independent assay based on the ability of Ponceau 4R to enter B-cells and quench the fluorescence of CFSE, a widely used vital dye that covalently labels cytosolic molecules without affecting cell viability. Ponceau 4R has been used to reduce the extracellular background of fluorescence-based assays because it is membrane-impermeable and potently quenches the emission of fluorophores in the 490-560 nm range[194]. We found that Ponceau 4R influx rapidly quenches the fluorescence of CFSE-labeled B-cells, providing us with an independent and accurate tool to determine the kinetics of antigen-induced PM permeabilization.

We also showed that endocytosis does not account for the sudden, massive influx of lipophilic dyes that occurs in B-cells binding surface-associated antigen. Cross-linking surface BCRs with soluble antibodies[192,202], which did not permeabilize the B-cell PM, induced the endocytosis of lipophilic dyes - as expected from a tracer that is associated with the outer leaflet of the PM. However, the endocytosed lipophilic dye appeared as small puncta that gradually accumulated at the cell periphery, in sharp contrast to the sudden, massive dye influx that reaches

the nuclear envelope in antigen-permeabilized cells. Consistent with this result, endocytosed fluorescent Fab' covalently attached to beads also appeared as small puncta in our live imaging assays. Thus, we conclude that the sudden, massive influx of lipophilic dyes is the result of PM permeabilization but not of dye endocytosis.

The PM of primary B-cells can be damaged by phototoxicity during prolonged live imaging, or by necrosis or apoptosis. To control for such events, in parallel to our assays with surface-associated antigen, we measured the permeabilization levels of cells interacting with Tf-beads or Tf-PLB, which bind the Tf receptor with similar affinity as antigen-BCR but without BCR activation[187]. Low levels of non-specific permeabilization of B-cells could be detected in all our assays, not surprisingly given that primary splenic B-cells are often injured during the purification process. Furthermore, we did not observe an increase in apoptotic markers in B-cells interacting with surface-associated antigen. Importantly, our assays involving sequential exposure to membrane-impermeable dyes revealed that a significant fraction of the antigen-permeabilized B-cells subsequently resealed. Thus, our findings cannot be explained by a loss in B-cell viability, strongly suggesting that B-cells can become transiently permeabilized when binding antigen that is tightly associated with surfaces.

We found that two different model antigens, αM and HEL, can induce B-cell PM permeabilization when attached to surfaces. This shows that BCR binding through *bona fide* antigen-binding sites is not a requirement for generation of the mechanical forces leading to B-cell PM permeabilization. Since stiffness of the antigen-presenting surface appears to impact BCR signaling and antigen capture[120,175], it could be argued that antigen tethered to latex beads or PLB assembled on glass coverslips represent unnaturally stiff surfaces that might cause B-cell permeabilization. To investigate this issue, we utilized COS-7 cells expressing mHEL, a surface-associated antigen previously shown to engage MD4 B-cells *in vivo* when expressed in mouse

models[203]. Our finding that BCR engagement of mHEL on the surface of COS-7 cells also induces PM permeabilization supports the notion that this process occurs under physiological conditions and is likely to be relevant *in vivo*.

Not all B-cells binding surface-associated antigen were permeabilized, possibly due to heterogeneity of the primary B-cell population used in our assays. Splenic B-cells are found at different stages of peripheral maturation and differentiation[204,205], binding antigen with variable affinities at different times and generating distinct responses. In subsequent studies, it will be interesting to determine which subsets of B-cells are more effective in capturing and presenting surface-associated antigen through NMII-dependent PM permeabilization.

The rapid exocytosis of lysosomes triggered by B-cell permeabilization uncovered in our study provides a mechanistic explanation for the previously reported affinity-dependent extraction and presentation of antigen associated with non-internalizable surfaces[45]. We showed that the low affinity DEL-I antigen induces markedly lower levels of PM permeabilization, lysosome exocytosis, and antigen presentation when compared to the higher affinity HEL, when the two antigens are displayed on surfaces at similar densities. Surface association significantly enhances the avidity of antigens by increasing their valency, a process that can reduce the impact of BCR-binding affinity on BCR signaling, antigen internalization, and presentation when compared to soluble forms of the same antigen. However, this avidity effect is primarily observed with antigen associated with surfaces that B-cells are able to internalize[45], and it is known that B-cell subsets such as native follicular B-cells have very low phagocytic capacity[181]. We envision that when antigen is strongly associated with non-internalizable surfaces, low-affinity BCR-antigen interactions are disrupted before B-cells can extract antigen. In this scenario, high-affinity BCR interactions would be critical for sustaining antigen binding under NMII-mediated traction forces, to promote PM permeabilization, lysosomal enzyme release, and antigen extraction. High-

affinity BCR-antigen binding is also expected to induce more robust signaling than low-affinity binding, enabling higher levels of NMII activation[44,85] and polarization to drive PM permeabilization. Collectively, in addition to supporting the notion that tight antigen attachment to non-internalizable surfaces facilitates B-cell affinity discrimination, our results expand the mechanistic understanding of why different physical and chemical forms of immunogens impact the efficacy of vaccines[206,207].

Lysosomal exocytosis is acutely dependent on rapid elevations in $[Ca^{2+}]_i$ [159,208]. PM tears cause immediate Ca^{2+} influx and massive lysosomal exocytosis [154,159], due to the markedly higher Ca^{2+} concentration in the extracellular space compared to the cytoplasm. BCR engagement of antigen also induces $[Ca^{2+}]_i$ increases [209,210], and we cannot rule out the possibility that BCR-mediated Ca^{2+} fluxes might contribute to the initiation of lysosomal exocytosis, which would then be amplified by PM permeabilization and more robust Ca^{2+} influx. However, while BCR-induced Ca^{2+} fluxes occur in most antigen-binding B-cells within seconds of antigen binding, we found that the majority of lysosomal exocytosis and antigen internalization events occur >30 min after antigen binding, a time frame that coincides with the period required for antigen-induced PM permeabilization. Thus, our data suggest that BCR-mediated $[Ca^{2+}]_i$ increases are unlikely to be the primary driver of the lysosomal exocytosis events that facilitate endocytosis of surface-associated antigen. However, BCR-triggered Ca^{2+} fluxes may have induced the small number of initial lysosomal exocytosis events that we detected during the first 15 min of B-cell interaction with surface-associated antigen. It is also conceivable that early BCR-induced Ca^{2+} fluxes contribute to antigen-induced B-cell PM permeabilization by activating NMII and actin reorganization[211].

Collectively, our results provide important insights into the spatiotemporal relationship of events initiated by interaction of the BCR with surface-associated antigen (*Figure 7I*). Our

findings suggest that high-affinity binding stabilizes BCR-antigen interactions, inducing strong BCR signaling and NMII activation to locally generate traction forces that permeabilize the PM. Ca^{2+} entry would then trigger a localized PM repair response mediated by lysosomal exocytosis, releasing hydrolases that can cleave antigen off surfaces, facilitating endocytosis and presentation to T-cells. Our results support the notion that B-cells utilize a cellular mechanism that evolved for surviving PM injury to promote the acquisition, presentation, and possibly affinity discrimination of surface-associated antigens.

2.5 Materials and Methods

2.5.1 Mice, B-cell isolation and culture

Primary B-cells were isolated from the spleens of wild type C57BL/6, MD4 transgenic (C57BL/6 background), B10.BR-*H2*^{k2} *H2-T18*^{a}/SgSnJJrep (Jackson Laboratories), and F1 of B10.BR-*H2*^{k2} *H2-T18*^{a}/SgSnJJrep x MD4 mice using a previously published protocol[146]. Briefly, mononuclear cells were isolated by Ficoll density-gradient centrifugation (Sigma-Aldrich). T-cells were removed with anti-mouse CD90.2 mAb (BD Biosciences) and guinea pig complement (Innovative Research, Inc.) and monocytes and dendritic cells by panning. B-cells were kept at 37°C and 5% CO_2 before and during experiments. All procedures involving mice were approved by the Institutional Animal Care and Usage Committee of the University of Maryland.

The A20 B-cell lymphoma line (ATCC #TIB-208) was cultured in DMEM (Lonza) supplemented with 10% of FBS (Thermo Fisher Scientific), 0.05 mM 2-mercaptoethanol (Sigma-Aldrich), 10 mM MOPS, 100 units/ml penicillin, and 100 µg/ml streptomycin (Gemini) at 37°C and 5% CO_2. The 3A9 T-cell hybridoma line (ATCC #CRL-3293) was cultured in DMEM (ATCC) supplemented with 5% FBS (Thermo Fisher Scientific), 0.05 mM 2-mercaptoethanol (Sigma-Aldrich) at 37°C and 5% CO_2. ATCC follows the highest manufacturing standards and uses the most reliable procedures to verify and authenticate every cell line and to ensure there is no mycoplasma contamination.

2.5.2 Antigen-coated beads

Latex NH_2-beads (3 μm diameter, 3.5 x 10^8 beads/preparation, Polysciences) were activated with 8% glutaraldehyde in 0.5 ml PBS for 120 min under rotation at room temperature, washed with PBS, and incubated overnight with equal molar amounts of F(ab')$_2$ goat-anti-mouse IgM+G (αM, 20 μg/ml, Jackson ImmunoResearch Laboratories), hen egg lysozyme (HEL, 5.8 μg/ml, Sigma-Aldrich), duck egg lysozyme (DEL)-I [119], holo-transferrin (Tf, 32 μg/ml, Sigma-Aldrich), Alexa Fluor (AF) 488-conjugated Tf (AF488-Tf, 32 μg/ml, Thermo Fisher Scientific), or AF488-F(ab')$_2$ goat-anti-mouse IgM+G (AF488-αM, 20 μg/ml, Jackson ImmunoResearch Laboratories) in 1 ml PBS. Protein content determination (BCA, Thermo Fisher Scientific) of coupling solutions before and after bead incubation confirmed that similar molar amounts of protein were conjugated in each case. The beads were then blocked with PBS 1% BSA for 30 min under rotation, washed to remove unconjugated proteins, counted in a Neubauer chamber and stored at 4°C in PBS containing 1% BSA and 5% glycerol. Streptavidin-conjugated Yellow-Green latex beads (2 μm diameter, 5 x 10^8 beads/preparation, Polysciences) were washed with 1% BSA in PBS and incubated with Biotin-SP (long spacer)-conjugated Fab fragments of goat-anti-mouse IgG (H+L) (40 μg of biotinylated antibody/mg of beads, Jackson ImmunoResearch Laboratories) for 30 min at 4°C, washed, counted in a Neubauer chamber and stored at 4°C in PBS containing 1% BSA and 5% glycerol.

2.5.3 Antigen-coated planar lipid bilayers (PLB)

PLB were prepared as previously described [79,120,188]. Briefly, liposomes were generated from 5 mM 1,2-dioleoyl-sn-glycero-3-phosphocholine plus 1,2-dioleoyl-sn-glycero-3-phosphoethanolamine-cap-biotin (Avanti Polar Lipids) at a 100:1 molar ratio by sonication. Eight-well coverslip chambers (Lab-Tek) were incubated with liposomes for 20 min at room temperature and washed with PBS. The chambers were then incubated with 1 μg/ml streptavidin (Jackson ImmunoResearch Laboratories) for 10 min, washed, and incubated with 10 μg/ml mono-

biotinylated Fab' goat-anti-IgM+G (αM-PLB)[79] or the same molar amount of biotinylated Tf (16 μg/ml, Sigma-Aldrich) (Tf-PLB) for 10 min at room temperature.

2.5.4 COS-7 cells expressing membrane hen egg lysozyme-GFP (mHEL-GFP)

COS-7 cells were transiently transfected with mHEL-GFP[75] (plasmid kindly provided by Dr. Michael Gold, University of British Columbia) using Lipofectamine 3000 (Thermo Fisher Scientific) and a published protocol[175], and used for experiments 24 h post-transfection.

2.5.5 Flow cytometry analysis of PM permeabilization

Mouse splenic B-cells were incubated with beads coated with αM, HEL, DEL-I or Tf in DMEM containing 6 mg/ml BSA (DMEM-BSA) at a cell:bead ratio of 1:2 (or as indicated), or with soluble $F(ab')_2$ goat-anti-mouse IgM+G (sαM, 0.5 μg/ml) for 30 min at 37°C with 5% CO_2. Propidium iodide (PI, Sigma-Aldrich) was present during the 37°C incubation as an indicator of PM permeabilization. Cells were then analyzed by flow cytometry (BD FACSCanto II) at 10,000 cell counts/sample. Bead-bound cells were identified based on their forward- (FSC) and side-scatter (SSC) properties and on fluorescence intensity (FI) when using fluorescent beads (*Figure 1-figure supplement 2*). The percentages of PI-positive (PI+) cells among the bead-bound cell populations were quantified using FlowJo 10.1 software.

2.5.6 Live cell imaging of PM permeabilization

To assess PM permeabilization by protein-coated beads, mouse splenic B-cells or a B-cell line (A20) were incubated for 30 min at 4°C in 35 mm glass-bottom dishes (MatTek) coated with poly-lysine and then with protein-coated beads at a cell:bead ratio of 1:2 for another 30 min at 4°C. Cells were washed with DMEM-BSA and imaged in a Live Cell System chamber (Pathology Devices) at 37°C with 5% CO_2 in the presence of 50 μg/ml PI (Sigma-Aldrich) with or without 50 μM blebbistatin (Sigma-Aldrich). Images were acquired for 60 min at 1 frame/15-30 s using a spinning disk confocal microscope (UltraVIEW VoX, PerkinElmer with a 63X 1.4

N.A. oil objective). Images were analyzed using Volocity Suite (PerkinElmer) and NIH ImageJ. More than 200 cells from 3 independent experiments were analyzed for each condition.

To assess PM permeabilization after binding to ligand-coated PLB, splenic B-cells were incubated with FM1-43FX or FM4-64FX (Thermo Fisher Scientific) in DMEM-BSA for 5 min at 4°C, added to coverslip chambers containing mono-biotinylated Fab' goat-anti-IgM+G or biotinylated Tf tethered to PLB, and imaged immediately at 37°C with 5% CO_2 using a spinning disk confocal microscope (UltraVIEW VoX, PerkinElmer with a 63X 1.4 N.A. oil objective) with or without 50 μg/ml PI and/or 10 μg/ml FM1-43FX or FM4-64FX (Thermo Fisher Scientific). Images were acquired at 1 frame/6-10 s and analyzed using Volocity (PerkinElmer) and NIH ImageJ. For quantitative analysis, the mean fluorescence intensity (MFI) of FM1-43FX or FM4-64FX in a defined area was measured using Volocity (PerkinElmer). More than 270 cells from 3 independent experiments were analyzed for each condition. For 4 h videos, DMEM without phenol red containing 2% FBS was used, and images were acquired at 1 frame/30 s in the presence of PI (50 μg/ml).

PM permeabilization was also assessed using Ponceau 4R-mediated quenching of a cytosolic fluorescent dye. B-cells were pre-stained with 1 μM CFSE (Thermo Fisher Scientific) for 10 min at 37°C, washed with DMEM, incubated with αM- or Tf -PLB and analyzed in a spinning disk confocal microscope (UltraVIEW VoX, PerkinElmer with a 40X 1.4 N.A. oil objective) in the presence or absence of 1 mM Ponceau 4R (Sigma-Aldrich). More than 480 cells from four independent experiments were analyzed for each condition. To validate this method, cells pre-stained with CFSE were incubated with or without 800 ng/ml SLO in the presence or absence of 1 mM Ponceau 4R (Sigma-Aldrich) for 10 min and analyzed by flow cytometry (BD FACSCanto II) at 10,000 cell counts/sample.

To assess the ability of antigen exposed on the surface of mammalian cells to permeabilize B-cells, COS-7 cells mock-transfected or transfected with mHEL-GFP were seeded on fibronectin-coated coverslips and cultured for 24 h. WT or MD4 B-cells pre-stained with

AF674-conjugated Fab fragments of donkey-anti–mouse IgM+G (Jackson ImmunoResearch Laboratories) were then added to the COS-7 cells in the presence of 50 μg/ml PI and imaged immediately at 37ºC with 5% CO_2 using a spinning disk confocal microscope (UltraVIEW VoX, PerkinElmer with a 40X 1.3 N.A. oil objective). Images were acquired at 1 frame/20s and analyzed using NIH ImageJ software. More than 240 cells from 3 independent experiments were analyzed for each condition.

2.5.7 Cleaved caspase-3 detection

Splenic B-cells were pretreated or not with 1 μM staurosporine (Abcam) for 24 h at 37ºC in DMEM-BSA to induce apoptosis[212], exposed to αM- or Tf-beads for 30 min at 37ºC, washed, fixed with 4% paraformaldehyde (PFA), blocked with 1% BSA, and permeabilized with 0.05% saponin. Cells were then incubated with antibodies specific for cleaved caspase-3 (Asp175) (Cell Signaling Technology) followed by AF488 donkey-anti-rabbit IgG (Life Technologies) and analyzed by flow cytometry (BD FACSCanto II) at 10,000 cell counts/sample. The percentages of cells with cleaved caspase-3 staining were determined using FlowJo 10.1 software.

2.5.8 BCR signaling

BCR signaling was analyzed using both flow cytometry and western blotting. For flow cytometry assays, splenic B-cells from MD4 mice were pretreated or not with 5 μM of the Src kinase inhibitor PP2 (Millipore)[30] for 30 min at 37ºC (conditions selected not to cause B-cell toxicity) and then incubated with HEL-beads in the presence or not of the inhibitor at 37°C for 30 min. Cells were fixed with 4% PFA, permeabilized with 0.05% saponin, incubated with mouse anti-phosphotyrosine mAb (4G10, Millipore) followed by AF488-goat-anti-mouse IgG_{2b} (Thermo Fisher Scientific) secondary antibodies, and analyzed by flow cytometry (BD FACSCanto II) at 10,000 cell counts/sample. The data were analyzed using FlowJo 10.1 software.

For western blot assays, splenic B-cells from MD4 mice were pretreated or not with 10 nM of the BTK inhibitor AVL-292 (Selleckchem)[213] for 30 min at 37ºC (conditions selected not

to cause B-cell toxicity) and incubated with HEL-beads in the presence or not of the inhibitor at 37°C for 30 min. Cells were then lysed using RIPA buffer (150 mM $NaCl_2$, 1% of NP40, 0.5% Sodium deoxycholate, 0.1% SDS, 50 mM Tris, pH 8.0) containing protease and phosphatase inhibitors (50 mM NaF, 1 mM Na_3VO_4 and 10 mM $Na_4P_2O_7$) at 4°C. Cell lysates were run in 4-20% gradient SDS-PAGE gels (Bio-Rad) ($5x10^6$ cells/ lane) and transferred (Bio-Rad Trans-Blot transfer system) to PVDF membranes (Millipore). The membranes were blotted with rabbit anti-phospho-BTK (pBTK; Abcam) or anti-BTK (Cell Signaling Technology) antibodies followed by HRP-conjugated anti-rabbit antibodies (Jackson ImmunoResearch Laboratories) and visualization using ECL substrate (Bio-Rad) and imaging (iBright FL-1500, (Thermo Fisher Scientific).

To check if signaling affected PM permeabilization, splenic B-cells from MD4 mice were pretreated or not with 5 μM PP2[30] or 10 nM AVL-292[213] for 30 min at 37°C and then incubated with HEL-beads in the presence or not of the inhibitor and 50 μg/ml PI (Sigma-Aldrich) at 37°C for 30 min. The percentage of PI+ cells was expressed relative to the untreated condition.

2.5.9 BCR and NMII polarization

BCRs on the surface of mouse splenic B-cells were stained with Cy3-Fab donkey-anti–mouse IgM+G (Jackson ImmunoResearch Laboratories) for 30 min at 4°C. Cells were then incubated with αM- or Tf-beads at 4°C for 30 min and 37°C for different lengths of time. Cells were fixed with 4% PFA, permeabilized with 0.05% saponin, and incubated with rabbit anti-phosphorylated myosin light chain 2 (pMLC2) antibodies (Cell Signaling Technology) to label activated NMII [214], followed by AF633-goat-anti-rabbit IgG (Invitrogen). Cells were analyzed by confocal fluorescence microscopy (Zeiss LSM710 with a 63X 1.4 N.A. oil objective). The percentages of cells with polarization of surface labeled BCRs and activated NMII towards bead-binding sites were quantified by visual inspection. More than 300 cells from 3 independent experiments were analyzed for each condition.

2.5.10 PM repair assays

Mouse splenic B-cells were pretreated or not with 12 μM bromoenol lactone (BEL, Sigma-Aldrich) in DMEM-BSA for 30 min at 37ºC before and during assays, to inhibit lysosomal exocytosis and PM repair (Fensome-Green *et al.* 2007). Cells were then incubated with αM-beads (1:2 cell:bead ratio) with or without inhibitors at 4ºC for 5 min and 37°C for 30 min in the presence of FM4-64FX (Thermo Fisher Scientific) to stain wounded cells. Cells were then incubated with SYTOX™ Blue nucleic acid stain (300 nM, Invitrogen) at 4ºC for 10 min to stain cells that failed to repair PM wounds during the 30 min incubation. Cells were analyzed by flow cytometry (BD FACSCanto II) at 10,000 cell counts/sample. Cells that were FM4-64FX positive but SYTOX Blue negative were identified as permeabilized cells that resealed. The percentages of resealed cells among all bead-bound permeabilized cells were quantified using FlowJo 10.1 software.

To assess the resealing capacity of B-cells permeabilized by ligand-coated PLB using live cell imaging, splenic B-cells were incubated with SYTOX Green (Thermo Fisher Scientific) in DMEM-BSA for 5 min at 4ºC and added to coverslip chambers containing mono-biotinylated Fab' goat-anti-IgM+G or biotinylated Tf tethered to PLB. Cells were imaged at 1 frame/30 s for 4 h at 37°C with 5% CO_2 using a spinning disk confocal microscope (UltraVIEW VoX, PerkinElmer with a 63X 1.4 N.A. oil objective), followed by addition of 50 μg/ml PI (Thermo Fisher Scientific) at the end of the assay and final image acquisition.

2.5.11 BCR polarization in relation to permeabilization

Surface BCRs of splenic B-cells were labeled with Cy5-Fab donkey-anti mouse IgG (Jackson ImmunoResearch) at 4ºC for 30 min. Cells were incubated with αM-PLB in the presence of FM 4-64FX (Thermo Fisher Scientific) and imaged immediately at 37°C with 5% CO_2 using a spinning disk confocal microscope (UltraVIEW VoX, PerkinElmer with a 60X 1.4 N.A. oil objective). Images were acquired at 1 frame/20 s for 60 min and analyzed using a custom-made MATLAB script (MathWorks) and NIH ImageJ software. BCR polarization was

analyzed using maximal projection of XZ images and quantified by the MFI ratio between defined regions within the bottom half (closer to PLB) and the top half (away from PLB) of individual cells. Cells with bottom to top ratios ≥2 were considered polarized. More than 20 cells from 3 independent experiments were analyzed.

2.5.12 Lysosome exocytosis

To detect LIMP-2 exposed on the cell surface, splenic B-cells (C57BL/6 or MD4) were incubated with αM-, HEL-, DEL-I or Tf-beads for 30 min at 37°C, cooled to 4°C, and incubated with rabbit-anti-LIMP-2 antibodies (Sigma-Aldrich) for 60 min at 4°C. Cells were then washed and fixed with 4% PFA, washed, blocked with 1% BSA in PBS and incubated with AF488 donkey-anti-rabbit IgG (Life Technologies) secondary antibodies. For intracellular LIMP-2 staining, B-cells were fixed with 4% PFA, washed, permeabilized with 0.05% saponin for 20 min, and incubated with rabbit anti-LIMP-2 antibodies followed by AF488 donkey-anti-rabbit IgG. Flow cytometry (BD FACSCanto II) was performed at 10,000 cell counts/sample. Cells were also analyzed by confocal fluorescence microscopy (Leica SPX5 with a 63X 1.4 N.A. oil objective). Polarization of LIMP-2 towards bound beads was quantified by calculating the fluorescence intensity ratio (FIR) of anti-LIMP-2 at the B-cell-bead contact site relative to the opposite side of the cell PM, using NIH ImageJ and a custom-made MATLAB script (MathWorks).

Individual events of lysosome exocytosis were captured using total internal reflection fluorescence (TIRF). Splenic B-cells were preloaded with SiR-Lysosome (1 µM, Cytoskeleton) in the presence of verapamil (10 µM, Cytoskeleton) for 30 min at 37°C. Cells were added to coverslip chambers containing mono-biotinylated Fab' goat anti-IgM+G tethered to PLB and imaged at 37°C with 5% CO_2 in the presence of PI (50 µg/ml, Sigma-Aldrich) using a TIRF microscope (NIKON Eclipse Ti-E TIRF, 63X 1.49NA oil objective). Images were acquired at 8 frames/s during 15-20 min intervals of the 45 min incubation and analyzed using NIH ImageJ and

Nikon NIS Elements software. Increases in the FI of individual SiR-Lysosome puncta (reflecting lysosome movement within the TIRF evanescent field towards the PM in contact with PLB) followed by sharp decreases within a period of 1-2 s (corresponding to a loss of the SiR-Lysosome signal upon PM fusion) were scored as exocytosis events[208]. More than 20 cells were analyzed in 4 independent experiments.

2.5.13 FM endocytosis after BCR crosslinking.

Mouse splenic B-cells were incubated with F(ab')$_2$ goat-anti-mouse IgM+G (10 μg/ml, Jackson ImmunoResearch Laboratories) for 10 min, followed by AF674-conjugated donkey-anti-goat (10 μg/ml, Invitrogen) for 30 min at 4ºC in coverslip chambers, to label and crosslink surface BCRs. FM1-43FX (10 μg/ml, Thermo Fisher Scientific) was added at the last 5 min of the 30 min incubation at 4ºC. Cells were washed and imaged at 37°C with 5% CO_2 in the presence of 50 μg/ml PI and 10 μg/ml FM1-43FX using a spinning disk confocal microscope (UltraVIEW VoX, PerkinElmer with a 63X 1.4 N.A. oil objective). Images were acquired at 1 frame/30 s for 60 min and analyzed using Volocity (PerkinElmer).

2.5.14 Assessment of BEL toxicity

Mouse splenic B-cells were pre-treated or not with 12 μM bromoenol lactone (BEL, Sigma-Aldrich) in DMEM-BSA for 30 min at 37ºC and then incubated with Tf-beads (1:2 cell-bead ratio) with or without the inhibitors at 37°C for 30 min in the presence of SYTOX™ Blue (300 nM, Invitrogen). Cells were analyzed by flow cytometry (BD FACSCanto II) at 10,000 cell counts/sample. Bead-bound cells and SYTOX Blue positive cells were gated. The percentages of SYTOX Blue positive cells among all bead-bound permeabilized cells were quantified using FlowJo 10.1 software.

2.5.15 Antigen internalization

For live imaging of antigen internalization, splenic B-cells were incubated with AF488-αM-beads (1:4 cell:bead ratio) in the presence of 1 μM SiR-Lysosome and 10 μM verapamil for 30 min at 4°C, washed with DMEM-BSA and imaged by confocal fluorescence microscopy (Leica SPX5 with a 63X 1.4 N.A. oil objective) for 60 min at 1 frame/min at 37ºC. Live time-lapse images were analyzed using NIH ImageJ.

For fixed cell imaging, splenic B-cells were pretreated or not with 50 μM blebbistatin on poly-lysine coated slides for 30 min at 4°C and incubated with AF488-αM beads or AF488-Tf-beads at 37°C for varying lengths of time in the presence or not of 50 μM blebbistatin. After fixation with 4% PFA, cells were imaged by confocal fluorescence microscopy (Zeiss LSM710 with a 63X 1.4 N.A. oil objective). Percentages of cells with intracellularly-located AF488-αM puncta were determined by visual inspection of images. More than 200 cells from 3 independent experiments were analyzed for each condition.

For live imaging of B-cells interacting with PLB, mouse splenic B-cells were added to coverslip chambers containing PLB coated with AF488-conjugated mono-biotinylated Fab' goat-anti-mouse IgM+G and incubated at 37°C with 5% CO_2 in the presence of 10 μg/ml FM 4-64FX (Thermo Fisher Scientific) for varying lengths of time. Samples were then moved to 4°C for 5 min and immediately imaged using a confocal microscope (Leica SPX5 with a 63X 1.4 N.A. oil objective). Internalization of antigen was quantified by determining the percentages of cells with intracellularly-located AF488-Fab' goat-anti-mouse IgM+G puncta in each field and by measuring the AF488 FI associated with intracellular puncta in individual cells, using a custom-made MATLAB (MathWorks) script. Cells with high FM staining were identified as wounded and those with low FM staining as unwounded. More than 15 fields or ~90 cells from 3 independent experiments (high or low FM staining) were analyzed for each condition.

2.5.16 Antigen presentation and T-cell activation

To detect antigen presentation to T-cells, splenic B-cells from F1 mice of a crossing

between B10.BR-*H2*^{k2} *H2-T18*^{a}/SgSnJJrep and MD4 mice were co-cultured with 3A9 T-cell hybridoma cells (ATCC® CRL-3293™) at equal concentrations ($3.75x10^6$ cells/ml). Cells were incubated in DMEM supplemented with 5% FBS and 0.05 mM 2-mercaptoethanol for 72 h in the presence or not of soluble HEL or DEL-I (10 µg/ml), or of beads coated with HEL, DEL-I or Tf (1:4 cell: bead ratio). After incubation, the concentration of IL-2 in the supernatant was measured using an IL-2 ELISA kit (Biolegend).

2.5.17 Statistical analysis

Statistical significance was assessed using unpaired, two-tailed Student's *t*-tests (Prism - GraphPad software) when only two groups were compared, and one-way ANOVA (parametric) or Kruskal-Wallis (non-parametric) when 3 or more groups were compared. All data were presented as the mean ± SD (standard deviation).

Chapter 3: The molecular requirements for B cell plasma membrane permeabilization during interaction with surface bound antigen

3.1 Abstract

B cell-mediated humoral immune responses play a crucial role in neutralizing pathogens and harmful foreign substances. Antigen (Ag) binding of the B cell receptor (BCR) induce signaling cascades and Ag internalization and presentation on the MHCII for T cell recognition. T cell help is essential for B cell differentiation into high-affinity antibody-producing cells and memory B cells. *In Vivo*, antigen encountered by B cells is often tightly associated with the surface of pathogens or Ag-presenting cells. Surface-associated Ags induce actin-mediated cell spreading and contraction, which allows B cells to engage more antigen and gather the antigen-BCR into a central cluster for internalization. Previously, we showed that BCR interaction with surface Ags induces B cell plasma membrane (PM) permeabilization in a non-muscle myosin IIA (NMIIA) and BCR-antigen affinity-dependent manner. B cell PM permeabilization facilitates Ag internalization and presentation by inducing lysosomal exocytosis. However, the cellular mechanisms underlying this PM permeabilization are unknown. Here, we showed that B cells undergoing PM permeabilization spread on Ag-presenting surfaces at a faster rate and to a larger area than cells remaining intact. Ag permeabilized B cells recruit more NMIIA at a faster rate and display a unique NMIIA organization at the immune synapse. Additionally, B cells undergo spreading and NMIIA recruitment for the second time 25-30 minutes after antigen engagement and before PM permeabilization. These results suggest that Ag-induced PM permeabilization requires rapid, high extent, and persistent B cell spreading on Ag presenting surfaces and strong NMIIA recruitment to the immune synapse, providing novel insights into the cellular mechanism underlying Ag-induced B cell PM permeabilization.

3.2 Introduction

B cells are essential in generating the antibody responses responsible for neutralizing unwanted foreign substances and pathogens. Binding of the B cell receptor (BCR) to a foreign substance initiates signaling cascades that prime B cells to internalize, process, and present antigen on MHCII for T cell recognition[9]. T cells in turn provide B cells with an additional activation signal for B cells to differentiate into high-affinity antibody-producing cells or memory B cells[178]. With a large pool of clonally specific BCRs, B cells detect and bind to a large variety of antigens in distinct physical, chemical, and biochemical forms[177]. B cells are selected to survive and differentiate based on the BCR affinity to antigens in a process called affinity maturation. Affinity-independent activation of B cells leads to the production of unspecific and self-reactive antibodies, causing autoimmune disorders[15]. To ensure an effective humoral immune response, B cells undergo a process known as affinity maturation. During affinity maturation B cells undergo changes to their BCR through somatic hypermutation of their Ig gene, and B cell clones with high affinity to the specific antigen are selected for[5,9]. Affinity maturation occurs in specialized cellular structures called germinal centers in secondary lymphoid tissues[5,37,178]. In germinal centers, antigen-activated B cells undergo somatic hypermutation to their immunoglobulin genes. Only B cells with high-affinity BCRs are competitive to engage and capture antigen for signaling and antigen presentation, consequently acquiring the essential signals for surviving and differentiating into antibody-producing cells or memory B cells. Several mechanisms for B cells to differentiate high and low-affinity antigens have been proposed[45,118,120,215]; however, this process remains incompletely understood.

In vivo, antigen encountered by B cells is often tightly associated with the surface of antigen-presenting cells, such as follicular dendritic cells (FDCs), or the surface of pathogens, such as parasites, bacteria, and viruses[179]. Unlike soluble antigen, when encountering surface-associated antigen, the ability of B cells to internalize and process antigen is highly dependent on

the BCR-antigen binding affinity[45]. This suggests that surface-bound antigen facilitates B cell affinity differentiation. The interaction of B cells with antigen exposed on the surface of FDCs during affinity maturation in germinal center reactions underscores this notion. When naïve B cells encounter antigen associated with an antigen-presenting surface, a BCR signaling cascade is initiated[9,18,19], causing a reorganization of the B cell cytoskeleton through activation of actin regulatory molecules such as ezrin, WASp/N-WASp, and Apr2/3[60,94,95]. Reorganization of the actin cytoskeleton drives B cells to spread over antigen-presenting surfaces, allowing B cells to engage more antigen and form BCR microclusters. Subsequently, B cells organize BCR microclusters into a central cluster, forming an organized interaction site before antigen internalization occurs[75,76].

Using various antigen-presenting models, recent studies have proposed two distinct mechanisms for B cells to internalize antigen from presenting surfaces[45,85,89]. B cells use NMII-generated contractile forces to pull antigen from presenting surfaces. If the mechanical force alone is insufficient, extracellular lysosomal hydrolases resulting from lysosome exocytosis are required to cleave antigen from presenting surfaces[120,121]. We have recently shown that lysosome exocytosis is triggered locally by antigen-induced B cell PM permeabilization as a part of a PM repair mechanism[147]. We have further shown that antigen induced B cell membrane permeabilization is dependent on BCR-antigen binding affinity, BCR signaling, and signaling activated NMII [147]. Our findings provide another mechanism for B cell affinity discrimination: low-affinity BCR-antigen interactions will likely break before inducing membrane damage, while high-affinity interactions will stay intact upon NMII-mediated pulling and induce membrane damage that in turn causes the release of lysosomal enzymes which facilitates antigen uptake. However, it is unclear what molecular cues are required to induce PM permeabilization during surface-bound antigen interaction with the BCR.

Here we show that B cell PM permeabilization requires rapid and a great extent of cell spreading and NMIIA recruitment to the BCR-antigen interaction site. Additionally, we

discovered an apparent shift in cytoskeletal recruitment at the contact area that may provide a switch for the B cell to change from gathering antigen to antigen endocytosis. These findings suggest that thresholding levels of antigen engagement, myosin recruitment, and lysosome polarization as well as a cytoskeletal switch are required to induce and maintain sufficient NMIIA-generated force to cause PM permeabilization and facilitate antigen extraction.

3.3 Results

3.3.1 Antigen-induced B cell PM permeabilization is associated with a rapid initial B cell spreading to a large area and a second spreading event

To study the interaction of B cells with surface-associated antigen, we utilized a widely used antigen presentation model, where the pseudo-antigen ($F(ab')_2$-anti-mouse IgM+G [αM], which binds and activates the BCR), were tethered to planar lipid bilayers (PLB) by biotin-streptavidin interaction[79,120,188]. PM permeabilization of B cells binding to the αM-PLB was detected using the membrane-impermeable dye propidium iodide (PI). Intact cells exclude PI, but when the PM is permeabilized, PI enters cells and their nuclei, becoming fluorescent upon binding nucleic acids. We used naïve B cells from the spleens of unimmunized mice and interference reflection microscopy (IRM) to analyze B cell spreading on αM-PLB. Upon engaging the αM-PLB, the B cell contact area increased rapidly in the first few minutes and then gradually reached a plateau (Figure 3.1A-B). B cells that eventually became PI positive (PI+), indicating PM permeabilization, spread on the presenting surface to a larger area when compared to cells that do not become permeabilized (PI-) by the end of the detecting time (Figure 3.1A-B). We further determined the rate of B cell spreading by plotting the contact area over time for individual cells and obtaining the initial linear slope of the area increase (Figure 3.1C). The results showed that cells that later become PI+ spread at a faster rate than those that remained PI- (Figure 3.1D). Notably, after B cell spreading reaches a plateau, a subset of B cells reduced their contact area, which was followed by a recovery of the B cell contact area around 25-30 minutes

after αM-PLB engagement, whereas the contact area of the rest of B cells remained stagnant or steadily decreased over time (Figure 3.1E-F). Here, we refer to this cell population for their second spreading event (2^{o} spreading). The 2^{o} spreading mostly occurred preceding PM permeabilization and antigen internalization and 30-45 minutes after antigen engagement[147]. Importantly B cells that undergo such 2^{o} spreading initially spread faster and to a larger total area (Figure 3.1F-G). Furthermore, a much higher percentage of B cells that ultimately become permeabilized exhibit a 2^{o} spreading event than those remaining PI- (Figure 3.1H). When comparing cells that did or did not exhibit the 2^{o} spreading event, we found that cells which experience this 2^{o} spreading event are more likely to ultimately become permeabilized, compared to cells that do not undergo a 2^{o} spreading event (Figure 3.1I). Collectively, these results show that B cells that are permeabilized by αM-PLB spread faster and more extensively than those cells that do not become permeabilized. Additionally, a 2^{o} spreading event that occurs approximately 25-30 minutes after antigen engagement is potentially required for antigen-induced B cell PM permeabilization.

Figure 3.1

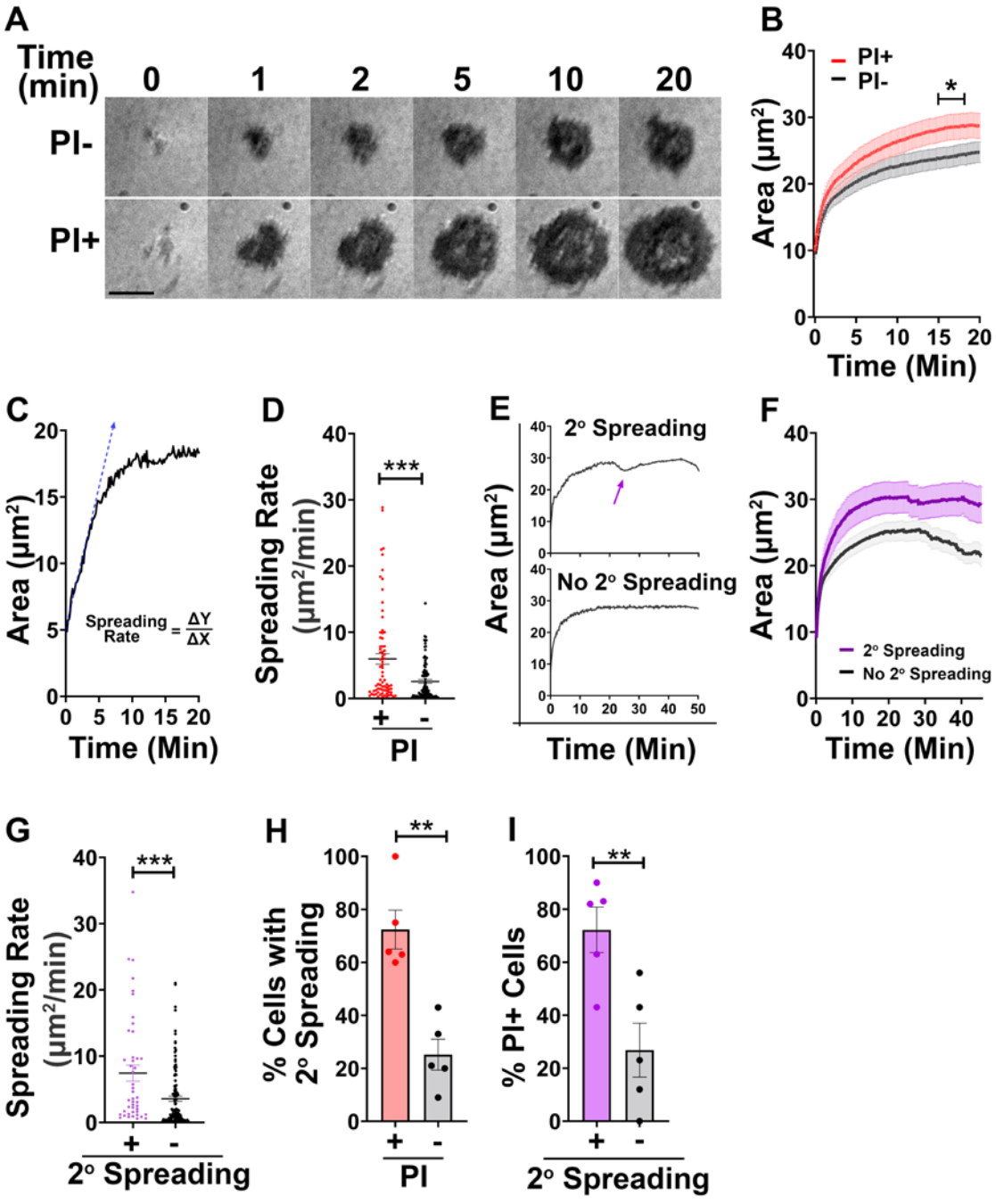
A
Time (min)
0
1
2
5
10
20
PI-
PI+
B
PI+
PI-
*
Area (μm²)
Time (Min)
C
Area (μm²)
Spreading Rate = ΔY/ΔX
Time (Min)
D
Spreading Rate (μm²/min)
***
+
-
PI
E
2° Spreading
No 2° Spreading
Area (μm²)
Time (Min)
F
Area (μm²)
2° Spreading
No 2° Spreading
Time (Min)
G
Spreading Rate (μm²/min)
***
+
-
2° Spreading
H
% Cells with 2° Spreading
**
+
-
PI
I
% PI+ Cells
**
+
-
2° Spreading

Figure 3.1. B cells permeabilized by surface-associated antigen spread rapidly to a great extent and a second spreading event. (A) Live internal reflection microscopy (IRM) imaging of primary mouse B cells interacting with F(ab')$_2$-anti-mouse IgM+G coated planar lipid bilayer (αM-PLB). Bars, 5 μm. **(B)** The average contact Area (in μm^2) of B cells on the PLB over time, comparing cells that do and do not become permeabilized. Data represent 79 cells from 3 independent experiments. **(C)** A representative plot of the contact area (in μm^2) of B cells on αM-PLB over time. The blue dotted line indicates the slope of B cell spreading. **(D)** Spreading rates (in μm^2/min) of individual B cells that do or do not become permeabilized. Data points represent individual cells from 3 independent experiments. **(C)** Representative plots of the contact area (in μm^2) of B cells on αM-PLB over time. Top panel, a cell showing a second (2^o) spreading event (purple arrow). Bottom pane, a cell not showing a 2^o spreading event. **(F)** The average contact area (in μm^2) of B cells that did or did not undergo a 2^o spreading event on αM-PLB over time. Data represent individual cells from 3 independent experiments. **(G)** Spreading rate (in μm^2/min) of individual B cells that did not undergo a 2^o spreading event. Data points represent individual cells from 3 independent experiments. **(H)** The percentage of cells undergoing a 2^o spreading event that did and did not become permeabilized. Data points indicate individual experiments. **(I)** The percentage of cells that become PIs that did and did not undergo a 2^o spreading event. Data points indicate individual experiments. Data points represent independent experiments (mean ± SEM). *$p \leq 0.05$, **$p \leq 0.01$, **$p \leq 0.005$, unpaired Student's *t*-test.

3.3.2 Surface-associated antigen-induced B cell PM permeabilization associates with a strong initial NMIIA recruitment, a secondary NMIIA recruitment event, and a NMIIA ring structure.

B cells are known to utilize myosin-generated force to extract antigen from presenting surfaces[85]. In addition to antigen extraction from the presenting surface, myosin also facilitates BCR microcluster merging into a central cluster at the interaction site[56,105,109]. We previously showed that B cell PM permeabilization in response to surface-bound antigen requires NMII activity[147]. To further examine how NMII contributes to B cell PM permeabilization, we utilized GFP-NMIIA transgenic mice. We imaged GFP-NMIIA B cells exposed to αM-PLB using live TIRF microscopy, which allowed us to visualize the recruitment and the organization of NMIIA in the contact area between B cells and αM-PLB. The mean fluorescence intensity (MFI) of GFP-NMII in the B cell contact zone increased rapidly in the first few minutes, peaked at 7~12 min, and then decreases (Figure 3.2A-B). The NMIIA MFI in the contact zone of B cells that later become PI+ was much higher than those cells remaining PI- (Figure 3.2A-B). The NMIIA MFI of PI+ cells peaked earlier (~7 min) than PI- cells (~12 min) (Figure 3.2B). To determine the rate of NMIIA recruitment, we plotted the GFP-NMIIA MFI over time for individual cells and found the linear slope in the first few minutes (Figure 3.2C). We found that cells that later became PI+ recruited MNIIA at a faster rate than cells that remained PI- (Figure 3.2D).

Figure 3.2

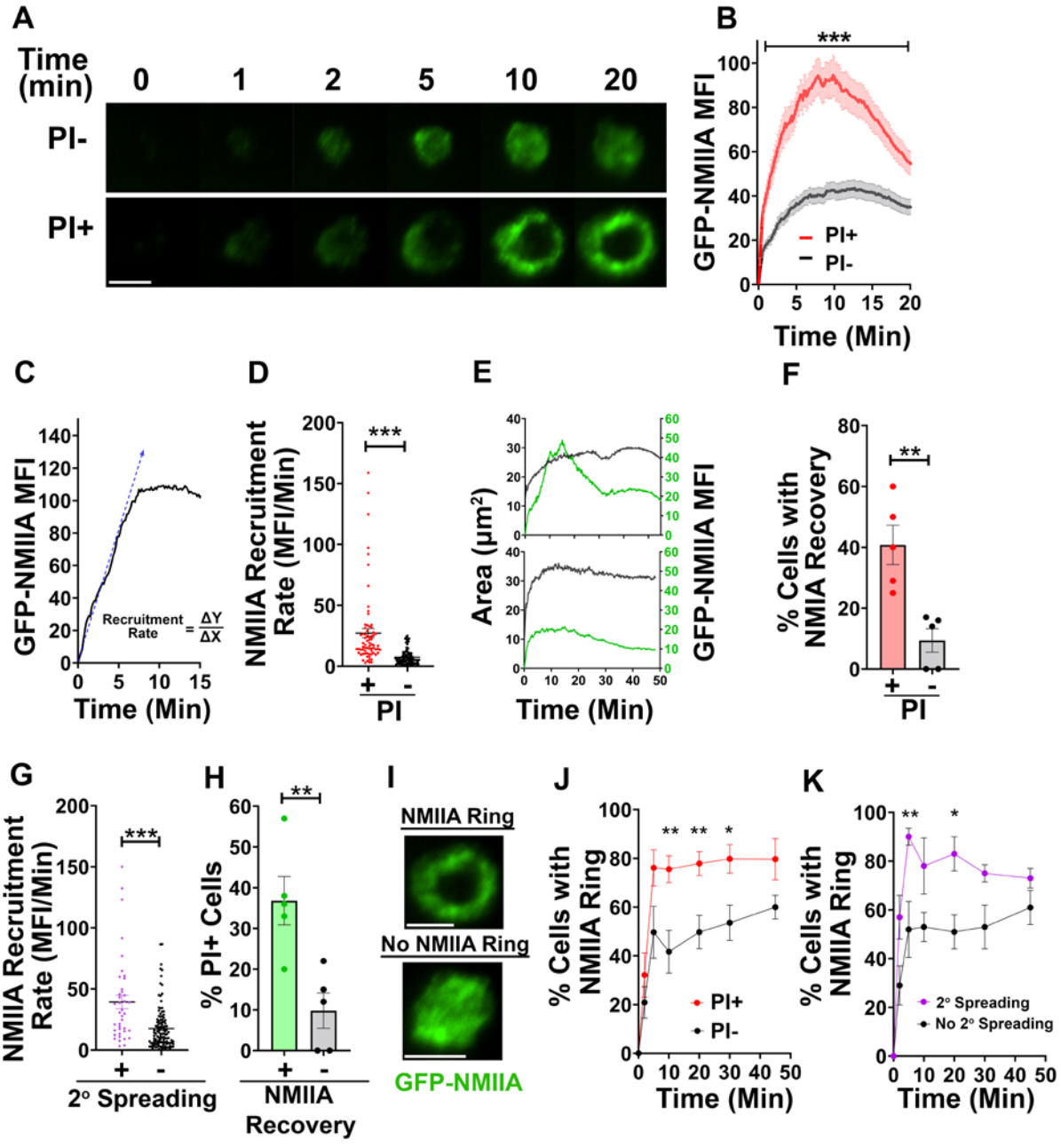
A
Time (min)
0
1
2
5
10
20
PI-
PI+
B
***
GFP-NMIIA MFI
PI+
PI-
Time (Min)
C
GFP-NMIIA MFI
Recruitment Rate = ΔY/ΔX
Time (Min)
D
NMIIA Recruitment Rate (MFI/Min)
***
PI
E
Area (μm²)
GFP-NMIIA MFI
Time (Min)
F
% Cells with NMIA Recovery
**
PI
G
NMIIA Recruitment Rate (MFI/Min)
***
2° Spreading
H
% PI+ Cells
**
NMIIA Recovery
I
NMIIA Ring
No NMIIA Ring
GFP-NMIIA
J
% Cells with NMIIA Ring
PI+
PI-
Time (Min)
K
% Cells with NMIIA Ring
2° Spreading
No 2° Spreading
Time (Min)

Figure 3.2. Surface-associated antigen-induced B cell PM permeabilization associates with a strong initial NMIIA recruitment, a secondary NMIIA recruitment event, and a NMIIA ring structure. (A) Total Internal Reflection Fluorescence (TIRF) time-lapse images of B cells from GFP-NMIIA transgenic mice interacting with αM-PLB. **(B)** The average GFP-NMIIA mean fluorescence intensity (MFI) at the contact zone of B cells that did or did not become permeabilized over time. Data represent 73 cells from 3 independent experiments. **(C)** A representative plot of the GFP-NMIIA MFI versus time in a B cell contact zone. Blue dotted line, the slope of the NMIIA MFI increase. **(D)** NMIIA recruitment rates (in MFI/min) of individual B cells comparing cells that became or did not become permeabilized. Data points represent individual cells from 3 independent experiments. **(F)** Representative plots of the contact Area (in μm^2) and GFP-NMIIA MFI at the contact area over time in B cells undergoing or not undergoing a 2^o spreading event. **(F)** Percentages of cells that experienced a NMIIA recovery after a decline among cells that did or did not become permeabilized. Data points represent individual experiments. **(G)** The average initial NMIIA recruitment rate of B cells that did or did not undergo a 2^o spreading. Data represent individual cells from 3 independent experiments. **(H)** Percentages of cells that became PI+ among cells that did or did not undergo a NMIIA recovery. Data points represent individual experiments. **(I)** Representative TIRF images of GFP-NMIIA transgenic B cells interacting with αM-PLB that did and did not exhibit a NMIIA ring structure. **(J)** Percentages of B cells with an organized NMIIA ring structure at the contact area among cells that did and did not become permeabilized. Data represent individual videos from 3 independent experiments. **(K)** Percentages of cells with NMIIA ring at the contact area among cells that did and did not undergo a 2^o spreading event. Data represent individual videos from 3 independent experiments. Data points represent independent experiments (mean ± SEM). Scale bars, 5 μm. *$p \leq 0.05$, **$p \leq 0.01$, **$p \leq 0.005$, unpaired Student's *t*-test.

After early recruitment of NMIIA to the contact area, most cells exhibited a steady decrease in NMIIA MFI (Figure 3.2A, E). However, a subset of B cells stopped this decrease and recovered or maintained their NMIIA MFI in the contact zone (Figure 3.2E). Interestingly, this recovery of NMIIA occurred at a time window similar to the 2º spreading event (Figures 3.1E and 3.2E). We also found that the B cell population that later became permeabilized, as determined by PI entry, were more likely to display a NMIIA recovery when compared to cells that remained PI- (Figure 3.2F). When comparing B cells that did not undergo a 2º spreading, B cells that undergo a 2º spreading event recruited NMIIA at a faster rate during the early stages of antigen engagement (Figure 3.2G). Furthermore, cells that exhibited a NMIIA recovery were more likely to become permeabilized later, compared to cells with a continuous decrease in NMIIA at the contact zone (Figure 3.2H). Collectively, these data show a potential threshold rate and level of NMIIA recruitment to the antigen interaction site for B cell permeabilization and suggest that the NMIIA recovery and persistence may support the 2º spreading event prior to B cell PM permeabilization.

We next analyzed the spatial organization of NMIIA at the contact area. When B cells engage antigen on the surface of presenting cells, B cells form an organized interaction site that facilitates the formation of a central BCR cluster. NMII is often observed to localize with actin at the distal area surrounding the central area of the contact zone. NMIIA associates with actin and facilitates the inward movement of BCR clusters into a central cluster[56,109,130]. Using TIRF microscopy, we visualized the formation of GFP-NMIIA ring structures at the antigen interaction surface in individual B cells upon interacting with an αM-PLB (Figure 3.2I) and determined the percentages of B cells with the NMII ring structures. We found that cells that become permeabilized were more likely to form NMII ring structures and do so more rapidly when compared to cells that remained intact (figure 3.2J). Furthermore, B cells which underwent a 2º spreading are more likely to form a NMIIA ring than those B cells that did not spread for the

second time (Figure 3.2K). These data suggest that the formation of a NMIIA ring structure may facilitate NMII-dependent B cell PM permeabilization by surface associated antigens.

3.3.3 Fast and strong polarization of lysosomes towards the antigen binding site is associated with surface-bound antigen-induced B cell PM permeabilization

Myosin-generated forces can cause B cell PM permeabilization during interactions with surface associated antigen, which induces lysosome exocytosis. Released lysosomal enzymes cleave antigen from presenting surfaces[89,120]. Lysosomal compartments recruited to the BCR-antigen interaction site have also been shown to facilitate antigen processing and loading onto MHCII for presentation to T cells[91]. To analyze lysosome dynamics during B cell-antigen interaction, we labeled lysosomes using the SiR-Lysosome probe designed for live imaging and tracked B cell PM permeabilization using a membrane-impermeable lipophilic FM dye. The FM dye has previously been used to determine PM integrity, as they stain only the outer leaflet of the PM in intact cells, but upon membrane disruption, the dye enters the cytoplasm and stains the inner leaflet of the PM and intracellular membranes, including the nuclear envelope[189–191]. Using these probes and spinning disc confocal fluorescence microscopy, we analyzed the localization of lysosomes in B cells during interaction with αM-PLB at different times. We found that the majority of B cells recruited lysosomes to the antigen interaction site upon engaging αM-PLB (Figure 3.3A-B). Notably, a higher percentage of B cells showing increased FM fluorescence intensity (FM^{Hi}), indicating membrane permeabilization, exhibited lysosomal polarization towards the interactions site than those without increased FM fluorescence intensity (FM^{Low}) (Figure 3.3B). Utilizing SiR-Lysosome probe and live-cell TIRF microscopy, we further measured the MFI of SiR-Lysosome at the antigen interaction site over time. We found that SiR-Lysosome MFI in the contact zone of B cells that later became permeabilized but not those that remained intact increased significantly and peaked at ~17 min, indicating more lysosome recruitment to the antigen interaction site (Figure 3.3C-D). However, the MFI of SiR-Lysosomes

decreased afterward in cells that became PI+ but remained higher than cells that remained PI-. We further measured the rate of this lysosome recruitment (Figure 3.3E) and found that cells that became PI+ recruited lysosomes at a much higher rate than cells that remain PI- (Figure 3.3F). Together, these data show that B cells exhibited a strong polarization of lysosomes towards antigen presenting surfaces before becoming permeabilized.

Figure 3.3

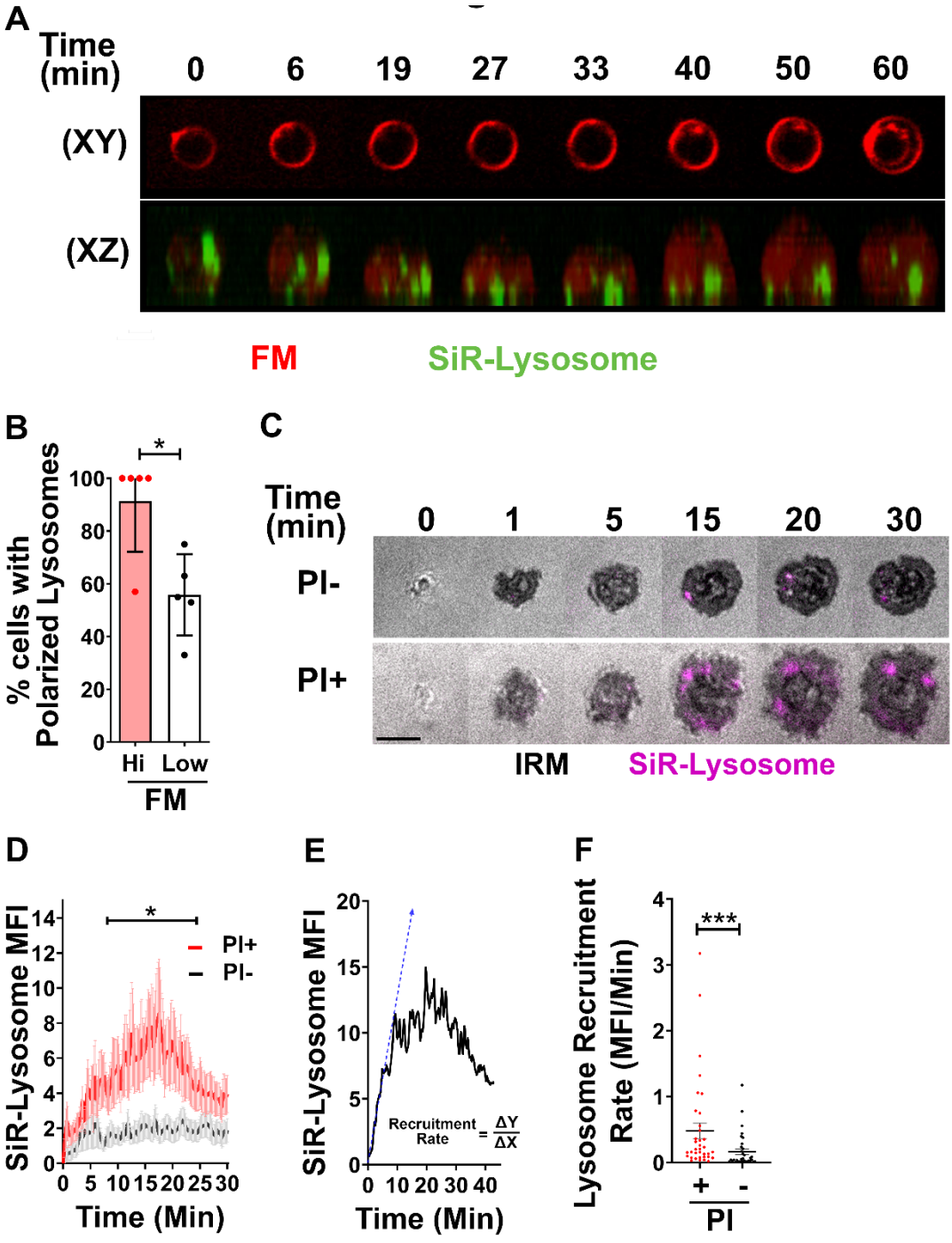
A
Time (min)
0
6
19
27
33
40
50
60
(XY)
(XZ)
FM
SiR-Lysosome
B
% cells with Polarized Lysosomes
*
Hi
Low
FM
C
Time (min)
0
1
5
15
20
30
PI-
PI+
IRM
SiR-Lysosome
D
SiR-Lysosome MFI
*
PI+
PI-
Time (Min)
E
SiR-Lysosome MFI
Recruitment Rate = ΔY/ΔX
Time (Min)
F
Lysosome Recruitment Rate (MFI/Min)
***
+
-
PI

Figure 3.3. A fast and strong lysosome polarization towards antigen presenting surface is associated antigen-induced B cell PM permeabilization. (A) Time-lapse images of SiR-Lysosome staining in mouse primary B cells interacting with αM-PLB in the presence of FM by spinning disk confocal microscopy. **(B)** Percentages of B cells with polarized lysosomes among cells that did and did not exhibit increased FM staining. **(C).** Time-lapse TIRF and IRM images of SiR-Lysosome staining at the contact zone of B cells interacting with αM-PLB. **(D)** The average SiR-Lysosome MFI (± SEM) at the contact zone of B cells that did and did not become permeabilized by αM-PLB. Data represent 37 cells from 3 independent experiments. **(E)** A representative plot of the SIR-Lysosome MFI in the contact zone of a B cell interacting with αM-PLB over time. Blue dotted line, the slope of SiR-Lysosome increase. **(F)** The average SiR-Lysosome recruitment rate (in MFI/min) (± SEM) of individual B cells that did or did not become permeabilized. Data points represent individual cells taken from 3 independent experiments. Scale bars, 5 μm. *$p \leq 0.05$, **$p \leq 0.01$, **$p \leq 0.005$, unpaired Student's *t*-test.

3.4 Discussion

Antigen extraction from the surface of presenting cells plays an important role in B cell affinity discrimination necessary for affinity maturation and generating high-affinity anybody producing and memory B cells. It has been shown that B cells utilize two district mechanisms to extract antigen from presenting surfaces, (1) the use of mechanical force to pull antigen from the presenting surface[85], and (2) the secretion of lysosomal enzymes to cleave the antigen from the presenting surface[89,120]. It has been hypothesized that B cells initially attempt to pull antigen from its presenting surface using myosin-generated force. In this case, the effectiveness of antigen endocytosis is determined by both the BCR-Ag binding affinity, and the mode of antigen presentation. During NMII-mediated pulling, low-affinity interactions will be broken while high-affinity interactions can overcome the pulling, providing a mechanism for B cells to differentiate between high and low-affinity antigen[120]. If high-affinity antigen is weakly associated with the presenting surface, myosin mediated traction force can pull the antigen from the presenting surface, allowing internalization. However, if antigen is strongly associated with the presenting surface, B cells cannot pull the antigen from the presenting surface. In this case, antigen internalization requires external lysosomal enzymes to cleave antigen off presenting surfaces[89,120].

Our recently published data show that myosin-generated forces can disrupt the B cell PM during extraction of high-affinity antigen strongly attached to presenting surfaces and induce lysosome exocytosis as part of a repair response, thus providing a molecular mechanism for the B cells to switch from mechanical to chemical antigen extraction[147]. These data demonstrate the importance of PM permeabilization for B cells to capture and present antigen strongly attached to rigid surfaces. However, the cellular requirement for inducing PM permeabilization remained unclear. In this study, we demonstrate the importance of rapid initial B cell spreading to a large area on the antigen-presenting surface and a 2^{o} B cell spreading event before B cell PM

permeabilization. We furthermore showed that the rapid initial recruitment of a large amount of NMIIA to the antigen interaction site and the ability to maintain NMII polarization may also play an important role in inducing PM permeabilization. NMIIA recruited to the contact zone organizes into a ring structure at the distal regions of the contact area. In addition to NMIIA recruitment, higher levels of lysosome polarization to the antigen interactions site are also associated with B cell PM permeabilization. Thus, fast and strong cell spreading and NMIIA and lysosome polarization are likely critical for inducing B cell PM permeabilization in response to surface-bound antigens.

We observed a heterogeneity in antigen-induced PM permeabilization in primary mouse B cells, among which some cells became permeabilized, while others did not. Splenic B cells from non-immunized mice are known to include various subsets, including transitional, marginal zoon, and follicular B cells[204,205]. As a result of this, individual cells are likely to respond differently to antigen stimulation. We previously found that only a percentage of all primary B cells exposed to the surface-bound αM become permeabilized[147]. We examined how individual cells responded to engaging surface-bound antigen in order to determine what is required to induce B cell PM permeabilization. B cells are known to spread on the antigen-presenting surface in response to antigen engagement, which allows B cells to engage and gather more antigen, increasing their BCR signaling and ultimately internalization of more antigen [44,56,75]. Here, we found that cells that ultimately undergo PM permeabilization initially spread faster and to a larger area than cells that do not undergo PM permeabilization. The increased B cell spreading suggests that B cell PM permeabilization requires BCR engagement of sufficient antigen, generating signaling over a certain threshold. It is important to note that in this study we did not examine whether B cells that become permeabilized and spread to a larger area engage more antigen and induce higher levels of BCR signaling. However, we previously showed that inhibition of BCR signaling does reduce B cell PM permeabilization[147], suggesting that cells with lower levels of

BCR signaling are less likely to become permeabilized. Furthermore, unpublished data from our lab show that reductions in antigen density on presenting surfaces decrease B cell spreading and B cell PM permeabilization, suggesting that high levels of antigen engagement may be important in inducing B cell PM permeabilization. This notion is further supported by previous findings that low affinity or low valency antigen is less effective in activating B cells and inducing a T cell response[32,43,77,117]. In future studies, we will slow down or reduce B cell spreading by perturbing the actin cytoskeleton to examine their effect on B cell PM permeabilization, which will establish a direct link between B cell spreading and B cell PM permeabilization.

Myosin-generated forces play an essential role in antigen extraction from presenting surfaces[85]. BCR signaling induces cytoskeleton reorganization. Actin polymerization drives B cells to spread on the antigen-presenting surface[44,56,102]. Cell spreading enables B cells to engage more antigen and form more BCR microclusters. The centripetal flow of actin moves antigen microclusters into a large central cluster, ultimately forming immune synapses prior to antigen uptake. It has been suggested that in addition to actin, myosin plays an important role in establishing a central BCR cluster by forming actomyosin arcs that facilitate the inward movement of antigen[56,101,104,110]. Our recently published data show that the motor activity of NMII is required for B cell PM permeabilization by surface associated antigen [147]. This study observed that cells that became permeabilized recruit more NMIIA to the contact area, and do so at a faster rate than cells that do not become permeabilized. Furthermore, B cells that eventually became permeabilized are more likely to form an NMIIA ring structure at the contact zone, which persisted at least until the PM became permeabilized. This myosin ring structure is similar to the myosin organization observed at immune synapses, where a central cluster of receptors, devoid of cytoskeletal protein, is surrounded by an area of organized actin and myosin[77,82,83]. These results together suggest that the organized cytoskeleton at the B cell-APC interaction site may be required to generate forces that induce B cell PM permeabilization. Future studies should analyze

the level, location, and timing of forces generated using traction force microscopy or molecular DNA-based force probes[136,215], which will provide insights into the specific myosin forces responsible for B cell PM permeabilization.

We additionally showed that cells that become permeabilized show higher levels of polarization of lysosomes to the BCR-antigen interaction site. Lysosome exocytosis is required to repair possible disruptions of the membrane. Meanwhile, lysosome exocytosis provides extracellular proteases for the cleavage of the antigen from its presenting surface. Furthermore, lysosomes play an important role in the processing of internalized antigen by fragmenting protein antigen into peptides for MHCII loading and presentation. B cell polarity is induced by polarized BCR signaling, suggesting that strong BCR signaling will cause more pronounced B cell polarization. Polarized B cells may recruit endocytic machinery to the interaction site. We found that cells with strong lysosome polarization are more likely to become permeabilized. Our findings are consistent with previous research which found that cell polarity and polarization of lysosomes are essential for B cell activation and the internalization and processing of antigen[61,91,216]. Furthermore, research has found that cell polarity facilitates the recruitment of various molecules that play an important role in exocytosis and secretion, including Vamp-7, and various exocyst associate proteins[61,164,217]. These together suggest that cell polarization may play an important role in B cell PM repair in response to antigen-induced permeabilization. Previous studies showed that BCR signaling activates polarity proteins, including Cdc42 and Par3, which facilitate the polarization of the B cell towards the antigen interaction site[61,90]. Dynein has been shown to mediate the polarization of the microtubule organization center (MTOC) towards BCR-antigen interaction sites, which is essential for the recruitment and exocytosis of lysosomes[61,89]. Cell polarity thus prepares B cells for PM repair upon permeabilization and provides localized releasing lysosomal enzymes to cleave antigen from presenting surfaces. Without MTOC and lysosome polarization, B cells may not be able to induce a prompt and efficient repair response

upon becoming permeabilized and may die before extracting antigen. It is important to note here that we only examined lysosome polarization and did not examine other indicators of cell polarity. In future studies, we will analyze the polarization of microtubules and MTOC as well as the activation of various polarization-associated proteins such as Cdc42 and Par3. It will be interesting to see how inhibition of cell polarization affects B cell permeabilization and its subsequent repair.

Surprisingly, a majority of B cells that became permeabilized underwent a 2^{o} spreading event, which was associated with a discontinuation of NMIIA decline at antigen interaction sites before PM permeabilization. We found a strong association between the 2^{o} spreading and PM permeabilized. After the initial recruitment of NMIIA during B cell spreading, there is a steady decrease in NMIIA fluorescence at the immune synapse. Such a decrease could be a result of BCR signaling downregulation. Upon central cluster formation, BCR signaling is downregulated to prevent overstimulation[56,78]. In cells that undergo a 2^{o} spreading event, this NMIIA decrease appears to be disrupted, often followed by a mild recovery of myosin recruitment. At this time, it is unclear what causes this 2^{o} spreading event. It is possible that upon BCR central cluster formation, B cells further reorganize the actin cytoskeleton from centripetal flow to exert forces to BCR-antigen binding sites for antigen extraction. Notably, the 2^{o} spreading event was often preceded by a decrease in the contact area, a transient contraction. Interestingly, a discontinuing decline of NMIIA occurs concurrently with the 2^{o} spreading event, further supporting the possibility of another cytoskeleton reorganization before PM permeabilization. The finding that B cells which underwent a 2^{o} spreading event are also more likely to show an organized ring structure of NMIIA suggests the immune synapse formation may be necessary for cells to extract antigen from presenting surfaces, and shows a correlation between the 2^{o} spreading and myosin recruitment event. As it is well established that B cells use NMII-generated forces to pull antigen from presenting surfaces[85], it is possible that this 2^{o} myosin recruitment event is responsible for

generating the force that ultimately leads to B cell PM permeabilization. Upon most surface BCRs clustering into a central cluster, B cells cannot further recruit antigen into a central cluster and switch to antigen uptake by recruiting NMIIA again, which facilitates the pulling of the antigen from the presenting surface. If B cells are not sufficiently activated and do not efficiently establish a central BCR cluster, they do not recruit sufficient amounts of NMIIA and maintain it, consequently failing to acquire antigen through PM permeabilization.

Taken together, our data provide a possible explanation for how B cells regulate their affinity maturation by inducing lysosome exocytosis mediated antigen extraction only in response to high avidity surface-associated antigen. It is known that surface associated antigen with low-affinity or low-density are ineffective in activating B cells for survival and differentiation, as low-avidity antigen induce low levels of BCR signaling that is insufficient for inducing antigen internalization. Antigen avidity is a determining factor for the extent of BCR signaling and antigen internalization[32,43,77,117]. Previous studies from the Batista lab and unpublished data from our lab show that the extent of B cell spreading depends on antigen affinity and density[44,45]. Furthermore, the accumulation and the reorganization of the cytoskeleton at the interaction surface are also dependent on antigen avidity on presenting surface. These findings explain what we observed previously that surface antigen with a low affinity is ineffective in inducing B cell PM permeabilization and the internalization and presentation of the antigen[147]. Together, these suggest that a certain level of BCR activation is required to induce sufficient B cell spreading on antigen presenting surfaces, cytoskeletal reorganization, and the formation of an organized B cell-APC interaction site. Multi-staged reorganization of the cytoskeleton is required to mediate B cell spreading, organization of the immune synapse, and pulling antigen from presenting surfaces. This leads the B cell to initiate antigen extraction through the recruitment of more myosin which generates the force required to pull the antigen from the presenting surface[85]. It thus stands to reason that only cells with sufficient BCR activation, and which create an organized B cell-APC

interaction site, are able to generate sufficient myosin pulling force to cause PM permeabilization and help facilitate the release of the antigen from the presenting surface.

3.5 Materials/methods

3.5.1 Mice and B-cell isolation

Primary B-cells were isolated from the spleens of wild type C57BL/6 or MNIIA-GFP transgenic (C57BL/6 background) mice using a previously published protocol[146]. Briefly, mononuclear cells were isolated by Ficoll density-gradient centrifugation (Sigma-Aldrich). T-cells were removed with anti-mouse CD90.2 mAb (BD Biosciences) and guinea pig complement (Innovative Research, Inc.), and monocytes and dendritic cells by panning. B-cells were kept at 37°C and 5% CO_2 before and during experiments. All procedures involving mice were approved by the Institutional Animal Care and Usage Committee of the University of Maryland.

3.5.2 Antigen-coated planar lipid bilayers (PLB)

PLBs were prepared as previously described[79,120,188]. Briefly, liposomes were generated from 5 mM 1,2-dioleoyl-sn-glycero-3-phosphocholine plus 1,2-dioleoyl-sn-glycero-3-phosphoethanolamine-cap-biotin (Avanti Polar Lipids) at a 100:1 molar ratio by sonication. Eight-well coverslip chambers (Lab-Tek) were incubated with liposomes for 20 min at room temperature and washed with PBS. The chambers were then incubated with 1 μg/ml streptavidin (Jackson ImmunoResearch Laboratories) for 10 min, washed, and incubated with 10 μg/ml mono-biotinylated Fab' goat-anti-IgM+G (αM-PLB)[79] for 10 min at room temperature. Chambers were washed and uses immediately.

3.5.3 Live TIRF microscopy imaging

Wild type C57BL/6 or MNIIA-GFP transgenic B cells were isolated from a mouse spleen. If required, splenic B-cells were preloaded with SiR-Lysosome (1 μM, Cytoskeleton) in

the presence of verapamil (10 µM, Cytoskeleton) for 30 min at 37ºC. Cells were added to coverslip chambers containing mono-biotinylated Fab' goat anti-IgM+G tethered to PLB and imaged at 37°C with 5% CO_2 in the presence of PI (50 µg/ml, Sigma-Aldrich) using a TIRF microscope (NIKON Eclipse Ti-E TIRF, 63X 1.49NA oil objective). Imaging was done in DMEM containing 6 mg/ml BSA (DMEM-BSA) and 50µg/ml PI. Images were acquired at 6 frames per minute for 60 minutes. Images analysis was done using NIH Image J and Matlab (Mathworks). The contact area (μm^2) was detected using IRM, while mean fluorescence intensity (MFI) was detected from the total fluorescence intensity/contact area.

3.5.4 Spreading rate and fluorescence recruitment rate

The rate of early B cell spreading and the rate of early fluorescence recruitment were calculated using Matlab (Mathworks). For this, the area (μm^2) or mean fluorescence intensity (MFI) were plotted against time. A linear fit line was found for the early spreading or fluorescence recruitment, and the slope of this line was calculated to provide a relative rate of spreading or fluorescence recruitment.

3.5.5 2º spreading event analysis

A 2º contact area spreading event was analyzed by plotting the contact area, as determined by IRM imaging, against time. A 2º spreading event was identified manually. Cells with a significant decrease over general fluctuations in contact area followed by a sustained increase were considered to have a 2º spreading event.

3.5.6 NMIIA recruitment recovery event analysis

A NMIIA recruitment recovery event was analyzed by plotting NMIIA MFI, as determined by TIRF imaging, against time. A NMIIA recruitment recovery event was identified manually. Cells with a significant and sustained increase over general fluctuations in MFI following a steady decrease in MFI were considered to have a NMIIA recruitment recovery event.

3.5.7 Spatial NMIIA organization analysis

NMIIA-GFP transgenic B cells interacting with a PLB were imaged using a TIRF microscope (NIKON Eclipse Ti-E TIRF, 63X 1.49NA oil objective). Cells were analyzed at various time points (2, 5, 10, 20, 30, and 45 minutes) to determine the presence of a NMIIA ring structure. The presence of a NMIIA ring structure was determined visually. Cells with a significant decrease in fluorescent intensity of NMIIA-GFP toward the center of the cell, when compared to the surrounding regions of the cell were considered to have a ring structure.

3.5.8 Lysosome polarization

Splenic B-cells were preloaded with SiR-Lysosome (1 μM, Cytoskeleton) in the presence of verapamil (10 μM, Cytoskeleton) for 30 min at 37ºC. Cells were incubated with αM-PLB in the presence of FM 4-64FX (Thermo Fisher Scientific) and imaged immediately at 37°C with 5% CO_2 using a spinning disk confocal microscope (UltraVIEW VoX, PerkinElmer with a 60X 1.4 N.A. oil objective). Images were acquired at 1 frame/20 s for 60 min and analyzed using a custom-made MATLAB script (MathWorks) and NIH ImageJ software. Lysosome polarization was analyzed using maximal projection of XZ images and quantified by the MFI ratio between defined regions within the bottom half (closer to PLB) and the top half (away from PLB) of individual cells. Cells with bottom to top ratios ≥2 were considered polarized.

3.5.9 Statistical analysis

Statistical significance was assessed using unpaired, two-tailed Student's *t*-tests (Prism - GraphPad software). All data were presented as the mean ± SEM (Standard Error of the Mean).

Chapter 4: Discussion

4.1 B cell PM permeabilization in response to surface-associated antigen

4.1.1 Permeabilization and repair

The research in this dissertation describes a novel mechanism B cells use to extract antigen from antigen-presenting surfaces. We found that B cell plasma membrane (PM) permeabilization occurs in response to surface-associated antigen, and identified a functional role for the subsequent repair response in B cell antigen internalization and presentation to T cells. Encountering foreign antigen initiates naïve follicular B cells to become activated and differentiate into antibody-producing cells or memory B cells. *In vivo*, B cells often encounter antigen associated with the surface of pathogens, such as parasites, bacteria, and viruses, or antigen-presenting cells, such as follicular dendritic cells[197]. Follicular dendritic cells capture antigen drained into the lymph node and present the antigen to B cells, increasing the likelihood of B cells encountering antigen and the avidity of the antigen presented to B cells[16]. B cells more efficiently differentiate high and low-affinity antigen when the antigen is presented on a surface than antigen in soluble form. Therefore, it is essential to understand how B cells interact with surface-associated antigen[45]. Internalization of surface-associated but not soluble antigen has been shown to involve myosin-generated pulling forces and the release of lysosomal enzymes to facilitate the release of antigen from the presenting surface[89,218]. Using membrane-impermeable dyes and a variety of antigen-presenting models, including antigen conjugated beads, antigen tethered to a planar lipid bilayer, and antigen presented on the surface of antigen-presenting cells, we demonstrated B cell PM permeabilization events occur in response to surface-bound antigen, but not in response to soluble antigen or interaction with surface-bound transferrin (which binds the transferrin receptor with similar affinity with which the HEL antigen binds the BCR). Importantly, we observed an influx of a membrane-impermeable dye originating from the antigen interaction site, indicating membrane disruptions occur specifically at the site of antigen

interaction. We demonstrated the permeabilization of the B cell membrane using various permeabilization markers, including the membrane-impermeable nucleic acid stain propidium iodide, the membrane-impermeable lipophilic probe FM, and the fluorescence quenching by the membrane-impermeable ponceau-4R.

Previous research from our lab showed that B cells can repair PM permeabilizations caused by the pore-forming toxin SLO using a repair process involving lysosome exocytosis and endocytosis[146]. Here we showed that B cells used a similar lysosome exocytosis mediated repair response to reseal their PM after becoming permeabilized in response to surface-bound antigen. Upon PM permeabilization, a rapid influx of extracellular Ca^{2+} into the cytoplasm from the disrupted site induces the exocytosis of lysosomes. Lysosome exocytosis releases enzymes extracellularly, including acid sphingomyelinase (ASM), which generates ceramide that is preferentially localized on lipid raft domains and induces endocytosis of the disrupted membrane to effectively repair the membrane[149,159]. We demonstrated lysosome exocytosis by significant increases in the surface detection of the luminal domain of LIMP-2, a lysosomal membrane protein, and by imaging events of lysosome fusion with the PM at antigen binding sides, specifically in cells that became permeabilized. Additionally, we confirmed that cells permeabilized by surface associated antigen are able to reseal their PM by their ability to exclude membrane impermeable dyes after becoming initially permeabilized. The requirement of lysosome exocytosis for membrane repair is supported by the observation that inhibition of lysosomal exocytosis using the inhibitor BEL reduces the ability of cells to reseal their PM. These results suggest that upon PM permeabilization by surface-associated antigen, B cells induce a lysosome exocytosis-dependent repair response to retain their membrane integrity.

Currently, the cellular process of surface antigen causing B cell PM permeabilization in response remains unclear. We hypothesize that the PM permeabilization is caused by membrane shearing due to mechanical stress, as significant traction and pulling forces have been shown to

be generated at BCR-antigen interaction sites[120,219]. However, we cannot rule out that the permeabilization we observe is caused by the opening of mechanosensitive channels due to the same forces[199,200]. Moving forward, it will be interesting to take a closer look at the physiology of the PM to determine the extent and the origin of the PM permeabilizations during the engagement of surface-bound antigen, and to determine the relationship between B cell PM permeabilization and intercellular forces. For this, the spatial origins of B cell forces generated at BCR-antigen interaction sites can be imaged using traction force microscopy or DNA-based molecular force probes. Furthermore, it would be of interest to determine if permeabilization occurs as a result of the opening of non-specific mechanosensitive channels or physical disruptions of the PM. For this, electron tomography could be used to directly visualize membrane disruptions at the B cell antigen interaction site.

4.1.2 The effect of PM permeabilization on B cell activation

Upon discovering B cell PM permeabilization in response to surface-bound antigen, we further examined whether this PM permeabilization and subsequent repair play a role in B cell activation. Previous research showed that the extracellular release of lysosomal enzymes facilitates antigen uptake into B cells[89]. Therefore, we hypothesized that the lysosome exocytosis repair response might facilitate antigen endocytosis when it occurs at antigen interaction sites. Indeed, B cells are able to internalize antigen from the presenting surface. Importantly, antigen internalization occurs within the same timeframe as PM permeabilization, supporting that PM permeabilization facilitates antigen endocytosis. Furthermore, inhibition of NMII-generated forces, which are required to induce PM permeabilization, inhibits B cell internalization of antigen. The finding that B cells which become permeabilized are more likely to internalize antigen and internalize more antigen at the same time window as B cell PM permeabilization shows a direct correlation between PM permeabilization and antigen endocytosis. Thus, antigen induced B cell PM permeabilization and subsequent repair facilitate antigen endocytosis by

triggering lysosome exocytosis and the extracellular release of lysosomal enzymes that cleave antigen at the interaction site.

After antigen internalization, B cells process and present antigen fragments to T cells on their MHCII in order to induce T cell activation and signaling. We determined the effect of B cell PM permeabilization on T cell activation, utilizing a T cells hybridoma that specifically recognizes a conserved HEL peptide displayed on the MHCII of B cells from the Ig transgenic mice MD4, whose BCRs specifically bind HEL. We additionally used a pair of high-affinity (HEL, recognized with high affinity by MD4 B cells' BCR) and low-affinity antigen (DEL, recognized with low affinity by the MD4 B cells' BCR)[147]. While no difference in T cell activation was detected after MD4 B cells were exposed to the soluble form of the high or low-affinity antigen, B cells exposed to surface-bound high-affinity antigen activate T cells more effectively than B cells that were exposed to low-affinity antigen. This suggests that low-affinity antigen, which fails to induce PM permeabilization, is not internalized to the same degree as high-affinity antigen, which does induce PM permeabilization. Together, our data show that PM permeabilization is a critical step for B cells to internalize and present antigen that is tightly attached to presenting surface in a binding affinity dependent manner. Moving forward, we will compare antigen presentation levels in individual B cells that are or are not permeabilized by antigen. Additionally, it would be interesting to see the effect of inhibition of the B cell PM repair response, using a lysosome exocytosis inhibitor such as BEL, on antigen presentation to T cells.

Our combined data suggest that B cell PM permeabilization in response to surface-bound antigen plays a critical role in antigen internalization and presentation to T cells. We suggest that when BCR engaging surface-associated antigen induces signaling, which activates actin reorganization and actomyosin-generated force at BCR-antigen interaction sites. NMII-generated forces pull antigen through engaging BCR, causing permeabilization of the B cell PM, likely through membrane shearing or possibly by activating mechanosensitive channels. This membrane

permeabilization will in turn induce a lysosomal exocytosis-dependent repair response. The release of lysosomes at the antigen interaction site will facilitate the cleavage of antigen from the presenting surface. This in turn facilitates the uptake of the antigen into the B cell for processing and presentation (Figure 2.7I). It is possible that in addition to the cleavage of antigen from the presenting surface, the release of lysosomal enzymes also induces B cell endocytosis. A lysosome enzyme, acid sphingomyelinase, cleaves sphingomyelin lipids and generates ceramide-rich lipid rafts at BCR-antigen interaction sites. Lipid rafts are known to be vital for both BCR signaling and antigen internalization[18,30,220]. The formation of ceramide-rich domains induces endocytosis by generating an inward membrane curvature[221–224]. Thus, in addition to providing extracellular proteases for the cleavage of the antigen from the presenting surface, the generation of ceramide-rich membrane domains likely further facilitates BCR signaling and antigen endocytosis by expanding lipid rafts and curving membranes. Furthermore, endophilin 2A, which has been shown to play an important role in membrane repair[201], is also involved in B cell activation and antigen internalization through clathrin-independent endocytosis[116]. These data suggest a close correlation between the mechanisms underlying PM repair and BCR endocytosis of antigen.

4.2 Cellular mechanisms driving B cell PM permeabilization

4.2.1 BCR activation requirements for PM permeabilization

The research presented in this thesis suggests that B cell PM permeabilization is a mechanism for B cells to discriminate between high and low affinity/avidity antigens that are associated with presenting membranes. Previous studies have shown that high-affinity BCR-antigen interactions, but not low-affinity interactions, allow B cells to pull the antigen from the presenting surface[77,120]. Here, we showed that only high-affinity, but not low-affinity, BCR-antigen interactions induce B cell PM permeabilization. We further show that BCR signaling is required for B cell PM permeabilization, as inhibition of BCR signaling reduces permeabilization. This finding also suggests that a certain level of BCR signaling induced by antigen with a certain

avidity (affinity and density) is required to induce B cell PM permeabilization. Such a signaling threshold for B cell PM permeabilization may be supported by the heterogeneous response of primary splenic B cells to surface associated antigen. Not all B cells, not even MD4 B cells expressing the Ig transgene, become permeabilized in response to surface-bound antigen. B cells isolated from the spleen of unimmunized mice are mature and native but at various differentiation stages, thereby interacting with antigen[204,205]. We found that B cells that become permeabilized spread over the presenting surface faster and to a larger area, allowing them to engage more antigen and inducing stronger signaling. This finding suggests that the amount of antigen engaged by a B cell, which determines the total levels of BCR signaling, may be important for inducing later PM permeabilization. This is further supported by B cell PM permeabilization does not occur in response to low-affinity[147] and low-density (unpublished data) antigen-presenting surfaces, which induce lower levels of BCR signaling than high-affinity and high-density antigen. My Ph.D. research did not examine directly BCR signaling. Therefore, in future studies, it would be interesting to ask whether the permeabilized cells gather more antigen and have higher levels of BCR signaling, which would shed light on the signaling threshold for antigen-induced B cell PM permeabilization.

In addition to increased spreading, B cells that became permeabilized also showed an increase in the rate of NMIIA recruitment as well as the total NMIIA recruited. This is consistent with an increase in signaling, as myosin is known to facilitate the formation of central BCR clusters at the interaction site[56,104]. Interestingly, cells that became permeabilized were more likely to reorganize NMII into a ring surrounding the B cell contact zone. These NMII rings also drive BCR-antigen microclusters into a central cluster at the center of the contact zone that is devoid of any cytoskeletal structures. Insufficient BCR signaling can reduce the ability of B cells to spread and gather antigen into a central cluster, consequently preventing the formation of a central BCR cluster. Our data suggest that only cells with sufficient initial BCR signaling, which

are able to spread on the presenting surface and engage enough antigen will progress to form a central BCR cluster and organized interaction site, and ultimately undergo PM permeabilization. Moving forward, it would be interesting to study the force generated upon the formation of NMII ring structures in different subsets of B cells, using DNA-based molecular force probes or traction force microscopy, which would determine the level and the location of NMII forces prior to PM permeabilization and examine the relationship of cell spreading and actomyosin reorganization with cellular forces[136,215].

Concurrent with NMIIA recruitment, lysosomes become polarized towards BCR-antigen interaction sites specifically in cells that became permeabilized. Lysosomes play an important role in antigen processing, fragmentation of antigen, and antigenic peptide loading onto MHCII[89,91]. Furthermore, lysosomal exocytosis facilitates antigen uptake by cleaving antigen from the presenting surface. Lysosome polarization to BCR-antigen interaction sites potentially increases the efficiency of transporting endocytosed antigen to the MIIC for process and lysosome exocytosis for PM repair. Lysosome polarization is a part of B cell polarization, and is induced by BCR signaling and mediated by the polarization of the actin cytoskeleton and the MTOC[61,88–90]. Our findings that a strong lysosome polarization that is associated with surface-associated antigen with high affinity and high percentages of PM permeabilization supports this notion. We detected a rapid decrease of lysosomes at BCR-antigen interaction site after peaking, specifically in cells that became permeabilized. This may be due to a loss in fluorescence as a result of lysosomal exocytosis occurring at the interaction site in response to PM permeabilization. Together, our data suggest that a strong level of early BCR signaling is required to induce B cell PM permeabilization, by inducing high levels of antigen engagement through cell spreading, strong myosin recruitment, and organization, and high levels of lysosome polarization. This data additionally suggests a possible mechanism by which B cells could differentiate high- and low-affinity and high- and low-density antigen (Figure 4.1).

Figure 4.1

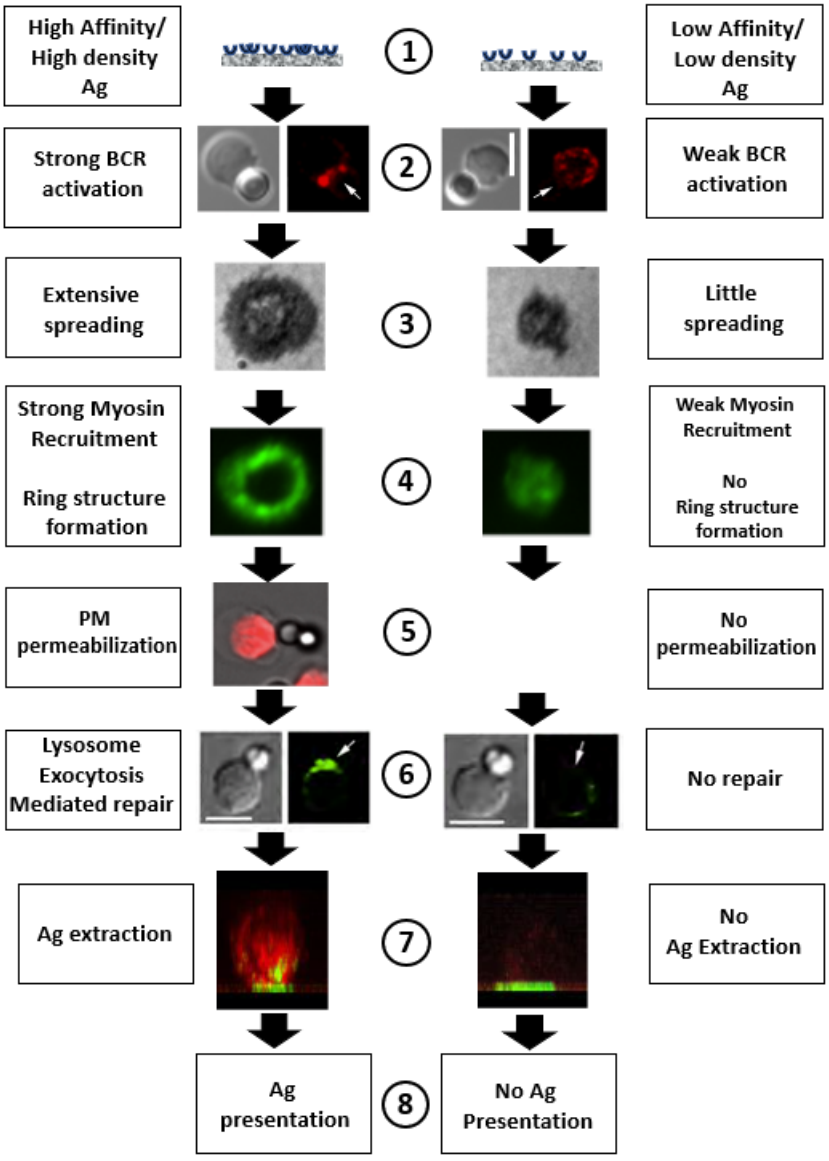
High Affinity/ High density Ag
1
Low Affinity/ Low density Ag
Strong BCR activation
2
Weak BCR activation
Extensive spreading
3
Little spreading
Strong Myosin Recruitment
Ring structure formation
4
Weak Myosin Recruitment
No Ring structure formation
PM permeabilization
5
No permeabilization
Lysosome Exocytosis Mediated repair
6
No repair
Ag extraction
7
No Ag Extraction
Ag presentation
8
No Ag Presentation

Figure 4.1. Working model. This figure proposes a working model of the mechanism by which B cells use B cell membrane permeabilization to differentiate high and low affinity and density antigen. In response to (1) high affinity and highly dense antigen (2) strong BCR activation occurs. (3) Early BCR signaling induces the B cell to spread on the presenting surface and engage more antigen. (4) B cells recruit myosin to the interaction site and organize the myosin in a ring-like structure around the center of the contact zone. (5) Myosin generated forces are generated to pull the antigen from the presenting surface and cause B cell PM permeabilization. (6) A lysosome exocytosis dependent repair response is initiated to reseal the plasma membrane. (7) lysosome enzymes secreted at the interaction site facilitate the cleavage of the antigen from the presenting surface and facilitate antigen endocytosis into the B cell. (8) antigen is processed and presented on the MHCII for T cell recognition. In response to low affinity or low-density antigen, there is less BCR activation, and less B cell spreading. This reduces the recruitment of myosin and inhibits the formation of a myosin ring structure around the center of the contact area. The lack of myosin prevents sufficient force from being generated to cause B cell PM permeabilization. Since no permeabilization occurs, there is no lysosome exocytosis dependent repair and thus antigen is not cleaved from the presenting surface, inhibiting antigen endocytosis and subsequent presentation in the MHCII for T cell recognition.

4.2.2 Cellular reorganization event leading up to B cell PM permeabilization

We observed a 2^{o} spreading event and a mild recovery of myosin recruitment prior to PM permeabilization. This phenomenon has not been previously described and was observed predominantly in cells that later became permeabilized. Furthermore, B cells that undergo this 2^{o} spreading event initially spread at a faster rate to a larger area, recruit myosin at a faster rate and are more likely to organize NMIIA into a ring structure at the immune synapse. Although it is unclear what the exact functions of this 2^{o} spreading and myosin recruitment events are, it could be an indication of the switch in the B cell's behavior from gathering antigen into a central cluster to pulling antigen from the presenting surface for internalization. Myosin-generated force is critical for pulling antigen from presenting surfaces; therefore, generation of such forces requires cytoskeleton reorganization, which potentially leads to a brief change in the contact area between B cells and the antigen-presenting surface, such as this 2^{o} B cell spreading event. The NMIIA recovery at the B cell contact zone may be a response to the pulling tension to facilitate BCR endocytosis of antigen. Only when antigen is strongly associated with a presenting surface, BCR binding to antigen with a high affinity, and enough force is generated, B cell PM permeabilization can occur. Future work will further characterize these observations and determine their impact on force generation and antigen internalization.

4.2.3 Future directions

Our research has revealed that PM permeabilization and repair is a vital step for B cells to capture and present antigen that is tightly associated with membranes, and identified the cellular requirements to induce PM permeabilization. To better characterize the membrane permeabilization of the B cell during interaction with surface-associated antigen, we will determine the exact location and the extent of the permeabilization of the PM and search for the direct cause of this permeabilization. We hypothesized that cellular forces generated by NMII at the B cell-APC interaction zone are directly responsible for B cell PM permeabilization. To test this hypothesis, we will examine cellular forces at the B cell contact zone in detail. Traction force

microscopy can analyze the relative level and distribution of traction forces at the contact zone[175,176,225]. Furthermore, DNA-based force probes in combination with BCR staining and TIRF microscopy can digitally pin dynamic forces to BCR-antigen interaction sites[136,215]. We will further characterize the molecular events leading to B cell PM permeabilization, including antigen engagement, BCR signaling, cytoskeleton reorganization, and B cell polarization. Particularly, we will examine how B cells mount the 2^{o} spreading and NMIIA recruitment events and whether these events are required for B cell PM permeabilization. Together, these proposed studies will expand our understanding of how surface-associated antigen induces B cell PM permeabilization and how B cells use PM permeabilization to discriminate antigen binding avidity.

This thesis has focused on mouse splenic B cells, which primarily consist of naïve mature follicular B cells but also contain several other subsets of mature B cells[204,205]. Naïve mature B cells go through multiple antigen-dependent steps to differentiate into high-affinity plasma cells and memory B cells. My thesis mainly examines what occurs to B cells when they first encounter surface-associated antigen. It would be interesting to determine how various B cell subsets at different differentiation stages behave when encountering surface associated antigen. In the germinal center, B cells undergo rapid proliferation, somatic hypermutation, and affinity maturation. Antigen specific high-affinity B cells are selected based on their ability to capture antigen on the surface of follicular dendritic cells and present antigen to T cells. It has been shown that germinal center B cells interact with surface-associated antigen differently from naïve B cells[76]. BCRs on the surface of germinal center B cells were shown to form persisted microclusters but not central clusters when interacting with surface associated antigen[76,226,227]. It will be of interest to see if germinal center B cells are more sensitive to the surface-associated antigen to become permeabilized and whether the antigen-induced PM permeabilization has an impact on the affinity maturation of germinal center B cells. I also speculate a possibility that

membrane wounding and subsequent repair may also be adapted to play roles in other immune cell-cell interactions. Indeed, membrane repair has been recently shown to play a role in cytotoxic T cell mediated killing of their target cells[167]. Whether membrane permeabilization occurs during B-T cell interactions through TCR and antigenic peptide loaded MHCII remains to be explored.

The research presented in this dissertation discovers and characterizes a novel step in B cell activation, B cell PM permeabilization by surface-associated antigen, which plays a vital role in B cell capturing and presentation of surface-associated antigens. Antigen induced B cell PM permeabilization triggers a lysosome exocytosis-dependent PM repair response, which provides proteases to cleave antigen off from the presenting surface and enables antigen uptake and presentation (Figure 2.7I). Antigen induced B cell PM permeabilization requires high affinity or high avidity antigen associated with membranes, BCR signaling, and signaling activated NMII. High affinity/avidity antigen induces faster and higher levels of B cell spreading on antigen presenting surfaces, recruits more myosin to BCR-antigen interaction sites, and organizes actomyosin into a ring structure. B cell PM permeabilization may also require a 2^{o} spreading and NMII recruitment. These findings demonstrate a close relationship between BCR signaling and B cell PM permeabilization. Our data identified a novel mechanism for B cells to capture antigen from the surface of pathogens and antigen presenting cells, which expands our understanding of the mechanisms by which B cells discriminate antigen based on binding affinity to differentiate into high-affinity antibody-producing cells and memory B cells. Understanding B cell activation mechanisms is critical for revealing the dysregulation steps of B cell activation that cause autoimmune disorders, such as rheumatoid arthritis and systemic lupus erythematosus, and immune deficiencies, such as Wiskott Aldrich syndrome[15]. Additionally, cellular mechanisms of B cell affinity discrimination potentially provide innovative designs to increase vaccine efficacy.

Bibliography:

1. Newton, K. & Dixit, V. M. Signaling in innate immunity and inflammation. *Cold Spring Harbor Perspectives in Biology* **4**, (2012).

2. Medzhitov, R. Recognition of microorganisms and activation of the immune response. *Nature* **449**, 819–826 (2007).

3. Iwasaki, A. & Medzhitov, R. Regulation of adaptive immunity by the innate immune system. *Science (1979)* **327**, 291–295 (2010).

4. Gaya, M. *et al.* Initiation of Antiviral B Cell Immunity Relies on Innate Signals from Spatially Positioned NKT Cells. *Cell* **172**, 517-533.e20 (2018).

5. Eisen, H. N. Affinity Enhancement of Antibodies : How Low-Af fi nity Antibodies Produced Early in Immune Responses Are Followed by High-Affinity Antibodies Later and in Memory B-Cell Responses. 381–393 (2014) doi:10.1158/2326-6066.CIR-14-0029.

6. McHeyzer-Williams, L. J. & McHeyzer-Williams, M. G. Antigen-Specific Memory B Cell Development. *Annual Review of Immunology* **23**, 487–513 (2005).

7. Cooper, M. D. & Alder, M. N. The evolution of adaptive immune systems. *Cell* **124**, 815–822 (2006).

8. Constant, S. L. B lymphocytes as antigen-presenting cells for CD4+ T cell priming in vivo. *J Immunol* **162**, 5695–703 (1999).

9. Harwood, N. E. & Batista, F. D. Early Events in B Cell Activation. *Annual Review of Immunology* **28**, 185–210 (2010).

10. Shulman, Z. *et al.* Germinal centers: Dynamic signaling by T follicular helper cells during germinal center B cell selection. *Science (1979)* **345**, 1058–1062 (2014).

11. Lanzavecchia, A. Antigen-specific interaction between T and B cells. *Nature* (1985).

12. Shulman, Z., Gitlin, A. D., Targ, S. & Jankovic, M. T Follicular Helper Cell Dynamics in Germinal Centers. *Science (1979)* 1–8 (2013) doi:10.1038/ni.2428.

13. Dieckmann, N. M. G., Frazer, G. L., Asano, Y., Stinchcombe, J. C. & Griffiths, G. M. The cytotoxic T lymphocyte immune synapse at a glance. *Journal of Cell Science* **129**, 2881–2886 (2016).

14. Tschopp, J. & Nabholz, M. Perforin-mediated target cell lysis by cytolytic T lymphocytes. *Annual Review of Immunology* **8**, 279–302 (1990).

15. Lebien, T. W. & Tedder, T. F. ASH 50th anniversary review B lymphocytes : how they develop and function. *The american society of hematology* **112**, 1570–1580 (2008).

16. Natarajan, K., Sahoo, N. C. & Rao, K. V. S. Signal Thresholds and Modular Synergy During Expression of Costimulatory Molecules in B Lymphocytes. *The Journal of Immunology* **167**, 114–122 (2001).

17. Stoddart, A. *et al.* Lipid rafts unite signaling cascades with clathrin to regulate BCR internalization. *Immunity* **17**, 451–462 (2002).

18. Cheng, P. C., Dykstra, M. L., Mitchell, R. N. & Pierce, S. K. A Role for Lipid Rafts in B Cell Antigen Receptor Signaling and Antigen Targeting. *Journal of Experimental Medicine* **190**, 1549–1560 (1999).

19. Reth, M. Antigen receptors on B lymphocytes. *Annual Review of Immunology* **10**, 97–121 (1992).

20. Mills, D. M. & Cambier, J. C. B lymphocyte activation during cognate interactions with CD4+T lymphocytes: Molecular dynamics and immunologic consequences. *Seminars in Immunology* vol. 15 325–329 Preprint at https://doi.org/10.1016/j.smim.2003.09.004 (2003).

21. Edelman, G. M. Antibody Structure and Molecular Immunology. *Science (1979)* **180**, 830–840 (1973).

22. Davies, D. R. & Chacko, S. Antibody Structure. *Accounts of Chemical Research* **26**, 421–427 (1993).

23. Jung, D., Giallourakis, C., Mostoslavsky, R. & Alt, F. W. Mechanism and Control of V(D)J Recombination At the Immunoglobulin Heavy Chain Locus. *Annual Review of Immunology* **24**, 541–570 (2006).

24. Hozumi, N. & Tonegawa, S. Evidence for somatic rearrangement of immunoglobulin genes coding for variable and constant regions. *PNAS USA* **73**, 3628–3632 (1976).

25. Cyster, J. G. & Allen, C. D. C. B Cell Responses: Cell Interaction Dynamics and Decisions. *Cell* **177**, 524–540 (2019).

26. Hardy, R. R. & Hayakawa, K. B cell development pathways. 595–621 (2001).

27. Klaus Schwarz, george H. G. leopold L. U. P. Z. L. D. L. W. F. R. A. S. T. E. H.-H. S. D. M. R. L. C. R. B. RAG Mutations in Human B Cell-Negative SCID. *Science (1979)* **274**, 97–99 (1996).

28. Reichman-Fried, M., Hardy, R. R. & Bosma, M. J. Development of B-lineage cells in the bone marrow of scid/scid mice following the introduction of functionally rearranged immunoglobulin transgenes. *Proc Natl Acad Sci U S A* **87**, 2730–2734 (1990).

29. Pillai, S. & Taylor, K. N. B-Cell Tolerance and Autoimmunity. *Systemic Lupus Erythematosus* **6**, 107–113 (2011).

30. Cheng, P. C., Brown, B. K., Song, W. & Pierce, S. K. Translocation of the B Cell Antigen Receptor into Lipid Rafts Reveals a Novel Step in Signaling. *The Journal of Immunology* **166**, 3693–3701 (2001).

31. Cahalan, M. D. & Parker, I. Choreography of Cell Motility and Interaction Dynamics Imaged by Two-Photon Microscopy in Lymphoid Organs. *Annual Review of Immunology* **26**, 585–626 (2008).

32. Schwickert, T. A. *et al.* A dynamic T cell–limited checkpoint regulates affinity-dependent B cell entry into the germinal center. *The Journal of Experimental Medicine* **208**, 1243–1252 (2011).

33. Shlomchik, M. J. Germinal Centers. **1623**, 5–10 (2012).

34. MacLennan, I. C. M. *Germinal Centers*. vol. 1623 (2017).

35. Pereira, J. P., Kelly, L. M. & jason, J. G. C. Finding the right niche: B-cell migration in the early phases of T-dependent antibody responses. *International Immunology* **22**, 413–419 (2010).

36. Allen, C. D. C. & Okada, T. Imaging of Germinal Center Selection. **315**, 528–532 (2007).

37. MacLennan, I. C. M. Germinal Centers. *Annu. Rev. Immunol* **1623**, (1994).

38. Allen, C. D. C., Okada, T. & Cyster, J. G. Germinal-Center Organization and Cellular Dynamics. *Immunity* vol. 27 190–202 Preprint at https://doi.org/10.1016/j.immuni.2007.07.009 (2007).

39. Allen, C. D. C. *et al.* Germinal center dark and light zone organization is mediated by CXCR4 and CXCR5. *Nature Immunology* **5**, 943–952 (2004).

40. Allen, C. D. C. & Okada, T. Imaging of Germinal Center Selection. *Science* **315**, 528–531 (2007).

41. Vinuesa, C. G., Linterman, M. A., Yu, D. & MacLennan, I. C. M. Follicular Helper T Cells. *Annual Review of Immunology* **34**, 335–368 (2016).

42. Liu, W., Meckel, T., Tolar, P., Sohn, H. W. & Pierce, S. K. Antigen affinity discrimination is an intrinsic function of the B cell receptor. *Journal of Experimental Medicine* **207**, 1095–1111 (2010).

43. Victora, G. D. *et al.* Germinal center dynamics revealed by multiphoton microscopy with a photoactivatable fluorescent reporter. *Cell* **143**, 592–605 (2010).

44. Fleire, S. J. *et al.* B cell ligand discrimination through a spreading and contraction response. *Science (1979)* **312**, 738–741 (2006).

45. Batista, F. D. & Neuberger, M. S. B cells extract and present immobilized antigen: Implications for affinity discrimination. *EMBO Journal* **19**, 513–520 (2000).

46. Thyagarajan, R., Arunkumar, N. & Song, W. Polyvalent Antigens Stabilize B Cell Antigen Receptor Surface Signaling Microdomains. *The Journal of Immunology* **170**, 6099–6106 (2003).

47. Paus, D. *et al.* Antigen recognition strength regulates the choice between extrafollicular plasma cell and germinal center B cell differentiation. *Journal of Experimental Medicine* **203**, 1081–1091 (2006).

48. Goroff, D. K., Stall, A., Mond, J. J. & Finkelman, F. D. In vitro and in vivo B lymphocyte-activating properties of monoclonal anti-δ antibodies. I. Determinants of B lymphocyte-activating properties. *Journal of Immunology* **136**, 2382–2392 (1986).

49. Sohn, H. W., Tolar, P., Jin, T. & Pierce, S. K. Fluorescence resonance energy transfer in living cells reveals dynamic membrane changes in the initiation of B cell signaling. *Proc Natl Acad Sci U S A* **103**, 8143–8148 (2006).

50. Aman, M. J. & Ravichandran, K. S. A requirement for lipid rafts in B cell receptor induced Ca2+flux. *Current Biology* **10**, 393–396 (2000).

51. Kurosaki, B. T., Johnson, S. A., Pao, L., Sada, K. & Cambier, J. C. Role of the Syk Autophosphorylation Site and SH2 Domains in B Cell Antigen Receptor Signaling. **182**, (1995).

52. Kurosaki, T. *et al.* Syk activation by the Src-family tyrosine kinase in the B cell receptor signaling. *J Exp Med* **179**, 1725–9 (1994).

53. Hae, W. S., Tolar, P. & Pierce, S. K. Membrane heterogeneities in the formation of B cell receptor-Lyn kinase microclusters and the immune synapse. *Journal of Cell Biology* **182**, 367–379 (2008).

54. Hao, J. J., Carey, G. B. & Zhan, X. Syk-mediated tyrosine phosphorylation is required for the association of hematopoietic lineage cell-specific protein 1 with lipid rafts and B cell antigen receptor signalosome complex. *Journal of Biological Chemistry* **279**, 33413–33420 (2004).

55. Ishiai, M. *et al.* BLNK required for coupling syk to PLCγ2 and rac1-JNK in B cells. *Immunity* **10**, 117–125 (1999).

56. Wenxia Song *et al.* Actin-mediated feedback loops in B-cell receptor signaling. *Immunological Reviews* 177–189 (2013).

57. Park, H. *et al.* Regulation of Btk function by a major autophosphorylation site within the SH3 domain. *Immunity* **4**, 515–525 (1996).

58. Liu, Q.-H. *et al.* Distinct Calcium Channels Regulate Responses of Primary B Lymphocytes to B Cell Receptor Engagement and Mechanical Stimuli. *The Journal of Immunology* **174**, 68–79 (2005).

59. Hartzell, C. A., Jankowska, K. I., Burkhardt, J. K. & Lewis, R. S. Calcium influx through CRAC channels controls actin organization and dynamics at the immune synapse. *Elife* **5**, 1–28 (2016).

60. Sharma, S., Orlowski, G. & Song, W. Btk Regulates B Cell Receptor-Mediated Antigen Processing and Presentation by Controlling Actin Cytoskeleton Dynamics in B Cells. *The Journal of Immunology* **182**, 329–339 (2009).

61. del Valle Batalla, F., Lennon-Dumenil, A. M. & Yuseff, M. I. Tuning B cell responses to antigens by cell polarity and membrane trafficking. *Molecular Immunology* **101**, 140–145 (2018).

62. Fujimoto, M. *et al.* Complementary Roles for CD19 and Bruton's Tyrosine Kinase in B Lymphocyte Signal Transduction. *The Journal of Immunology* **168**, 5465–5476 (2002).

63. Carroll, D. T. F. and M. C. Regulation of B Lymphocte Resonses to Foreign and Self-Antigens by the CD19/CD21 Complex. **11**, 128–148 (2015).

64. Engel, P. *et al.* Abnormal B lymphocyte delevopment, activation, and differentiation in mice that lack or overexpress the CD19 signal transduction molecule. *Immunity* **3**, 39–50 (1995).

65. Sohn, H. W., Pierce, S. K. & Tzeng, S.-J. Live Cell Imaging Reveals that the Inhibitory FcγRIIB Destabilizes B Cell Receptor Membrane-Lipid Interactions and Blocks Immune Synapse Formation. *The Journal of Immunology* **180**, 793–799 (2008).

66. Conley, M. E. *et al.* Genetic analysis of patients with defects in early B-cell development. *Immunological Reviews* **203**, 216–234 (2005).

67. Magro, C. M., Clair, E. W. S. & Tedder, T. F. B-lymphocyte contributions to human autoimmune disease. *Immunological Reviews* 284–299 (2008).

68. Castiello, M. C. *et al.* In vivo chronic stimulation unveils autoreactive potential of Wiskott-Aldrich syndrome protein-deficient b cells. *Frontiers in Immunology* **8**, (2017).

69. Wilson, W. H. Treatment strategies for aggressive lymphomas: what works? *Hematology / the Education Program of the American Society of Hematology. American Society of Hematology. Education Program* **2013**, 584–590 (2013).

70. Carrasco, Y. R. & Batista, F. D. B Cells Acquire Particulate Antigen in a Macrophage-Rich Area at the Boundary between the Follicle and the Subcapsular Sinus of the Lymph Node. *Immunity* **27**, 160–171 (2007).

71. Junt, T. *et al.* Subcapsular sinus macrophages in lymph nodes clear lymph-borne viruses and present them to antiviral B cells. *Nature* **450**, 110–114 (2007).

72. Suzuki, K., Grigorova, I., Phan, T. G., Kelly, L. M. & Cyster, J. G. Visualizing B cell capture of cognate antigen from follicular dendritic cells. *Journal of Experimental Medicine* **206**, 1485–1493 (2009).

73. Bergtold, A., Desai, D. D., Gavhane, A. & Clynes, R. Cell surface recycling of internalized antigen permits dendritic cell priming of B cells. *Immunity* **23**, 503–514 (2005).

74. Wykes, M. *et al.* Dendritic Cells Interact Directly with Naive B Lymphocytes to Transfer Antigen and Initiate Class Switching in a Primary T-Dependent Response. *The Journal f Immunology* **161**, (2018).

75. Batista, F. D., Iber, D. & Neuberger, M. S. B cells acquire antigen from target cells after synapse formation. *Nature* **411**, 489–494 (2001).

76. Nowosad, C. R., Spillane, K. M. & Tolar, P. Germinal center B cells recognize antigen through a specialized immune synapse architecture. *Nature Immunology* **17**, 870–877 (2016).

77. Carrasco, Y. R., Fleire, S. J., Cameron, T., Dustin, M. L. & Batista, F. D. LFA-1/ICAM-1 Interaction Lowers the Threshold of B Cell Activation by Facilitating B Cell Adhesion and Synapse Formation. *Immunity* **20**, 589–599 (2004).

78. Liu, C. *et al.* N-WASP Is Essential for the Negative Regulation of B Cell Receptor Signaling. *PLoS Biology* **11**, (2013).

79. Liu, C. *et al.* Actin Reorganization Is Required for the Formation of Polarized B Cell Receptor Signalosomes in Response to Both Soluble and Membrane-Associated Antigens. *The Journal of Immunology* **188**, 3237–3246 (2012).

80. Kupfer, A., Swain, S. L. & Singer, S. J. The specific direct interaction of helper T cells and antigen-presenting B cells II. Reorientation of the Microtubule Organizing Center and Reorganization of the Membrane-associated Cytoskeleton inside the Bound Helper T Cells. (1987).

81. Grakoui, A. *et al.* The Immunological Synapse: A Molecular Machine Controlling T Cell Activation. *Science (1979)* (1999).

82. Harwood, N. E. & Batista, F. D. New Insights into the Early Molecular Events Underlying B Cell Activation. *Immunity* vol. 28 609–619 Preprint at https://doi.org/10.1016/j.immuni.2008.04.007 (2008).

83. Tolar, P., Hanna, J., Krueger, P. D. & Pierce, S. K. The Constant Region of the Membrane Immunoglobulin Mediates B Cell-Receptor Clustering and Signaling in Response to Membrane Antigens. *Immunity* **30**, 44–55 (2009).

84. Schnyder, T. *et al.* B Cell Receptor-Mediated Antigen Gathering Requires Ubiquitin Ligase Cbl and Adaptors Grb2 and Dok-3 to Recruit Dynein to the Signaling Microcluster. *Immunity* **34**, 905–918 (2011).

85. Natkanski, E., Molloy, J. E. & Tolar, P. B cells Use Mechanical Energy to Discriminate Antigen Affinities. *Science (1979)* 1587–1590 (2013).

86. Heesters, B. A., van der Poel, C. E., Das, A. & Carroll, M. C. Antigen Presentation to B Cells. *Trends in Immunology* vol. 37 844–854 Preprint at https://doi.org/10.1016/j.it.2016.10.003 (2016).

87. Vertii, A., Hehnly, H. & Doxsey, S. The centrosome, a multitalented renaissance organelle. *Cold Spring Harbor Perspectives in Biology* **8**, 1–14 (2016).

88. Obino, D. *et al.* Actin nucleation at the centrosome controls lymphocyte polarity. *Nature Communications* **7**, (2016).

89. Yuseff, M. I. *et al.* Polarized Secretion of Lysosomes at the B Cell Synapse Couples Antigen Extraction to Processing and Presentation. *Immunity* **35**, 361–374 (2011).

90. Reversat, A. *et al.* Polarity protein Par3 controls B-cell receptor dynamics and antigen extraction at the immune synapse. *Molecular Biology of the Cell* **26**, 1273–1285 (2015).

91. Yuseff, M.-I., Pierobon, P., Reversat, A. & Lennon-Duménil, A.-M. How B cells capture, process and present antigens: a crucial role for cell polarity. *Nature Reviews Immunology* **13**, 475–486 (2013).

92. Treanor, B. *et al.* The Membrane Skeleton Controls Diffusion Dynamics and Signaling through the B Cell Receptor. *Immunity* **32**, 187–199 (2010).

93. Kusumi, A. *et al.* Dynamic Organizing Principles of the Plasma Membrane that Regulate Signal Transduction: Commemorating the Fortieth Anniversary of Singer and Nicolson's Fluid-Mosaic Model. *Annual Review of Cell and Developmental Biology* **28**, 215–250 (2012).

94. Freeman, S. A. *et al.* Cofilin-Mediated F-Actin Severing Is Regulated by the Rap GTPase and Controls the Cytoskeletal Dynamics That Drive Lymphocyte Spreading and BCR Microcluster Formation. *The Journal of Immunology* **187**, 5887–5900 (2011).

95. Treanor, B., Depoil, D., Bruckbauer, A. & Batista, F. D. Dynamic cortical actin remodeling by ERM proteins controls BCR microcluster organization and integrity. *Journal of Experimental Medicine* **208**, 1055–1068 (2011).

96. Rey-Suarez, I. *et al.* WASP family proteins regulate the mobility of the B cell receptor during signaling activation. *Nature Communications* **11**, (2020).

97. Ketchum, C., Miller, H., Song, W. & Upadhyaya, A. Ligand mobility regulates B cell receptor clustering and signaling activation. *Biophysical Journal* **106**, 26–36 (2014).

98. Ochs, H. D. *The Wiskott-Aldrich syndrome*. *Springer Semin Immunopathol* vol. 19 (1998).

99. Miki, H., Miura, K. & Takenawa, T. N-WASP, a novel actin-depolymerizing protein, regulates the cortical cytoskeletal rearrangement in a PIP2-dependent manner downstream of tyrosine kinases. *EMBO Journal* **15**, 5326–5335 (1996).

100. Liu, C. *et al.* A Balance of Bruton's Tyrosine Kinase and SHIP Activation Regulates B Cell Receptor Cluster Formation by Controlling Actin Remodeling. *The Journal of Immunology* **187**, 230–239 (2011).

101. Dustin, M. L. *et al.* Arp2/3 complex-driven spatial patterning of the BCR enhances immune synapse formation, BCR signaling and B cell activation. *Elife* (2019) doi:10.7554/eLife.44574.001.

102. Weber, M. *et al.* Phospholipase C-γ2 and Vav cooperate within signaling microclusters to propagate B cell spreading in response to membrane-bound antigen. *The Journal of Experimental Medicine* **205**, 853–868 (2008).

103. Westerberg, L. *et al.* Wiskott-Aldrich syndrome protein deficiency leads to reduced B-cell adhesion, migration, and homing, and a delayed humoral immune response. *Blood* (2005) doi:10.1182/blood.

104. Seeley-Fallen, M. K. *et al.* Non-Muscle Myosin II Is Essential for the Negative Regulation of B-Cell Receptor Signaling and B-Cell Activation. *Frontiers in Immunology* **13**, (2022).

105. Liu, C. *et al.* A Balance of Bruton's Tyrosine Kinase and SHIP Activation Regulates B Cell Receptor Cluster Formation by Controlling Actin Remodeling. *The Journal of Immunology* **187**, 230–239 (2011).

106. Leung, W. H. *et al.* Aberrant antibody affinity selection in SHIP-deficient B cells. *European Journal of Immunology* **43**, 371–381 (2013).

107. Rey-Suarez, I. *et al.* WASP family proteins regulate the mobility of the B cell receptor during signaling activation. *Nature Communications* **11**, (2020).

108. Murugesan, S. *et al.* Formin-generated actomyosin arcs propel t cell receptor microcluster movement at the immune synapse. *Journal of Cell Biology* vol. 215 383–399 Preprint at https://doi.org/10.1083/jcb.201603080 (2016).

109. Baldari, C. T. & Dustin, M. L. *The Immune Synapse*. vol. 1584 (2017).

110. Hoogeboom, R. *et al.* Myosin IIa Promotes Antibody Responses by Regulating B Cell Activation, Acquisition of Antigen, and Proliferation. *Cell Reports* **23**, 2342–2353 (2018).

111. Busman-Sahay, K., Drake, L., Sitaram, A., Marks, M. & Drake, J. R. Cis and Trans Regulatory Mechanisms Control AP2-Mediated B Cell Receptor Endocytosis via Select Tyrosine-Based Motifs. *PLoS ONE* **8**, (2013).

112. Kaksonen, M. & Roux, A. Mechanisms of clathrin-mediated endocytosis. *Nature Reviews Molecular Cell Biology* **19**, 313–326 (2018).

113. Seeley-Fallen, M. K. *et al.* Actin-binding protein 1 links B-cell antigen receptors to negative signaling pathways. *Proceedings of the National Academy of Sciences* **111**, 9881–9886 (2014).

114. Stoddart, A., Jackson, A. P. & Brodsky, F. M. Plasticity of B cell receptor internalization upon conditional depletion of clathrin. *Molecular Biology of the Cell* **16**, 2339–2348 (2005).

115. Miller, H. *et al.* Lipid raft-dependent plasma membrane repair interferes with the activation of B lymphocytes. *Journal of Cell Biology* **211**, 1193–1205 (2015).

116. Malinova, D. *et al.* Endophilin A2 regulates B-cell endocytosis and is required for germinal center and humoral responses. *EMBO Rep* **22**, (2021).

117. Tien-An Yang Shih, E. M. M. R. & M. C. N. Role of BCR affinity in T cell–dependent antibody responses in vivo. *Nat Immunol* **3**, 5780–575 (2002).

118. Batista, F. D. & Neuberger, M. S. Affinity dependence of the B cell response to antigen: A threshold, a ceiling, and the importance of off-rate. *Immunity* **8**, 751–759 (1998).

119. Langley, D. B. *et al.* Structural basis of antigen recognition: Crystal structure of duck egg lysozyme. *Acta Crystallographica Section D: Structural Biology* **73**, 910–920 (2017).

120. Spillane, K. M. & Tolar, P. B cell antigen extraction is regulated byphysical properties of antigen presenting cells. *Journal of Cell Biology* **2**, 1–19 (2016).

121. Spillane, K. M. & Tolar, P. Mechanics of antigen extraction in the B cell synapse. *Molecular Immunology* **101**, 319–328 (2018).

122. Evans, E. Probing the Regulation Between Force - Lifetime - And Chemistry in Singgle Molecular Bonds. *Annu. Rev. Biophys. Biomol. Struct.* (2001).

123. Julie, T. *et al.* Active trans-synaptic capture of membrane fragments by natural killer cells. *European Journal of Immunology* **32**, 1502–1508 (2002).

124. Huang, J. F. *et al.* TCR-mediated internalization of peptide-MHC complexes acquired by T cells. *Science (1979)* **286**, 952–954 (1999).

125. Sprent, J. Swapping molecules during cell-cell interactions. *Sci STKE* **273**, pe8 (2005).

126. Drake, L., McGovern-Brindisi, E. M. & Drake, J. R. BCR ubiquitination controls BCR-mediated antigen processing and presentation. *Blood* **108**, 4086–4093 (2006).

127. Sohn, H. W., Gu, H. & Pierce, S. K. Cbl-b negatively regulates B cell antigen receptor signaling in mature B cells through ubiquitination of the tyrosine kinase Syk. *Journal of Experimental Medicine* **197**, 1511–1524 (2003).

128. Vascotto, F. *et al.* Antigen presentation by B lymphocytes: how receptor signaling directs membrane trafficking. *Current Opinion in Immunology* vol. 19 93–98 Preprint at https://doi.org/10.1016/j.coi.2006.11.011 (2007).

129. Cyster, J. G., Dang, E. V., Reboldi, A. & Yi, T. 25-Hydroxycholesterols in innate and adaptive immunity. *Nature Reviews Immunology* **14**, 731–743 (2014).

130. Dustin, M. L., Chakraborty, A. K. & Shaw, A. S. Understanding the structure and function of the immunological synapse. *Cold Spring Harb Perspect Biol* **2**, 1–15 (2010).

131. Cullinan, P., Sperling, A. I. & Burkhardt, J. K. The distal pole complex: A novel membrane domain distal to the immunological synapse. *Immunological Reviews* **189**, 111–122 (2002).

132. Billadeau, D. D. & Burkhardt, J. K. Regulation of cytoskeletal dynamics at the immune synapse: New stars join the actin troupe. *Traffic* **7**, 1451–1460 (2006).

133. Singer, A. & Hodes, R. J. Mechanisms of Mechanisms of T cell-B cell interaction. *Ann. Rev. Immunol* (1983).

134. Allison, J. P. & Lanier, L. L. Structure, Function, and Serology of the T-Cell Antigen Receptor Complex. *Annual Review of Immunology* **5**, 503–540 (1987).

135. Clevers, H., Alarcon, B., Wileman, T. & Terhorst, C. The T cell receptor/CD3 complex: a dynamic protein ensemble. *Ann. Rev. Immunol* **6**, 629–62 (1988).

136. Liu, Y. *et al.* DNA-based nanoparticle tension sensors reveal that T-cell receptors transmit defined pN forces to their antigens for enhanced fidelity. *Proceedings of the National Academy of Sciences* **113**, 5610–5615 (2016).

137. Wange, R. L. & Samelson, L. E. Complex complexes: Signaling at the TCR. *Immunity* **5**, 197–205 (1996).

138. Zaretsky, I. *et al.* ICAMs support B cell interactions with T follicular helper cells and promote clonal selection. *Journal of Experimental Medicine* **214**, 1–17 (2017).

139. Paul L. McNeil. *Cellular and molecular adaptations to injurious mechanical stress*. (1993).

140. McNeil, P. L. & Steinhardt, R. A. Loss, restoration, and maintenance of plasma membrane integrity. *Journal of Cell Biology* **137**, 1–4 (1997).

141. McNeil, P. L. & Khakee, R. Disruptions of muscle fiber plasma membranes. Role in exercise-induced damage. *Am J Pathol* **140**, 1097–1109 (1992).

142. Los, F. C. O., Randis, T. M., Aroian, R. v & Ratner, J. Role of Pore-Forming Toxins in Bacterial Infectious Diseases. *Microbiology and Molecular Biology Reviews* **77**, 173–207 (2013).

143. Fernandes, M. C. *et al.* Trypanosoma cruzi subverts the sphingomyelinase-mediated plasma membrane repair pathway for cell invasion. *The Journal of Experimental Medicine* **208**, 909–921 (2011).

144. Markiewski, M. M. & Lambris, J. D. The role of complement in inflammatory diseases from behind the scenes into the spotlight. *American Journal of Pathology* **171**, 715–727 (2007).

145. Bischofberger, M., Gonzalez, M. R. & van der Goot, F. G. Membrane injury by pore-forming proteins. *Current Opinion in Cell Biology* vol. 21 589–595 Preprint at https://doi.org/10.1016/j.ceb.2009.04.003 (2009).

146. Miller, H. *et al.* Lipid raft-dependent plasma membrane repair interferes with the activation of B lymphocytes. *Journal of Cell Biology* **211**, 1193–1205 (2015).

147. Maeda, F. Y. *et al.* Surface-associated antigen induces permeabilization of primary mouse B-cells and lysosome exocytosis facilitating antigen uptake and presentation to T-cells. *Elife* (2021) doi:10.7554/eLife.

148. Andrews, N. W. & Corrotte, M. Plasma membrane repair. *Current Biology* vol. 28 R392–R397 Preprint at https://doi.org/10.1016/j.cub.2017.12.034 (2018).

149. Andrews, N. W., Almeida, P. E. & Corrotte, M. Damage control: Cellular mechanisms of plasma membrane repair. *Trends in Cell Biology* vol. 24 734–742 Preprint at https://doi.org/10.1016/j.tcb.2014.07.008 (2014).

150. Miyake, K. & McNeil, P. L. Vesicle accumulation and exocytosis at sites of plasma membrane disruption. *Journal of Cell Biology* **131**, 1737–1745 (1995).

151. McNeil, P. L., Vogel, S. S., Miyake, K. & Terasaki, M. Patching plasma membrane disruptions with cytoplasmic membrane. *Journal of Cell Science* **113**, 1891–1902 (2000).

152. Purwada, A. *et al.* Ex vivo synthetic immune tissues with T cell signals for differentiating antigen-specific, high affinity germinal center B cells. *Biomaterials* 1–10 (2018) doi:10.1016/j.biomaterials.2018.06.034.

153. Bi, G. Q., Alderton, J. M. & Steinhardt, R. A. Calcium-regulated exocytosis is required for cell membrane resealing. *Journal of Cell Biology* **131**, 1747–1758 (1995).

154. Tam, C. *et al.* Exocytosis of acid sphingomyelinase by wounded cells promotes endocytosis and plasma membrane repair. *Journal of Cell Biology* **189**, 1027–1038 (2010).

155. Joaquina, A. *et al.* ESCRT Machinery Is Required for Plasma Membrane Repair. *Science (1979)* **343**, (2014).

156. Idone, V. *et al.* Repair of injured plasma membrane by rapid Ca2+ dependent endocytosis. *Journal of Cell Biology* **180**, 905–914 (2008).

157. Steinhardt, R. A., Togo, T. & Krasieva, T. B. A Decrease in Membrane Tension Precedes Successful Cell-Membrane Repair. *Molecular Biology of the Cell* **11**, 4339–4346 (2000).

158. Tardieux, I. *et al. Lysosome Recruitment and Fusion Are Early Events Required for Trypanosome Invasion of Mammalian Cells*. *Cell* vol. 71 (1117).

159. Reddy, A., Caler, E. v. & Andrews, N. W. Plasma membrane repair is mediated by Ca2+-regulated exocytosis of lysosomes. *Cell* **106**, 157–169 (2001).

160. Roy, D. *et al.* A process for controlling intracellular bacterial infections induced by membrane injury. *Science (1979)* **304**, 1515–1518 (2004).

161. Keefe, D. *et al.* Perforin triggers a plasma membrane-repair response that facilitates CTL induction of apoptosis. *Immunity* **23**, 249–262 (2005).

162. Corrotte, M., Fernandes, M. C., Tam, C. & Andrews, N. W. Toxin Pores Endocytosed During Plasma Membrane Repair Traffic into the Lumen of MVBs for Degradation. *Traffic* **13**, 483–494 (2012).

163. Keyel, P. A. *et al.* Streptolysin O clearance through sequestration into blebs that bud passively from the plasma membrane. *Journal of Cell Science* **124**, 2414–2423 (2011).

164. Obino, D. *et al.* Vamp-7–dependent secretion at the immune synapse regulates antigen extraction and presentation in B-lymphocytes. *Molecular Biology of the Cell* **28**, 890–897 (2017).

165. Vietri, M., Radulovic, M. & Stenmark, H. The many functions of ESCRTs. *Nature Reviews Molecular Cell Biology* vol. 21 25–42 Preprint at https://doi.org/10.1038/s41580-019-0177-4 (2020).

166. Schöneberg, J., Lee, I. H., Iwasa, J. H. & Hurley, J. H. Reverse-topology membrane scission by the ESCRT proteins. *Nature Reviews Molecular Cell Biology* vol. 18 5–17 Preprint at https://doi.org/10.1038/nrm.2016.121 (2016).

167. Ritter, A. T. *et al.* ESCRT-mediated membrane repair protects tumor-derived cells against T cell attack. *Science* **376**, 377–382 (2022).

168. Andrews, N. W. Resisting attack by repairing the damage. *Science (1979)* **376**, 346–347 (2022).

169. Corrotte, M. *et al.* Caveolae internalization repairs wounded cells and muscle fibers. *Elife* **2013**, 1–30 (2013).

170. Andrews, N. W. Solving the secretory acid sphingomyelinase puzzle: Insights from lysosome-mediated parasite invasion and plasma membrane repair. *Cellular Microbiology* vol. 21 Preprint at https://doi.org/10.1111/cmi.13065 (2019).

171. Sandvig, K., Kavaliauskiene, S. & Skotland, T. Clathrin-independent endocytosis: an increasing degree of complexity. *Histochemistry and Cell Biology* **150**, 107–118 (2018).

172. Li, R., Blanchette-Mackie, E. J. & Ladisch, S. Induction of endocytic vesicles by exogenous C6-ceramide. *Journal of Biological Chemistry* **274**, 21121–21127 (1999).

173. Pelkmans, L. & Helenius, A. Endocytosis Via Caveolae. *Traffic* **3**, 311–320 (2002).

174. Fra, A. M., Williamson, E. & Simons, K. Communication Microdomains in Lymphocytes in the Absence of Caveolae ". *Biochemistry* 2–5 (1994).

175. Wang, J. *et al.* Profiling the origin, dynamics, and function of traction force in B cell activation. *Science Signaling* **11**, (2018).

176. Upadhyaya, A. Mechanosensing in the immune response. *Seminars in Cell and Developmental Biology* vol. 71 137–145 Preprint at https://doi.org/10.1016/j.semcdb.2017.08.031 (2017).

177. Reth M. B cell antigen receptors. *Current Opinion in Immunology* (1994).

178. Shlomchik, M. J. *et al.* Germinal centers. *Immunological Reviews* **247**, 5–10 (2012).

179. Gonzalez, S. F. *et al.* Trafficking of B cell antigen in lymph nodes. *Annual Review of Immunology* **29**, 215–233 (2011).

180. Jason G Cyster. B cell follicles and antigen encounters of the third kind. *Nature Immunology* **11**, 989–996 (2010).

181. Vidard, L. *et al.* Analysis of M H C Class I I Presentation of Particulate Antigens by B-Lymphocytes'. *The Journal of Immunology* **156**, 2809–281 (1996).

182. Rodríguez, A., Webster, P., Ortego, J. & Andrews, N. W. Lysosomes Behave as Ca 2+-regulated Exocytic Vesicles in Fibroblasts and Epithelial Cells. *Cell* **137**, 93–104 (1997).

183. Zhang, Z. *et al.* Regulated ATP release from astrocytes through lysosome exocytosis. *Nature Cell Biology* **9**, 945–953 (2007).

184. Naegeli, K. M. *et al.* Cell Invasion In Vivo via Rapid Exocytosis of a Transient Lysosome-Derived Membrane Domain. *Developmental Cell* **43**, 403-417.e10 (2017).

185. Villeneuve, J. *et al.* Unconventional secretion of FABP4 by endosomes and secretory lysosomes. *Journal of Cell Biology* **217**, 649–665 (2018).

186. Ibata, K. *et al.* Activity-Dependent Secretion of Synaptic Organizer Cbln1 from Lysosomes in Granule Cell Axons. *Neuron* **102**, 1184-1198.e10 (2019).

187. Fuchs, H. & Geßner, R. Iodination significantly influences the binding of human transferrin to the transferrin receptor. *Biochimica et Biophysica Acta - General Subjects* **1570**, 19–26 (2002).

188. Dustin MLStarr TVarma RThomas VK. Supported planar bilayers for study of the immunological synapse. *Current Protocols in Immunology* **76**, 76 (2007).

189. Bansal DMiyake KVogel SSGroh SChen CCWilliamson RMcNeil PLCampbell KP. Defective membrane repair in dysferlin-deficient muscular dystrophy. *Nature* **423**, 168–172 (2003).

190. Mcneil, P. L., Miyake, K. & Vogel, S. S. The endomembrane requirement for cell surface repair. *PNAS* (2003).

191. Demonbreun, A. R. *et al.* Recombinant annexin A6 promotes membrane repair and protects against muscle injury. *Journal of Clinical Investigation* **129**, 4657–4670 (2019).

192. Song, W., Cho, H., Cheng, P. & Pierce, S. K. Entry of B cell antigen receptor and antigen. *The Journal of Immunology* (1995).

193. Robbert Hoogeboom & Pavel Tolar. Molecular Mechanisms of B Cell Antigen Gathering and Endocytosis. in *B Cell Receptor Signaling* vol. 393 45–63 (2015).

194. Tay, B., Stewart, T. A., Davis, F. M., Deuis, J. R. & Vetter, I. Development of a high-throughput fluorescent no-wash sodium influx assay. *PLoS ONE* **14**, (2019).

195. Fensome-Green, A., Stannard, N., Li, M., Bolsover, S. & Cockcroft, S. Bromoenol lactone, an inhibitor of Group V1A calcium-independent phospholipase A2 inhibits antigen-stimulated mast cell exocytosis without blocking Ca2+ influx. *Cell Calcium* **41**, 145–153 (2007).

196. Allen, P. M. & Unanue, E. R. Differential requirements for antigen processing by macrophages for lysozyme-specific T cell hybridomas. *The Journal of Immunology* (1984).

197. Batista, F. D. & Harwood, N. E. The who, how and where of antigen presentation to B cells. *Nature Reviews Immunology* vol. 9 15–27 Preprint at https://doi.org/10.1038/nri2454 (2009).

198. Gitlin, A. D., Shulman, Z. & Nussenzweig, M. C. Clonal selection in the germinal centre by regulated proliferation and hypermutation. *Nature* **509**, 637–640 (2014).

199. Liu, C. S. C. *et al.* Cutting Edge: Piezo1 Mechanosensors Optimize Human T Cell Activation. *The Journal of Immunology* **200**, 1255–1260 (2018).

200. Chinky Shiu Chen Liu, D. G. Mechanical Cues for T Cell Activation: Role of Piezo1 Mechanosensors. *Critical Reviews in Immunology* **39**, 15–38 (2019).

201. Corrotte, M., Cerasoli, M., Maeda, F. Y. & Andrews, N. W. Endophilin-A2-dependent tubular endocytosis promotes plasma membrane repair and parasite invasion. *Journal of Cell Science* **134**, (2021).

202. Michael A. Cousin, S. L. G. K. J. S. Using FM Dyes to Monitor Clathrin-Mediated Endocytosis in Primary Neuronal Culture. in *Clathrin-Mediated Endocytosis* 239–249 (2018).

203. Suzanne B. Hartley, J. C. R. B. A. B. K. A. B. C. C. G. Elimination from peripheral lymphoid tissues of self-reactive B lymphocytes recognizing membrane-bound antigens. *Letters to Nature* **353**, (1991).

204. Sagaert, X. & de Wolf-Peeters, C. Classification of B-cells according to their differentiation status, their micro-anatomical localisation and their developmental lineage. *Immunology Letters* **90**, 179–186 (2003).

205. Allman, D. & Pillai, S. Peripheral B cell subsets. *Current Opinion in Immunology* vol. 20 149–157 Preprint at https://doi.org/10.1016/j.coi.2008.03.014 (2008).

206. Bachmann, M. F. & Jennings, G. T. Vaccine delivery: A matter of size, geometry, kinetics and molecular patterns. *Nature Reviews Immunology* vol. 10 787–796 Preprint at https://doi.org/10.1038/nri2868 (2010).

207. Khan, F. *et al.* Head-to-head comparison of soluble vs. Qβ VLP circumsporozoite protein vaccines reveals selective enhancement of NANP repeat responses. *PLoS ONE* **10**, (2015).

208. Jaiswal, J. K., Andrews, N. W. & Simon, S. M. Membrane proximal lysosomes are the major vesicles responsible for calcium-dependent exocytosis in nonsecretory cells. *Journal of Cell Biology* **159**, 625–635 (2002).

209. Shinya Tanaka & Yoshihiro Baba. B Cell Receptor Signaling. in *B Cells in Immunity and Tolerance* 23–36 (2020).

210. Yoshihiro Baba & Tomohiro Kurosaki. Role of Calcium Signaling in B Cell Activation and Biology. in *B Cell Receptor Signaling* vol. 393 (2015).

211. Izadi, M., Hou, W., Qualmann, B. & Kessels, M. M. Direct effects of Ca2+/calmodulin on actin filament formation. *Biochemical and Biophysical Research Communications* **506**, 355–360 (2018).

212. Diaz, D. *et al.* Loss of lineage antigens is a common feature of apoptotic lymphocytes. *Journal of Leukocyte Biology* **76**, 609–615 (2004).

213. Aalipour, A. & Advani, R. H. Bruton tyrosine kinase inhibitors: A promising novel targeted treatment for B cell lymphomas. *British Journal of Haematology* vol. 163 436–443 Preprint at https://doi.org/10.1111/bjh.12573 (2013).

214. Anne R Bresnick. Molecular mechanisms of nonmuscle myosin-II regulation. *Current Opinion in Cell Biology* **11**, 26–33 (1999).

215. Katelyn M. Spillane & Pavel Tolar. DNA-Based Probes for Measuring Mechanical Forces in Cell-Cell Contacts: Application to B Cell Antigen Extraction from Immune Synapses. in *B Cell Receptor Signaling* 69–80 (2018).

216. Ibañez-Vega, J., del Valle Batalla, F., Saez, J. J., Soza, A. & Yuseff, M. I. Proteasome dependent actin remodeling facilitates antigen extraction at the immune synapse of B cells. *Frontiers in Immunology* **10**, (2019).

217. Sáez, J. J. *et al.* The exocyst controls lysosome secretion and antigen extraction at the immune synapse of B cells. *Journal of Cell Biology* **218**, 2247–2264 (2019).

218. Natkanski, E., Lee, W., Mistry, B., Molloy, J. E. & Tolar, P. B Cells Use Mechanical Energy to Discriminate Antigen Affinities. *Science (1979)* (2013) doi:10.1038/ni.1745.

219. Brockman, J. M. & Salaita, K. Mechanical proofreading: A general mechanism to enhance the fidelity of information transfer between cells. *Frontiers in Physics* vol. 7 Preprint at https://doi.org/10.3389/fphy.2019.00014 (2019).

220. Stoddart, A. *et al. Lipid Rafts Unite Signaling Cascades with Clathrin to Regulate BCR Internalization initiates a cascade of protein tyrosine phosphorylation events which drives B cells into cycle and increases expression of cell surface molecules involved in B cell*. *Immunity* vol. 17 (2002).

221. Grassmé, H., Riethmüller, J. & Gulbins, E. Biological aspects of ceramide-enriched membrane domains. *Progress in Lipid Research* vol. 46 161–170 Preprint at https://doi.org/10.1016/j.plipres.2007.03.002 (2007).

222. Gulbins, E. & Kolesnick, R. Raft ceramide in molecular medicine. *Oncogene* vol. 22 7070–7077 Preprint at https://doi.org/10.1038/sj.onc.1207146 (2003).

223. Holopainen, J. M., Angelova, M. I. & Kinnunen, P. K. J. Vectorial budding of vesicles by asymmetrical enzymatic formation of ceramide in giant liposomes. *Biophysical Journal* **78**, 830–838 (2000).

224. van Blitterswijk, W. J., van der Luit, A. H., Veldman, R. J., Verheij, M. & Borst, J. Ceramide: second messenger or modulator of membrane structure and dynamics? *Biochem. J* **369**, 199–211 (2003).

225. Ivan Rey, D. A. G. B. A. W. W. S. and A. U. Biophysical Techniques to Study B Cell Activation: Single-Molecule Imaging and Force Measurements. in *B cell receptor signaling* 51–68 (2018).

226. Kwak, K. , Q. N. , S. H. , S. A. , M.-L. J. , H. P. , et al. Intrinsic properties of human germinal center B cells set antigen affinity thresholds. *Science (1979)* (2018).

227. Li, Y., Bhanja, A., Upadhyaya, A., Zhao, X. & Song, W. WASp Is Crucial for the Unique Architecture of the Immunological Synapse in Germinal Center B-Cells. *Frontiers in Cell and Developmental Biology* **9**, (2021).

Supplemental figures and videos:

Figure 2.1-Sup.1

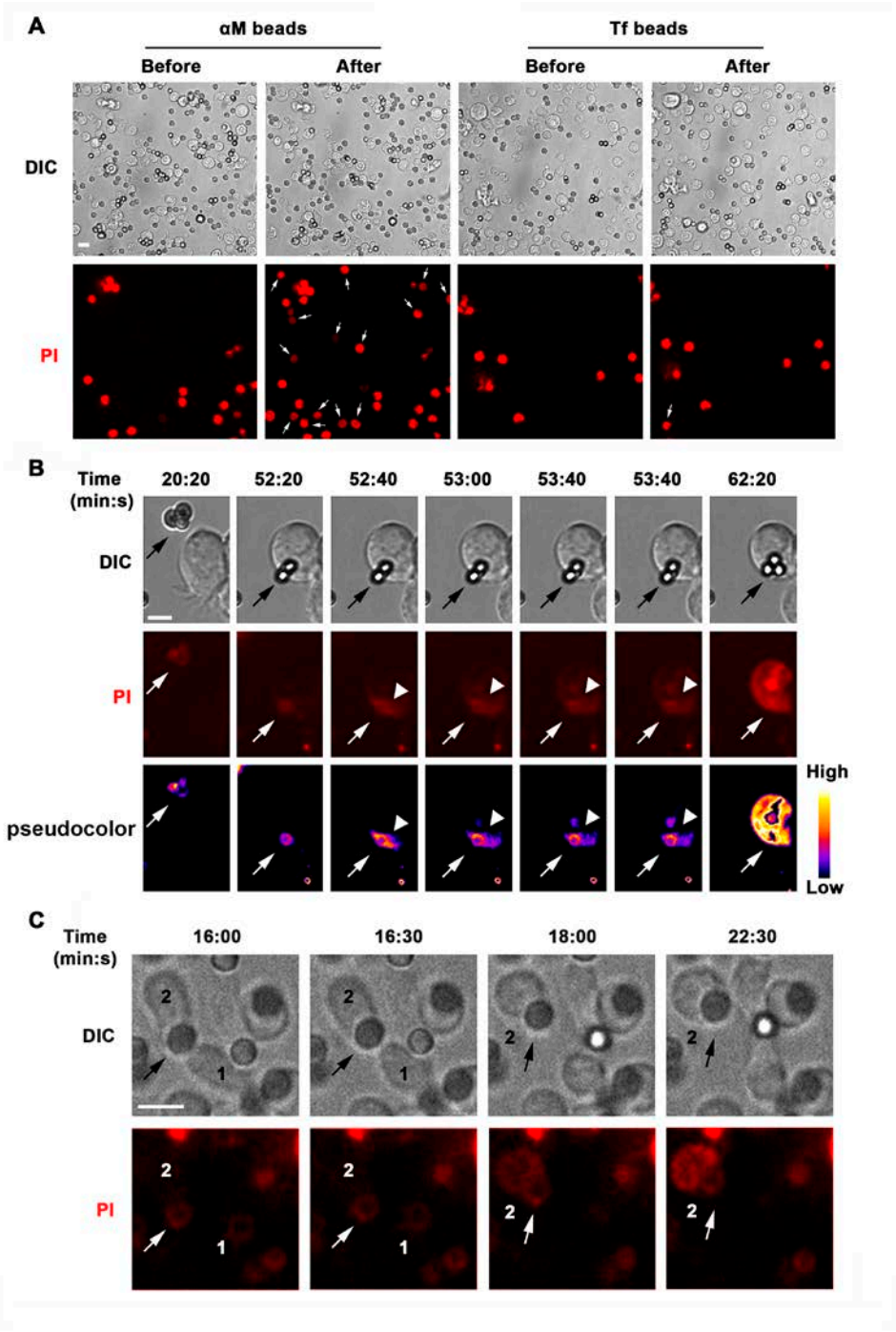

Figure 2.1-Sup. 1. BCR binding to αM-beads causes localized PM permeabilization in B-cells. (A) Live spinning-disk microscopy images of splenic B-cells incubated with αM- or Tf-beads before and after 60 min at 37°C in the presence of PI. The arrows point to bead-bound B-cells that became PI+ during the incubation (Video 1). **(B)** Live spinning disk time-lapse images and corresponding fluorescence intensity (FI) pseudo-color images of A20 B-cells incubated with αM-beads in the presence of PI. The arrow points to beads that caused permeabilization; the arrowhead points to the site of PI entry (Video 2). Beads appear faintly red due to autofluorescence. **(C)** Live spinning disk time-lapse images of splenic B-cells incubated with αM-beads in the presence of PI. The arrow points to a bead that was exchanged between cells (#1, #2) and caused permeabilization of cell #2 (Video 3). Bars, 5 μm. Work for figures 2.1-Sup.1 A and B was executed by Fernando Maeda.

Figure 2.1-Sup.2

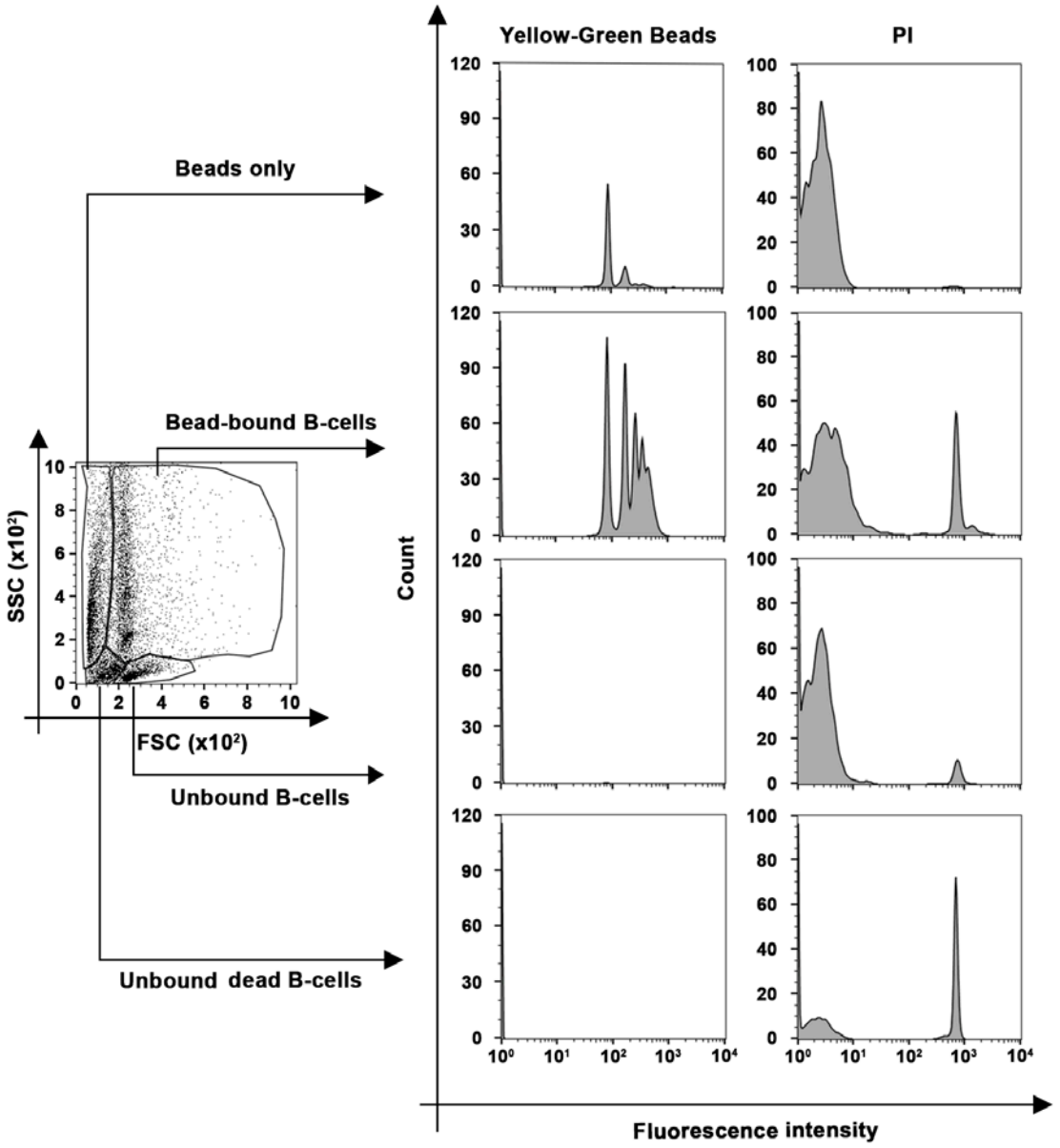

Figure 2.1-Sup.2. Identification of bead-bound B-cells by flow cytometry. Splenic B-cells were incubated with αM-conjugated yellow-green fluorescence beads in the presence of PI and analyzed by flow cytometry. Representative dot plots of side scatter (SSC) versus forward scatter (FSC) and fluorescence intensity histograms of yellow-green beads and PI are shown. Bead-bound B-cells were identified by sizes and the presence of yellow-green fluorescence. Work for figure 2.1-Sup.2 was executed by Fernando Maeda.

Figure 2.1-Sup.3

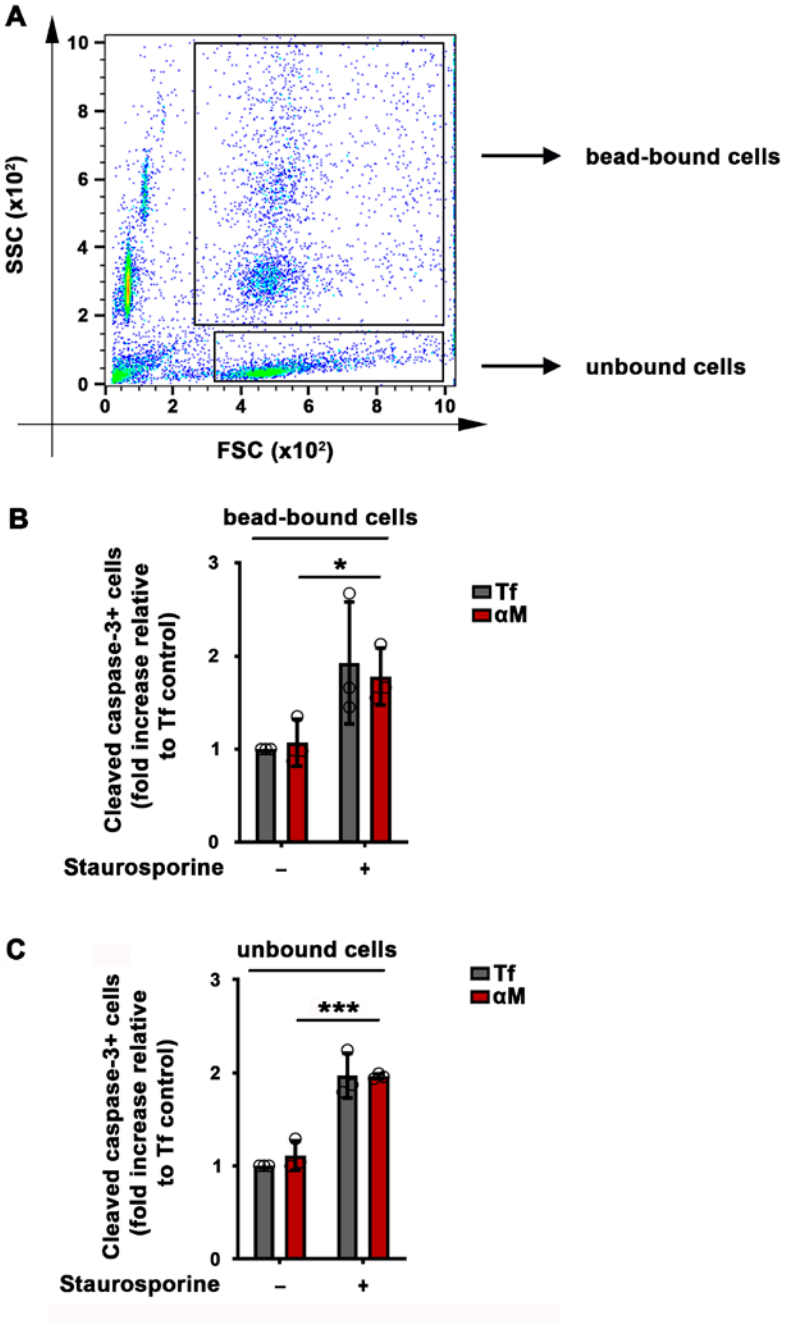

Figure 2.1-Sup.3. BCR binding to αM-beads does not increase apoptosis in B-cells. Splenic B-cells treated or not with staurosporine for 24 hr were incubated with αM- or Tf-beads for 30 min at 37°C, fixed, permeabilized, stained with antibodies against cleaved caspase-3, and analyzed by flow cytometry. **(A)** Identification of bead-bound and unbound B-cell populations on a side scatter (SSC) versus forward scatter (FSC) plot. The percentage of cells positive for cleaved caspase-3 was determined in the bead-bound **(B)** or unbound **(C)** cell populations and expressed relative to the Tf-bead control. Data points represent independent experiments (mean ± SD). *$p \leq 0.05$; ***$p \leq 0.005$, unpaired Student's *t*-test. Work for figure 2.1-Sup.3 was executed by Fernando Maeda.

Figure 2.1-Sup.4

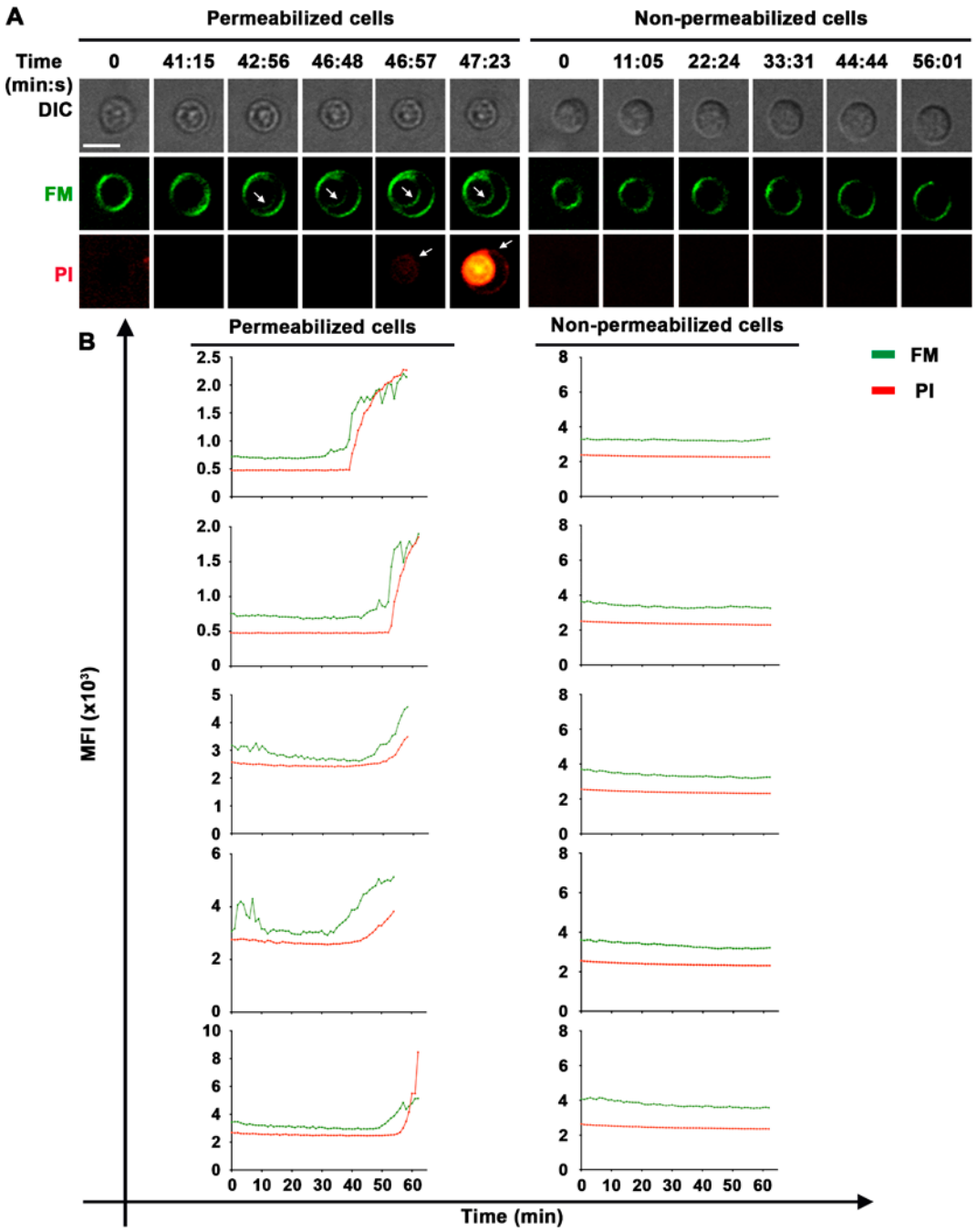

Figure 2.1-Sup.4. Sudden increases in intracellular staining with the lipophilic FM dye in B-cells permeabilized by interaction with αM-PLB. (A) Live spinning disk time-lapse images of splenic B-cells (permeabilized or non-permeabilized) after contact with αM-PLB in the presence of FM1-43 and PI at 37 °C. The arrows point to B-cell sites where intracellular FM or PI was initially detected. **(B)** Mean fluorescence intensity (MFI) of FM (green) and PI (red) over time in a defined intracellular region (Video 4) in permeabilized (left, 5 examples) or non-permeabilized cells (right, 5 examples). Bar, 5 μm. Work for figure 2.1-Sup.4 was executed by Fernando Maeda.

Figure 2.1-Sup.5

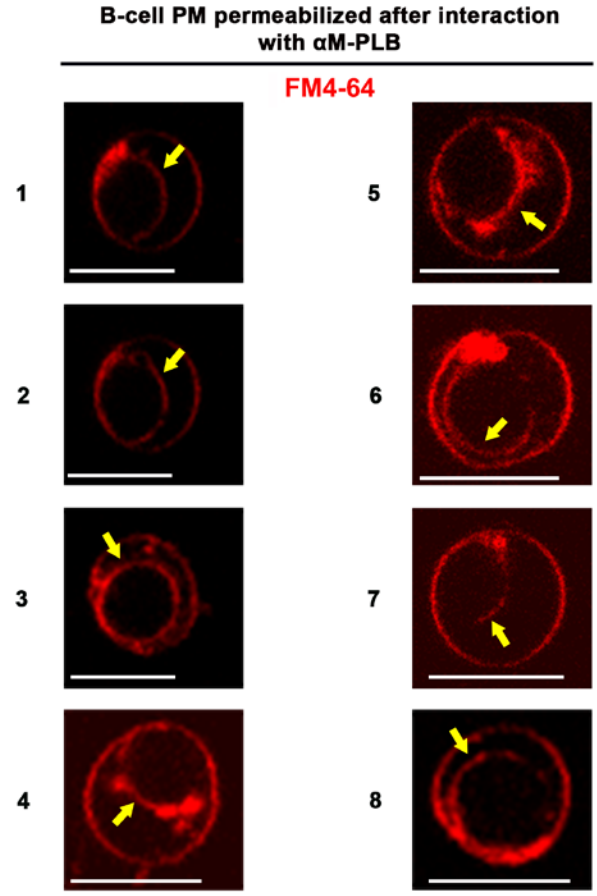

Figure 2.1-Sup 5. The lipophilic FM dye enters B-cells permeabilized by αM-PLB and stains the nuclear envelope. The images show eight examples of FM4-64 nuclear envelope staining (arrows) in splenic B-cells permeabilized by αM-PLB after 60 min incubation at 37°C and imaged by live spinning disk fluorescence microscopy. Bar, 5 µm.

Figure 2.1-Sup.6

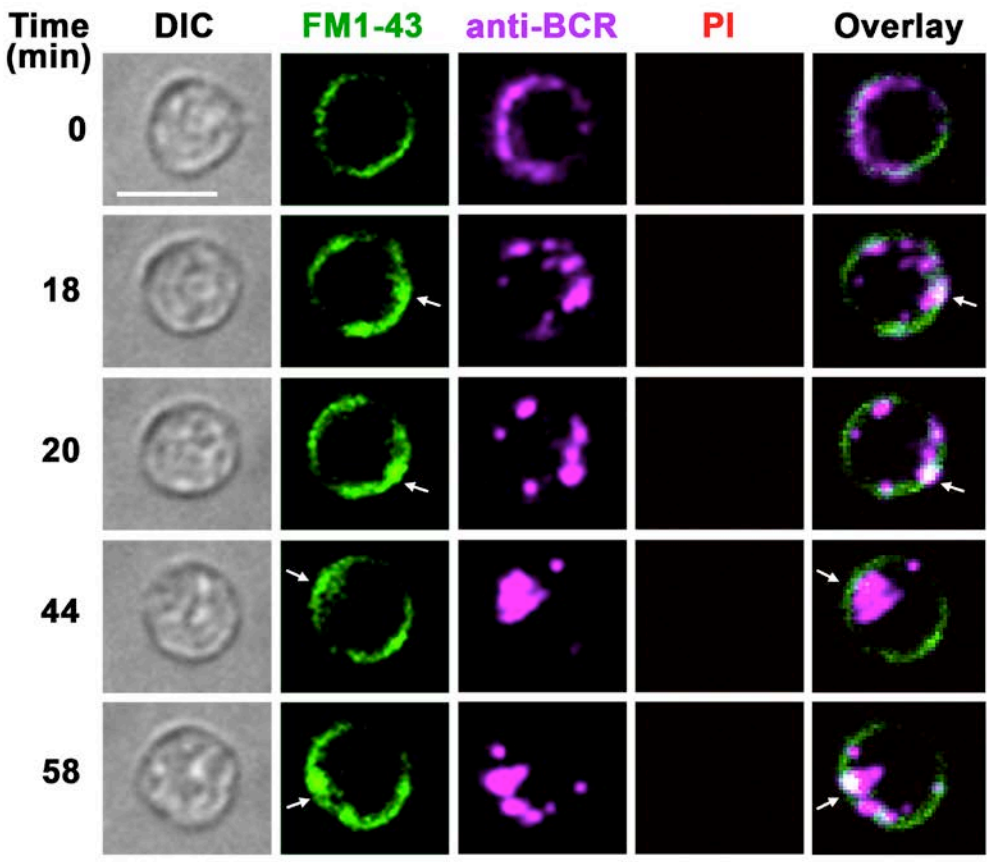

Figure 2.1-Sup.6. BCR cross-linking with soluble ligands does not permeabilize B-cells but induces a punctate form of FM uptake at the cell periphery that is distinct from the massive FM influx induced by surface-associated ligands. Spinning disk time-lapse images of B-cells pre-labeled with soluble anti-BCR antibodies and FM1-43 (green) at 4°C and then imaged at 37°C after addition of secondary fluorochrome-labeled crosslinking antibodies (magenta), in the presence of FM1-43 (green) and PI (red, not detected). The arrows point to areas at the cell periphery where small puncta of internalized FM1-43 were visualized next to anti-BCR clusters (Video 4). No PI influx was detected, indicating that the B-cells were not permeabilized. Bars, 5 μm. Work for figure 2.1-Sup.6 was executed by Fernando Maeda.

Figure 2.4-Sup.1

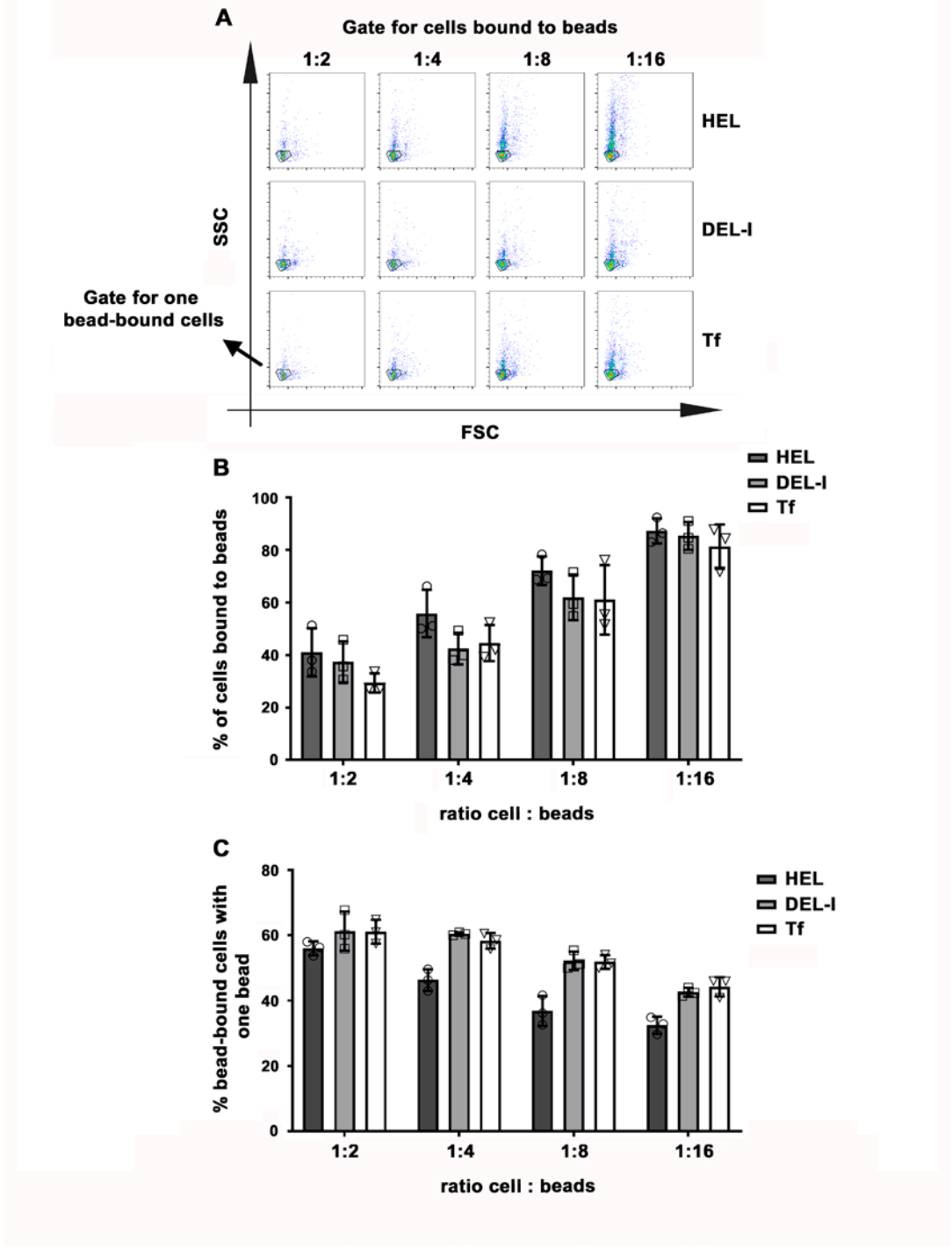

Figure 2.4-Sup.1. Impact of BCR-antigen affinity on B-cell-bead binding. Splenic B-cells were incubated with HEL, DEL-I or Tf-beads at the indicated cell:bead ratios for 30 min at 37 °C and analyzed by flow cytometry. **(A)** Representative SSC versus FSC dot plots gated for bead-bound populations. Outlined areas indicate populations of cells binding one single bead. **(B)** Percentages of total B-cells that bound to beads. Data points represent independent experiments (mean ± SD). **(C)** Percentages of bead-bound B-cells binding one single bead. Data points represent independent experiments (mean ± SD). No statistically significant differences were detected (one-way ANOVA). Work for figure 2.4-Sup.1 was executed by Fernando Maeda.

Figure 2.4-Sup.2

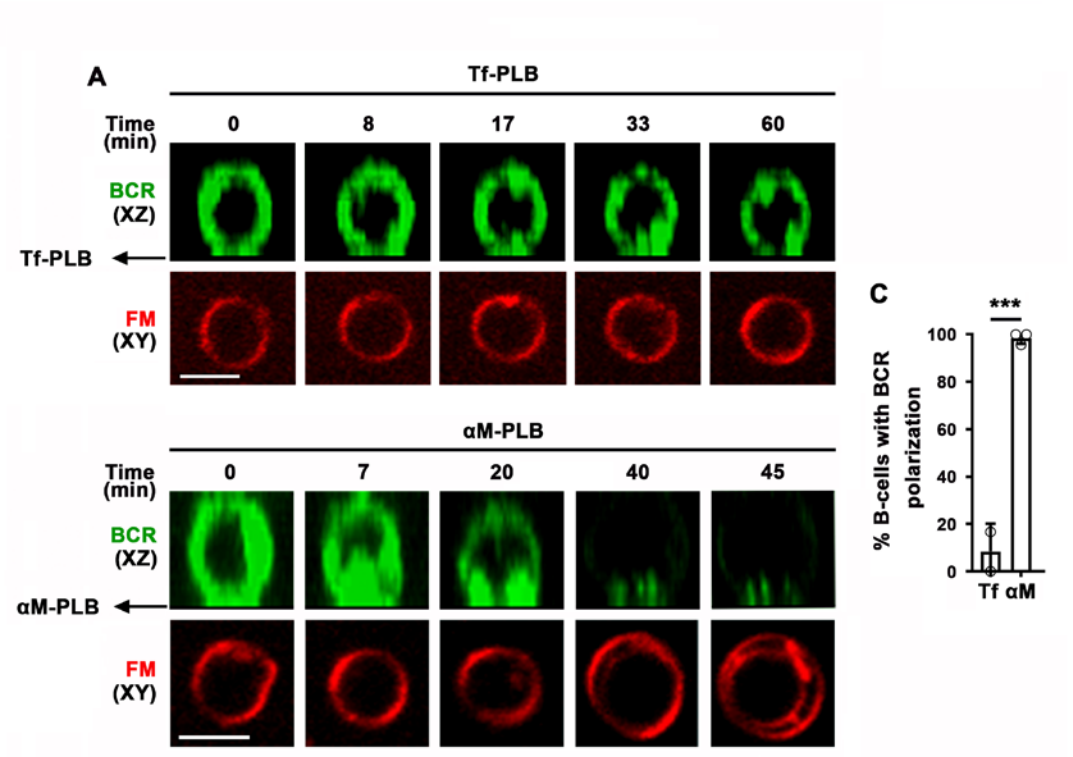

Figure 2.4-Sup.2. B-cell binding to αM-PLB but not to Tf-PLB triggers BCR polarization first and PM permeabilization later. (A) Splenic B-cells stained for surface BCR (green) were incubated with Tf-PLB (top panels) or αM-PLB (bottom panels) for 60 min at 37 °C in the presence of FM4-64 (red) and imaged by live spinning disk fluorescence microscopy. **(B)** Percentages of B-cells with BCR polarization after incubation with Tf- or αM-PLB. Data points represent independent experiments (mean ± SD). ***$p \leq 0.005$, unpaired Student's *t*-test.

Figure 2.4-Sup.3

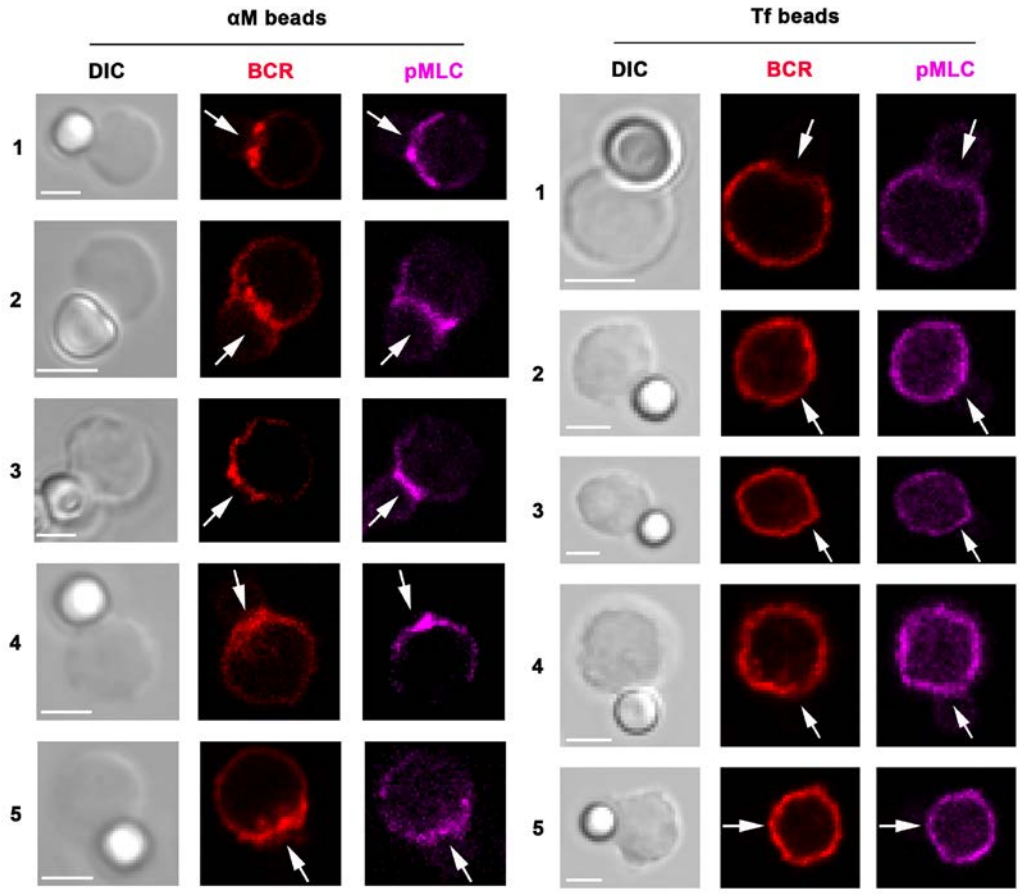

Figure 2.4-Sup.3. BCR and phosphorylated myosin light chain (pMLC) polarize toward αM-bead binding sites. The images show several examples of splenic B-cells stained for surface BCRs with a Cy3-labeled Fab fragment of donkey anti-mouse IgM+G (red), incubated with αM (left, 5 examples)- or Tf (right, 5 examples)-beads, fixed, permeabilized, and stained for pMLC (magenta) and analyzed by confocal fluorescence microscopy. The arrows point to bead contact sites in B-cells. Bars, 3 μm.

Figure 2.5-Sup.1

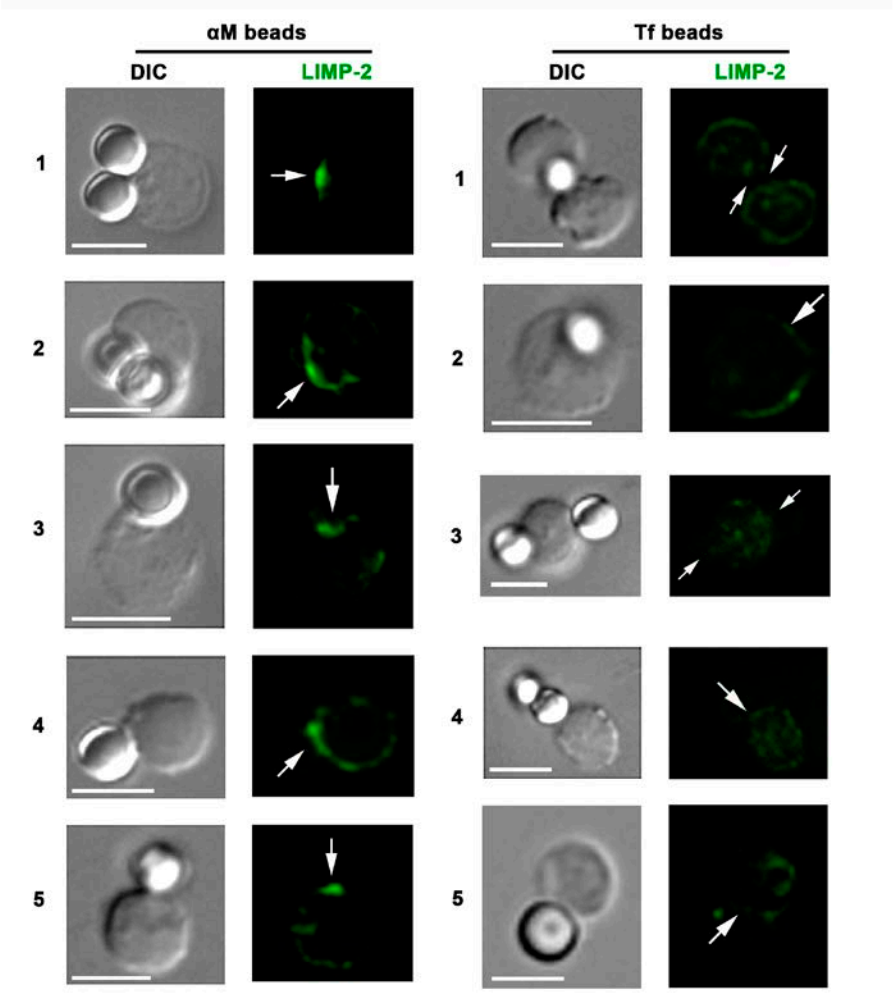

Figure 2.5-Sup.1. BCR-mediated binding of αM-beads induces surface exposure of the LIMP-2 luminal domain at bead contact sites. The images show several examples of splenic B-cells incubated with αM (left)- or Tf (right)-beads for 30 min at 37 °C, stained with LIMP-2-specific antibodies (green) at 4 °C without detergent permeabilization, followed by fixation, staining with secondary antibodies, and analysis by confocal fluorescence microscopy. Arrows, sites of bead binding on B-cells. Bar, 5 μm. Work for figure 2.5-Sup.1 was executed by Fernando Maeda.

Figure 2.5-Sup.2

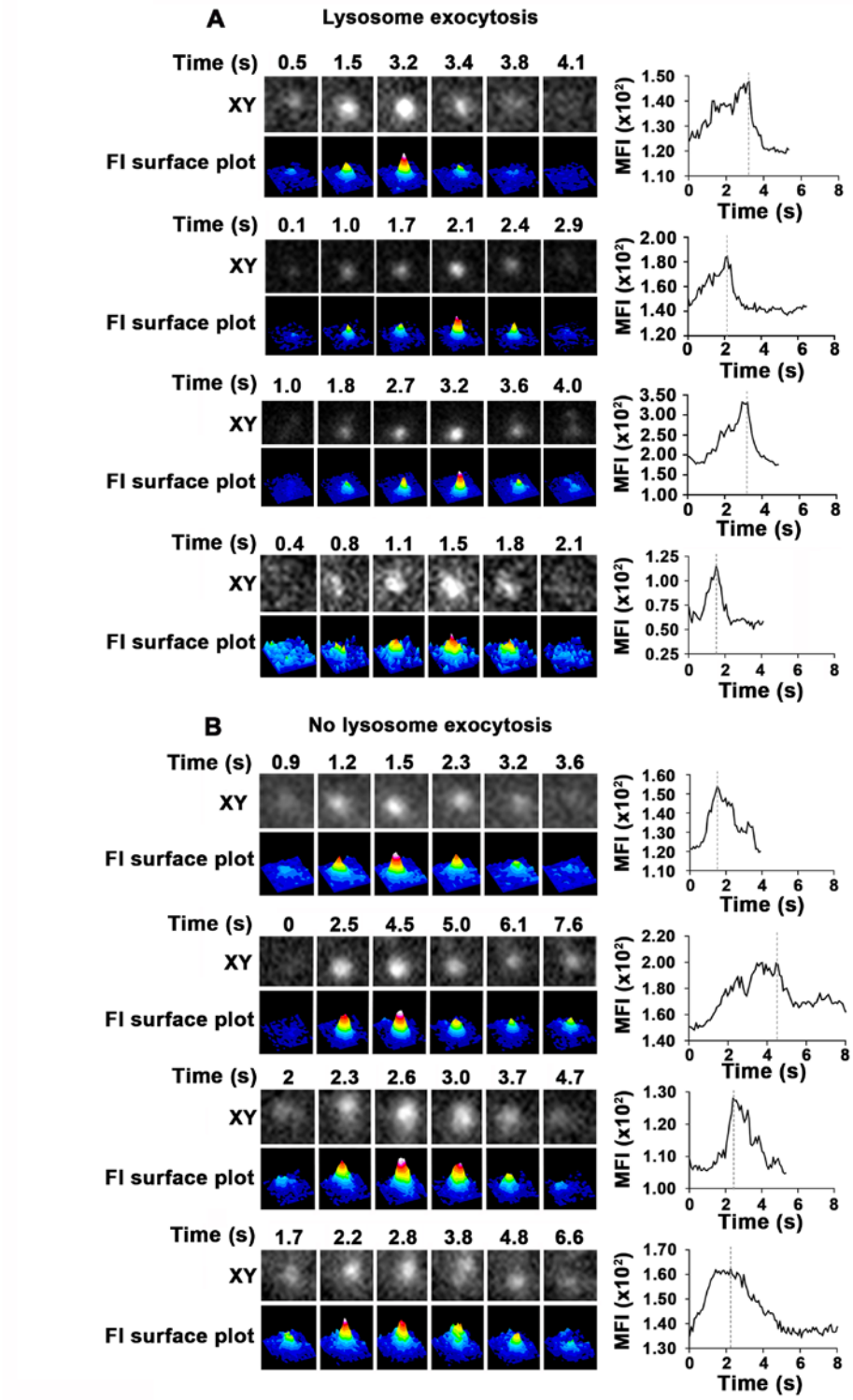

Figure 2.5-Sup.2. Detection of lysosomal exocytosis by TIRF microscopy. Splenic B-cells were added to αM-PLB and imaged by TIRF at eight frames/s. Live time-lapse XY images of individual SiR-Lyso puncta (top rows), their FI surface plots (bottom rows), and MFI (plots on right) within the TIRF evanescent field over time are shown for four examples where lysosomal exocytosis occurred (A, rapid decrease in MFI, consistent with rapid dye loss upon PM fusion) or not (B, slow reduction in MFI, likely due to lysosome movement away from the PM).

Figure 2.6 Sup.1

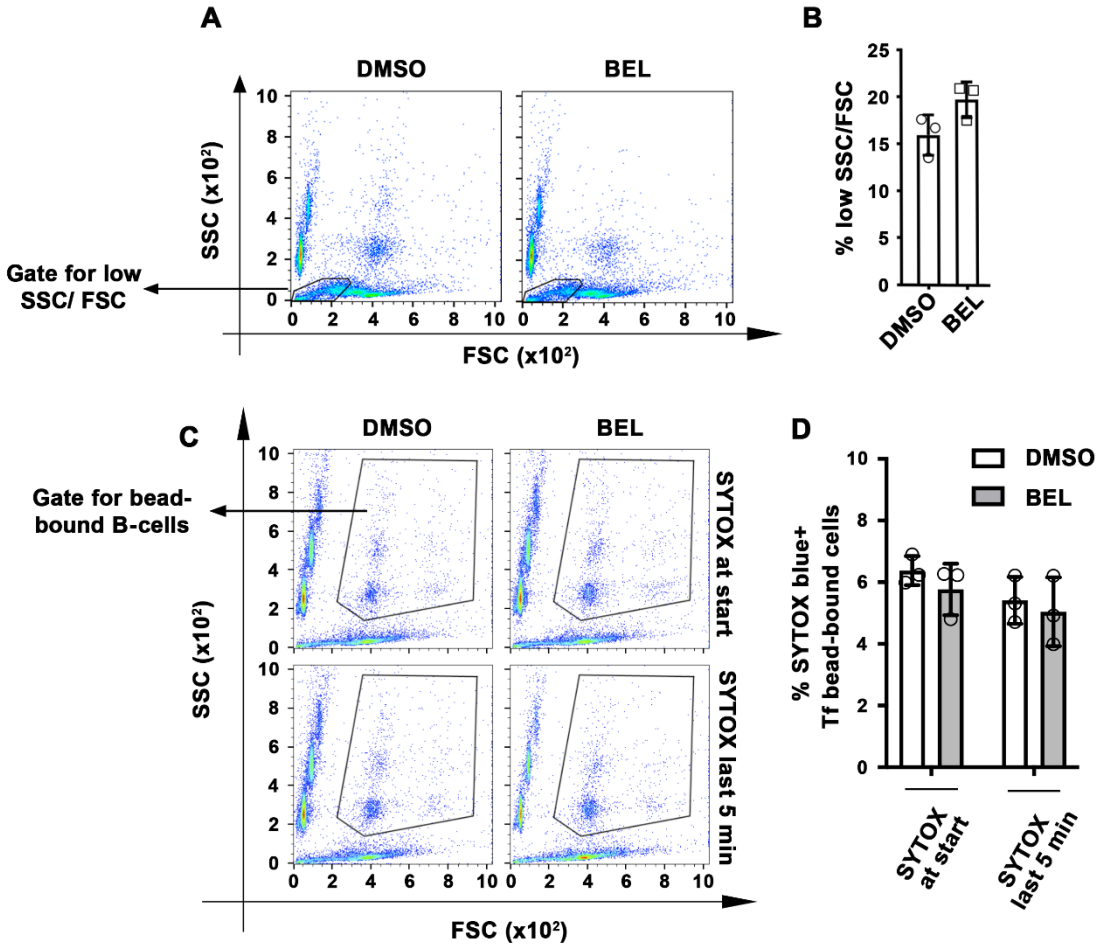

Figure 2.6-Sup.1. BEL does not affect the PM integrity and viability of B-cells. Splenic B-cells were pretreated or not with BEL and incubated with αM-beads in the presence of FM4-64 and analyzed by flow cytometry. **(A)** Representative dot plots of side scatter (SSC) versus forward scatter (FSC) of B-cells incubated with αM-beads. Outlined areas indicate the low SSC/FSC populations that correspond to dead cells. **(B)** Percentage of low SSC/FSC B-cells incubated with αM-beads treated or not with BEL. Data points represent independent experiments (mean ± SD). **(C)** Representative dot plots of side scatter (SSC) versus forward scatter (FSC) of B-cells incubated with Tf-beads in the presence of SYTOX Blue throughout the experiment (30 min) or only in the last 5 min. Outlined areas indicate B-cell populations binding Tf beads. **(D)** Percentages of SYTOX Blue-positive (+) Tf-bead-bound cells. Data points represent independent experiments (mean ± SD). No statistically significant differences were detected (Student's *t*-test). Work for figure 2.6-Sup.1 was executed by Fernando Maeda.

Figure 2.6-Sup.2

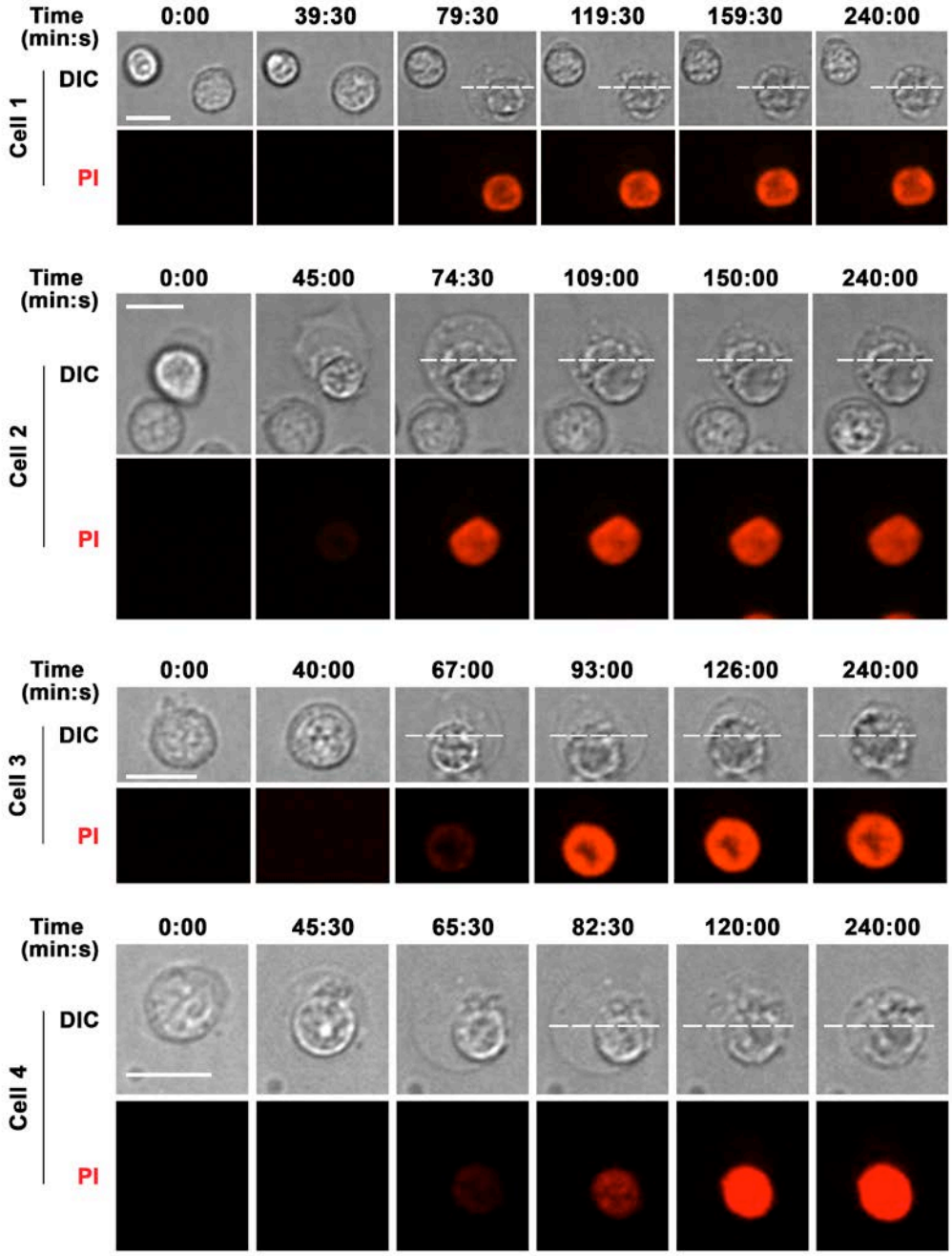

Figure 2.6-Sup.2. B-cell morphological changes occurring during permeabilization by surface-associated antigen are reversible. Spinning disk time-lapse images of B-cells interacting with αM-PLB in the presence of PI (red). The dashed line indicates the maximum cell diameter initially reached by a B-cell that became permeabilized, allowing PI influx (Video 12). The later frames indicate that the cell gradually recovers its original morphology. Bars, 5 μm. Work for figure 2.6-Sup.1 was executed by Fernando Maeda.

Supplemental video legends:

Video 1. BCR binding to αM-beads permeabilizes the PM of splenic B-cells.

Splenic B-cells were incubated with αM-beads at 4°C and warmed to 37°C in a live imaging chamber with 5% CO_2 in DMEM-BSA. Time-lapse images were acquired for 60 min at 1 frame/15 s in the presence of PI (red) using a spinning disk fluorescence microscope (UltraVIEW VoX, PerkinElmer with a 63X 1.4 N.A. oil objective). The arrow indicates the moment of PI entry. Time is displayed as hours: minutes: seconds. The video is displayed at 20 frames/s. Bar, 5 μm.

Video 2. BCR binding to αM-beads causes localized PM permeabilization in A20 B-cells (cell line). A20 B-cells were incubated with αM-beads in a live imaging chamber at 37°C with 5% CO_2 in DMEM/BSA. Time-lapse images were acquired for 65 min at 1 frame/20 s in the presence of PI using a spinning disk fluorescence microscope (UltraVIEW VoX, PerkinElmer with a 63X 1.4 N.A. oil objective). The arrow points to the beads and the arrowhead points to the site of entry and subsequent flow of PI into the cell. Beads appear red as a result of autofluorescence. Time is displayed as hour: minutes: seconds. The video is displayed at 20 frames/s. Bar, 5 μm. Work for Video 2 was executed by Fernando Maeda.

Video 3. Bead exchange between B-cells causes PM permeabilization. Splenic B-cells were incubated with αM-beads in a live imaging chamber at 37ºC with 5% CO_2 in DMEM-BSA. Images were acquired for 60 min at 1 frame/30 s in the presence of PI using a spinning disk fluorescence microscope (UltraVIEW VoX, PerkinElmer with a 63X 1.4 N.A. oil objective). The arrow points to the bead that was exchanged between cells (#1 and #2) and caused

permeabilization of cell #2. Beads appear red as a result of autofluorescence. Time is displayed as hour: minutes: seconds. The video is displayed at 10 frames/s. Bar, 5 μm. Work for Video 3 was executed by Fernando Maeda.

Video 4. Surface-associated ligand induces B-cell permeabilization and massive FM influx, while soluble ligand does not cause permeabilization but induces endocytosis, detected as puncta at the cell periphery. Top: B-cells pre-labeled with FM1-43 (green) were added to αM-PLB (surface-associated ligand). Bottom: B-cells pre-labeled with FM1-43 (green) and anti-BCR antibodies followed by secondary fluorochrome-labeled crosslinking antibodies (magenta) (soluble ligand). Under both conditions cells were imaged at 37°C in the presence of FM1-43 (green), and PI (red) was added to detect PM permeabilization. Images were acquired for 60 min at 1 frame/30 s or 15 s using a spinning disk fluorescence microscope (UltraVIEW VoX, PerkinElmer with a 60X 1.4 N.A. oil objective). Time is displayed as minutes: seconds after cells contacted αM-PLB. The white box indicates the intracellular area used to measure FI levels of intracellular FM1-43 (see Figure 1I and Figure 1-figure supplement 4). The arrow indicates the massive influx of FM1-43 in cells permeabilized during contact with αM-PLB. The arrowheads indicate areas where peripheral FM1-43 puncta (likely endosomes) were observed next to clusters of crosslinked BCR (magenta). The video is displayed at 20 frames/s. Bar, 5 μm. Work for Video 4 was executed by Fernando Maeda.

Video 5. B-cell PM permeabilization during binding to αM-PLB enables membrane-impermeable Ponceau 4R to quench cytoplasmic CSFE fluorescence. Splenic B cells pre-labeled with CFSE in the cytosol were added to αM-PLB in a live imaging chamber at 37ºC with 5% CO_2 in DMEM/BSA. Images were acquired for 60 min at 1 frame/10 s in the presence of

Ponceau 4R using a spinning disk fluorescence microscope (UltraVIEW VoX, PerkinElmer with a 40X 1.4 N.A. oil objective). The arrow indicates CFSE-labeled B-cells that lost their cytosolic fluorescence as a result of PM permeabilization and Ponceau 4R influx. Time is displayed as hour: minutes: seconds. The video is displayed at 30 frames/s. Bar, 5 μm. Work for Video 5 was executed by Fernando Maeda.

Video 6. Binding of MD4 B-cells to COS-7 cells expressing surface mHEL-GFP induces antigen clustering and PM permeabilization at interaction sites. MD4 splenic B-cells were incubated with mHEL-GFP-expressing COS-7 cells cultured on fibronectin-coated coverslips at 37ºC with 5% CO_2 in DMEM/BSA. Images were acquired for 120 min at 1 frame/20 s in the presence of PI using a spinning disk fluorescence microscope (UltraVIEW VoX, PerkinElmer with a 40X 1.3 N.A. oil objective). Shown are representative videos of XY (top) and XZ (bottom) views showing clustering of mHEL-GFP (arrows) and the intracellular influx of PI (arrowheads) at cell interacting sites. Time is displayed as minutes: seconds after the cell contacted the mHEL-GFP expressing COS cell. The video is displayed at 15 frames/s. Bar, 5 μm.

Video 7. Binding of WT B-cells to COS-7 cells expressing surface mHEL-GFP does not induce antigen clustering and PM permeabilization at interaction sites. WT splenic B-cells were incubated with mHEL-GFP-expressing COS-7 cells cultured on fibronectin-coated coverslips at 37ºC with 5% CO_2 in DMEM/BSA. Images were acquired for 120 min at 1 frame/20 s in the presence of PI using a spinning disk fluorescence microscope (UltraVIEW VoX, PerkinElmer with a 40X 1.3 N.A. oil objective). Shown are representative videos of XY (top) and XZ (bottom) views. Time is displayed as minutes: seconds after the cell contacted the mHEL-GFP expressing COS cell. The video is displayed at 15 frames/s. Bar, 5 μm.

Video 8. The BCR polarizes towards antigen-binding sites before PM permeabilization. Splenic B-cells stained with anti-BCR antibodies were added to αM-PLB and imaged in a live imaging chamber at 37ºC with 5% CO_2 in DMEM/BSA. Images were acquired for 60 min at 1 frame/20 s in the presence of FM4-64 using a spinning disk fluorescence microscope (UltraVIEW VoX, PerkinElmer with a 60X 1.4 N.A. oil objective). Top: XZ view showing BCR (green) polarization towards the αM-PLB (white arrow). Bottom: XY view showing intracellular influx of FM4-64 (red, yellow arrow). Time is displayed as minutes: seconds after the cell contacted the αM-PLB. The video is displayed at 15 frames/s. Bar, 5 μm.

Video 9. BCR and phosphorylated non-muscle myosin II (pMLC) polarize towards αM-bead-binding sites on a B-cell. Shown is a 3D representation of co-polarization of the BCR (red) and pMLC (green) towards the site of αM-bead (white) binding in a splenic B-cell. Z-stack images were acquired using a Zeiss LSM710 confocal fluorescence microscope (63X 1.4 N.A. oil objective) and the 3D reconstruction was generated using Volocity software (PerkinElmer). Bar, 3 μm.

Video 10. A lysosomal exocytosis event detected by total internal reflection fluorescence (TIRF) microscopy. Splenic B-cells preloaded with SiR-Lyso were incubated with αM-PLB in a coverslip chamber at 37ºC with 5% CO_2 in DMEM/BSA for 30 min. Time-lapse images were acquired for 20 min at 8 frames/s using a TIRF microscope (NIKON Eclipse Ti-E TIRF, 63X 1.49NA oil objective). Top: TIRF images of a lysosome appearing in the TIRF evanescent field and then rapidly losing the SiR-Lyso signal due to fusion with the B-cell PM. Bottom: FI surface

plot corresponding to the video on the top. Time is displayed in seconds. The video is displayed at 15 frames/s.

Video 11 – B-cells exclude a second membrane-impermeable tracer after antigen-dependent permeabilization. Splenic B-cells were added to αM-PLB and imaged in a live imaging chamber at 37ºC with 5% CO2 in DMEM 2% of FBS in the presence of SYTOX Green (green). Images were acquired for 4 h at 1 frame/30 s using a spinning disk fluorescence microscope (UltraVIEW VoX, PerkinElmer with a 60X 1.4 N.A. oil objective). PI (red) was added for 10 min at the end of the time-lapse image acquisition. The video is displayed as minutes: seconds after the cell contacted the αM-PLB. White arrows indicate cells that became permeabilized and later excluded PI. The yellow arrow indicates a cell that was stained by SYTOX Green since the beginning of the video and was not able to exclude PI. The video is displayed at 20 frames/s. Bar, 5 μm. Work for Video 11 was executed by Fernando Maeda.

Video 12. B-cell morphological changes occurring during permeabilization by surface-associated antigen are reversible. Splenic B-cells were added to αM-PLB and imaged in a live imaging chamber at 37ºC with 5% CO2 in DMEM without phenol red containing 2% FBS in the presence of PI (red). Images were acquired for 4 h at 1 frame/30 s using a spinning disk fluorescence microscope (UltraVIEW VoX, PerkinElmer with a 60X 1.4 N.A. oil objective). Time is displayed as minutes: seconds after the cells first contacted the αM-PLB. The arrow points to a cell that became permeabilized. The dashed line indicates the maximum diameter of the B-cell after permeabilization. The video is displayed at 20 frames/s. Bar, 5 μm. Work for Video 12 was executed by Fernando Maeda.

Video 13. B-cell with polarized surface BCRs and containing fluorescent αM extracted from beads. The surface BCRs of splenic B-cells were labeled with Cy3-Fab-donkey anti-mouse IgM+G at 4^{o}C. Labeled B-cells were incubated with AF488-αM-beads at 37^{o}C with 5% CO_2 for 60 min and then fixed. Images were acquired using a Zeiss LSM710 (63X 1.4 N.A. oil objective), and the 3D reconstruction was generated with Volocity software (PerkinElmer). The arrow points to internalized AF488-αM.